UNIVERSIDADE FEDERAL DE MINAS GERAIS

Programa de Pós-Graduação em Engenharia Metalúrgica Materiais e de Minas

Dissertação de mestrado

"**Metrologia aplicada a nanomateriais: estudo comparativo de técnicas e métodos**"

Autor: Taiane Guedes Fonseca de Souza

Orientador: Prof.ª Virginia Sampaio T. Ciminelli

Co-orientador: Prof.ª Nelcy Della Santina Mohallem

Abril de 2015

UNIVERSIDADE FEDERAL DE MINAS GERAIS

Programa de Pós-Graduação em Engenharia Metalúrgica, Materiais e de Minas

Taiane Guedes Fonseca de Souza

"Metrologia aplicada a nanomateriais: estudo comparativo de técnicas e métodos"

"Metrology applied to nanomaterials: comparative study of techniques and methods"

Dissertação apresentada ao Programa de Pós-Graduação em Engenharia Metalúrgica, Materiais e de Minas da Escola de Engenharia da Universidade Federal de Minas Gerais, como requisito parcial para obtenção do Grau de Mestre em Engenharia Metalúrgica, Materiais e de Minas.

Área de concentração: Ciência e Engenharia de Materiais

Orientador: Prof.ª Virginia Sampaio T. Ciminelli

Co-orientador: Prof.ª Nelcy Della Santina Mohallem

Belo Horizonte

Escola de Engenharia da UFMG

2015

Agradecimentos

Durante o desenvolvimento deste trabalho contei com o apoio de diversas pessoas as quais gostaria de agradecer.

Agradeço a Deus por me guiar e me dar forças durante a caminhada.

Agradeço imensamente às minhas orientadoras, Prof.ª Virginia S. T. Ciminelli e Prof.ª Nelcy D. S. Mohallem, pela oportunidade que me deram, pela confiança em mim depositada, pelo suporte e pelos ensinamentos científicos e de vida.

À minha querida família, Dad, Leo e Nina, pelo amor e pelo incentivo de toda uma vida. A Dona Marlene, meu exemplo e orgulho. E a Claudinha, Jujubinha e Lívia por serem minha inspiração e apoio. Amo vocês!

Ao Breno Galvão pelo amor, pela paciência, pelo inglês, pela parceria incondicional, pelas férias perdidas, por tantas outras coisas impossíveis de enumerar e, principalmente, por fingir saber estatística. Amo-te.

Aos amados amigos Betão, Nubinha, Nabo, Tatá, Sabrina, Ana Flávia, Clebinho e Juninho por suportar minha ausência e continuar me amando. E também por todas as alegrias divididas, juntamente com Walisson, Mayrex, Aline, Vitinho, Olidio,Val, Gessy, Amira, Raquel, Luís, Pim, Vinícius, Nairinha e Neal.

À Nair pelo carinho, paciência e pelos puxões de orelha.

À Christina Salvador pelo carinho, atenção e disponibilidade em ajudar sempre.

À Marina Guedes, Gil Camargo, Matheus Queiroz e a Tarlene Miranda pela imensa ajuda em partes tão difíceis deste trabalho.

À Nanum nanotecnologia S.A. pelo suporte e tempo disponibilizados. E aos queridos amigos da Nanum por tornarem meus dias mais leves, pelo carinho, por me ouvirem, pela preocupação, compreensão, pela convivência harmoniosa do dia-a-dia. Vocês são muito especiais!!!

Aos colegas do Centro de Microscopia, Breno, Raquel Souza, Raquel Fonseca, Paulo Cota, Lu, Denilson e Miquita pelas análises realizadas, pelas contribuições e pela atmosfera divertida.

Aos colegas do Laboratório de Materiais por dividirmos momentos de desespero e de alegria, especialmente à Anne por estar sempre pronta a ajudar.

Ao Centro de Microscopia da Universidade Federal de Minas Gerais por fornecer equipamentos e suporte técnico para experimentos envolvendo microscopia eletrônica.

E, finalmente, ao apoio das entidades CNPq, CAPES-PROEX, FAPEMIG e INCT-Acqua.

OUTLINE

1 Introduction 1
1.1 Objectives 2
1.2 Specific objectives.. 2
1.3 Structure and organization 2
2 Literature review.. 4
2.1 Nanomaterial.. 4
2.2 Nanometrology.. 5
2.2.1 Mesurement 6
2.2.2 Error.. 6
2.2.3 Uncertainty.. 8
2.2.4 Statistical analysis.. 9
2.3 Nanoparticle characterization 12
2.3.1 Transmission Electron Microscopy (TEM) 13
2.3.2 Scanning Electron Microscopy (SEM) (Barbosa, 2012). 15
2.3.3 Atomic force microscopy (AFM) 21
2.3.4 Dinamic light scattering (DLS) 24
2.3.5 Digital image 27
3 An assessment of errors in sample preparation and data processing for nanoparticle size analyses by AFM 29
3.1 Introduction 29
3.2 Materials and methods..31
3.3 Results and discussion..32
3.3.1 Sample Preparation 32
3.3.2 Effect of Data Processing..36
3.4 Conclusions 42
4 Errors associated to basic metrology methods applied to the characterization of non-conductive nanoparticles..43
4.1 Introduction 43
4.2 Materials and methods..45
4.3 Results and discussion..47
4.3.1 Number of particles to count 47
4.3.2 Test for normality 49

4.3.3 Microscopy analysis 49
4.3.4 Dynamic light scattering (DLS) 58
4.3.5 Comparison of NPs size distribution by the different measurement techniques 60
4.4 Conclusions 62
5 Final considerations 64
6 References 66

LIST OF FIGURES

Figure 2.1	Nanoparticles formats: (a) nanospheres; (b) nanorods; (c) nanobowls with 55-nm Au seed inside; (d) coreshell; (e) nanocubes and nanocages (inset); (f) nanostars; (g) nanobipyramids; (h) octahedral nanoparticles.	4
Figure 2.2	Measurement errors causes.	6
Figure 2.3	Schematic representation of the error types.	7
Figure 2.4	Function diagram of a TEM.	13
Figure 2.5	Focus position difference in the horizontal and vertical axis.	15
Figure 2.6	Schematic drawing of a scanning electron microscope.	16
Figure 2.7	Filamento de tungstênio, hexaboreto de lantânio e monocristal de tungstênio	17
Figure 2.8	Signals resulting from the beam-sample interaction	17
Figure 2.9	Scheme of the sample-beam interaction volume in different situations	18
Figure 2.10	Scattering of the incident electron beam for different working distances and vacuum	19
Figure 2.11	Optimum brightness and contrast.	20
Figure 2.12	Function diagram of an AFM.	21
Figure 2.13	Tapping mode AFM.	22
Figure 2.14	Operating regime of the AFM.	22
Figure 2.15	AFM contact and non-contact mode.	23
Figure 2.16	Formation of artifacts in the image of AFM.	24
Figure 2.17	Hypothetical DLS of two samples, one with larger particles, other minor.	25
Figure 2.18	Particle size distribution by number, volume and intensity for a hypothetical sample with 50% of the particles with 5nm and the remainder with 50nm.	26
Figure 2.19	Representation of the mean value of a pixel: (a) original image, (b) region of red rectangle, (c) gray-scale value.	28

Figure 3.1	AFM images of (a and b) SRM-S and (c and d) SRM-SW. Images acquired at 10 x 10 µm and 2 x 2 µm.	33
Figure 3.2	SEM image of sample SRM-SW and AFM microscopy images of the highlighted regions.	34
Figure 3.3	AFM images of samples (a) SRM-SW, (b) SRM-SG and (c) SRM-M.	35
Figure 3.4	AFM images of the SRM-SD samples: (a) height and (b) phase contrast images and (c) the profile of region 1.	35
Figure 3.5	3D image of the SRM-SG sample (original image with artefacts).	37
Figure 3.6	Height retrace images of the SRM-SG sample: (a) 2-D original with artefacts; (b) 2-D after treatment 1 with Gwyddion; (c) 2-D after treatment 2 with Gwyddion, (d) 2-D after treatment 3 by Asylum MFP-3D; and (e) 3-D after treatment 2 with Gwyddion.	38
Figure 3.7	Profile, height and length measurements of sample SRM-SG with treatment 2 using Gwyddion .	39
Figure 3.8	Round (a) and key (b) interpolation using Gwyddion software and their profiles from the AFM image of the SRM-SG sample.	40
Figure 4.1	Probability paper and p-value for normality tests of nanoparticles sizes analyzed by a) TEM, b) SEM and c) AFM, by Shapiro-Wilk test.	49
Figure 4.2	Images of SRM NPs by TEM (a), SEM (b) and AFM(c) showing low drying-induced agglomeration. Particle size distribution of SRM NPs measured by TEM (d), SEM (e) and AFM (f).	50
Figure 4.3	ANOVA results for SRM naoparticle measured using TEM at three replicated sample and two image measurement methods.	52
Figure 4.4	Sequential images of the same particle, by SEM with high vacuum and 15kV.	55
Figure 4.5	- SEM images from SRM NPs with (a) carbon coating, high vacuum and low energy; (b) no coating, low vacuum and energy beam of 15keV; (c) no coating, high vacuum and energy beam of 10keV and (d) no coating, low vacuum and energy beam of 10keV	57
Figure 4.6	Height retrace image from the SRM-sample (a) with artifacts; (b) after image treatment at Gwyddion.	58
Figure 4.7	Particle size distribution of SRM by DLS: at normal operational mode, no dispersant, and SRM concentrations of 0.1%(v/v) (a), 5%(v/v) (d), 1x10-4%(v/v) (e) and 1x10-4%(v/v) (f). At monodisperse operational mode, no dispersant, and SRM concentration of 0.1%(v/v) (b). At normal operational mode, with dispersant (disperbik 348), and SRM concentration of 0.1%(v/v) (c);	59
Figure 4.8	Mean value for SRM obtained by TEM, SEM, AFM and DLS. The center line marks the certified value and the gray zone indicate its standard deviation.	61

LIST OF TABLES

Table 2.1 Parameters to be maintained for different conditions of precision. 8

Table 2.2 Running time variation in function of particle size 27

Table 3.1 Experimental conditions employed and their acronyms 32

Table 3.2 Particle size measurements of SEM SG and SEM-SD samples 36

Table 3.3 Height measurements (SEM SG sample) without and with treatments by Gwyddion and Asylum MFP-3D software 38

Table 3.4 Measurements of height and FWHM of sample SRM-SG with treatment 2 using Gwyddion and with treatment 3 using Asylum MFP 3D 39

Table 3.5 Comparison of values obtained using round and key interpolation 41

Table 3.6 Particle size measurements from the height with two different resolutions and the key interpolation in Gwyddion 41

Table 4.1 Calculated Diameters of TEM nanoparticles. Random Sampling Summary 48

Table 4.2 Mean diameter of three replicate of SRM particles obtained by TEM 51

Table 4.3 Mean particle size of SRM samples and their standard deviation (SD) on three different days measured using TEM. 53

Table 4.4 Mean diameter of three replicate of SRM particles obtained by SEM at the same day , with : same operator, resolution of 2048x1887dpi, 100.000 times magnification, high vacuum and 15 kV. 55

Table 4.5 Particle size of SRM samples on three different days, by SEM, with : same operator, resolution of 2048x1887dpi, 100.000 times magnification, high vacuum and 15 kV.. 55

Table 4.6 Influence of analyses parameters at particle size measurement by SEM. 56

Table 4.7 Average particle size and standard deviation associted to SRM measurement by AFM with replicate and at different days 58

Table 4.8 Average particle size and standard deviation associated to SRM measurement by DLS. 59

Table 4.9 Span ratio and median values from SRM by TEM, SEM, AFM and DLS. 62

RESUMO

O desenvolvimento de nanomateriais e suas aplicações científicas e comerciais têm aumentado significativamente e, para tanto, a precisão e a confiabilidade da medição de suas propriedades tornam-se essenciais. Apesar da existência de estudos devotados a aumentar a acurácia das medições na escala nano e no desenvolvimento de equipamentos, lacunas são frequentemente identificadas, tais como a falta de reprodutibilidade de resultados obtidos por diferentes laboratórios, de padrões, de rastreabilidade, de metodologias padronizadas, entre outras.

O presente trabalho avaliou os vários parâmetros que podem influenciar as medidas de tamanho de nanopartículas não condutivas (NPs) por meio da análise de amostras de poliestireno com tamanho certificado de (102 ± 3)nm utilizando as técnicas de microscopia eletrônica de transmissão (MET), microscopia eletrônica de varredura (MEV), microscopia de força atômica (MFA) e espalhamento dinâmico de luz (DLS). Demonstrou-se que, através de manipulação adequada dos parâmetros e considerando as limitações inerentes aos métodos, todas as técnicas permitem a determinação de tamanhos compatíveis com o valor certificado, utilizando-se o teste t de Student, em um nível de confiança de 95%. A técnica MET apresentou os melhores resultados em termos de repetibilidade e de tendência para o valor certificado. A preparação de amostra mostrou-se como a maior fonte de erro desta técnica. Medições por MEV não apresentaram repetibilidade ao longo do tempo, de acordo com o teste de Dunnett, em um nível de confiança de 95%, além de apresentarem o maior erro, dentre as técnicas estudadas, em relação ao valor certificado. Resultados de MFA apresentaram o maior desvio padrão, apesar da sua elevada precisão associada com o eixo Z. Verificou-se que tanto o software para tratamento de dados quanto o tipo de procedimento de tratamento de imagens influenciam a medição do tamanho das partículas. Os resultados obtidos com a técnica de DLS mostraram-se sensíveis a diversos parâmetros operacionais (tais como a diluição e o uso de dispersantes) e apresentaram um grande desvio padrão. Além disso, a comparação dos resultados de tamanhos obtidos por DLS com aqueles obtidos por técnicas de microscopia deve ser realizada com cuidado, uma vez que a técnica mede o diâmetro hidrodinâmico e fornece distribuição em intensidade (não em número). Adicionalmente, os erros associados aos diferentes métodos de preparação das amostras sobre substratos de silício e mica para as medidas de tamanho por MFA foram investigados. Mostrou-se que a diluição da suspensão de nanopartículas foi o suficiente para obter uma boa dispersão sobre o substrato de mica. Para substrato de silício a preparação da amostra foi significativamente melhorada pelo tratamento do substrato com *glow discharge.*

Em resumo, a identificação dos desvios no tamanho das nanopartículas, obtido a partir das diferentes técnicas, e dos parâmetros que podem contribuir para estes desvios constituíram um estudo metrológico que possibilitou uma maior compreensão dos erros associados à medição de nanopartículas, contribuindo assim para o aumento da precisão destas medições.

ABSTRACT

Nanomaterial manipulation has increased scientifically and commercially, and for both, the reliability of measurement is essential. Measurements at the nanoscale must be comparable and reliable whenever the measurement is made.

In this work we discuss several parameters that may influence the non conductive nanoparticles (NP) size measurements by analysing polystyrene samples with certified sizes (102 ± 3)nm using transmission electron microscopy (TEM), scanning electron microscopy (SEM), atomic force microscopy (AFM) and dynamic light scattering (DLS) techniques. It was shown that by an adequate manipulation of their parameters and regarding their inherent limitation (e.g. hydrodynamic diameter for DLS) all techniques allow finding values compatible with the certified ones, according to one sample Student's t-test at a 95% confidence level. The TEM technique presented the best results in terms of repeatability and bias to the certified value. The sample preparation is the major source of error of this technique. Measurements by SEM did not present repeatability over time and showed the highest bias to the certified value, according to Dunnet's test at a 95% confidence level. AFM results presented the highest standard deviation, despite its high precision associated with the Z-axis. It was found that both the software for data treatment and the type of flattening procedure were shown to influence the particle size measurement. The results obtained from the DLS technique proved to be sensitive to several operating parameters (such as dilution and the use of dispersant) and showed a large standard deviation. Furthermore, comparison of results of NPs sizes obtained by DLS with those obtained by microscopy techniques should be performed carefully, since the technique measures hydrodynamic diameter and provides intensity distribution (not by number). In addition, the errors associated with different methods of sample preparation on silicon and mica substrates for measurement in AFM were investigated. It was shown that the dilution of the polymeric nanoparticle suspension was enough to achieve good dispersion on the mica substrate. For silicon substrate the sample preparation was significantly improved by treating the substrate with glow discharge.

In summary, the identification of the deviations in nanoparticles' size, obtained from each technique, and the parameters that contribute to these deviations constitute a metrological study that allows a better understanding of the size measurement errors and contribute to increasing their accuracy.

1 Introduction

The importance of nanotechnology is growing in several segments of industry (Malinovsky *et al.,* 2014; Linkov *et al.,* 2013). Due to its unique properties, nanoparticles have increased applications in the fields of microelectronics, catalysis, composite materials and biotechnologies, among others (Brown *et al.,* 2013). The production of nanoparticles (particles with at least one dimension between 1 and 100nm (Linkov *et al.,* 2013)) on an industrial scale is an essential bridge between the findings of nanoscience and the nanotechnology products for "the real world". Thus the nanomaterials need to be manufactured attending the market requirements, such as reliability, repeatability and economic viability. Reliable measurements are essential for nanomaterials production and trade, while emerging fields of research and industry place even newer demands on measurements. For the frequent measurements that are necessary over the whole range of applications, metrological traceability and calibration are needed, but unfortunately old calibration methods are not suitable at the nanometre scale (Tanaka *et al.,* 2011; Korpelaine, 2014). Therefore, the development of nanoscience and nanotechnology is also connected with the development of measurement systems to assure reliable and comparable measures. Scientific research requires that measurements are comparable even if performed with different instruments by different people at different times or places (Korpelainen, 2014; Sepä, 2014). In addition, increase in the use of nanomaterials also implies the need of a regulation for nanotechnologies and this also demands reliable measurements to support legislation and testing (Sepä, 2014).

Given the complexity and the importance of metrology to the development of nanoscience, and its application in various industrial sectors, standardization becomes necessary (Lojkowski et al., 2006). According to the European Commission (EC) Framework Programme 7, there is a high demand in developing methods to detect nanomaterials in biological matrices, in the environment, and in the laboratory, enabling studies of exposure to such materials (Burke *et al.,* 2011). The need for infrastructure in nanoparticle production industries also influences improvements in certification, standardization and procedures for calibration and measurement tools (Todua, 2008; Leach et al., 2012) as well as requires costs concerns. There are now numerous nanomaterials characterization techniques and some even already standardized, but there is still the need for the development of methodologies for standardization (Aleksandrov, 2012).

Particle size is the main parameter to be evaluated, since it has a direct correlation with many properties of these materials (Attota and Silver, 2010; Minary-Jolandan et al., 2012). It is also important to be able to measure size in situ (e.g. in suspended nanoparticles in different media) because the behaviour of nanomaterials may be strongly influenced by the matrix, and this is still considered a challenge (Burke *et al.*, 2011)

Accurate dimensional metrology and characterization of nanomaterials for

nanomanufacturing remains an issue regarding concepts, regulatory purposes and technological advances, which are needed to enable practical metrology (Postek *et al.,* 2011; Brown *et al.,* 2013). Imaging techniques and high-resolution microscopes are important for nanoobjects development. Even so, high resolution does not mean high accuracy; new reliable measurement methods are necessary for nanotechnology further development (Korpelainen, 2014) and nanometrology is therefore the key.

1.1 Objectives

The main goal of this study is to compare particle size measurements in nanometer scale by transmission electron microscopy (TEM), atomic force microscopy (AFM), scanning electron microscopy (SEM) and dynamic light scattering (DLS).

1.2 Specific objectives

Considering that each technique for particle size analysis has its own peculiarity, application, cost and uncertainty the work has also the following aims:

i. Contribute to nanometrology advances by comparing techniques and methodologies.
ii. Compare the results of average size measurement and distribution of nanoparticles for each technique.
iii. Evaluate the difference in the results obtained by each technique by performing statistical hypothesis testing methods.
iv. Assess the reproducibility of the sample preparation methods.
v. Assess the reproducibility of the techniques over time, for the chosen working conditions.
vi. Enable the usage of the techniques with knowledge of the error associated with that measurement.

1.3 Structure and organization

This work is organized in five chapters. Chapter 1 provides an introduction to the theme and discusses the importance of nanometrology.

Chapter 2 offers a detailed and critical review of the literature on basic statistics concepts used in this work, such as errors and measurements. It also discusses the applications and limitations of some hypothesis tests. Finally, a short description of the selected techniques for particle size measurement is presented.

Chapter 3 investigates the errors in sample preparation and data processing for nanoparticle size analyses by AFM with the aim to contribute to more accurate particle size measurements. The influence of software (Gwyddion and Asylum MFP-3D) and other parameters for data treatment on image resolution, such as the flattening technique, are also studied and, finally, the importance of resolution and image size for accurate results is evaluated.

Chapter 4 explores several parameters that may influence the nanoparticle size measurements using TEM, SEM, AFM and DLS techniques as well as their underlying metrology. It also presents some statistical tools for comparing a wide range of reported results and identifying potential mistakes when reporting nanoparticle sizes and size distributions.

Finally, Chapter 5 summarizes the main results obtained in the present work, as well as conclusions and original contributions.

2 Literature review

2.1 Nanomaterial

According to the International Organization for Standardization (ISO), nanoobjects are objects whose one dimension is on the nanoscale. The term nanoscale refers to a size between 1 and 100 nm. Included as nanoobjects are nanoparticles (nanoscale in all three dimensions), nanofibers (nanoscale in two dimensions) and nanoplates or nanolayers (nanoscale in only one dimension) (Linkov *et al.*, 2013). Nanoparticles are found in several shapes such as illustrated in Figure 2-1, but only for spherical particles, the size can be represented by a single parameter, the diameter. For the description of a particle of any other shape, length or breadth can be used, or the concept of equivalent sphere, yielding the diameter of a sphere expected to show the same behaviour as the particle or group of particles under consideration. There are also some other diameters or lengths used to characterize particles, which are dependent of particle orientation such as the Ferret diameter, which is the distance between two parallel tangents on opposite sides of the image of a randomly oriented particle (Merkus, 2009). In general, the spherical assumption does not cause serious problems, unless the particles have a very large aspect ratio, such as fibers. Particle size measured with different analysers may diverge because of the shape factor, since each measurement technique detects size through the use of its own physical principle (Horiba, 2014).

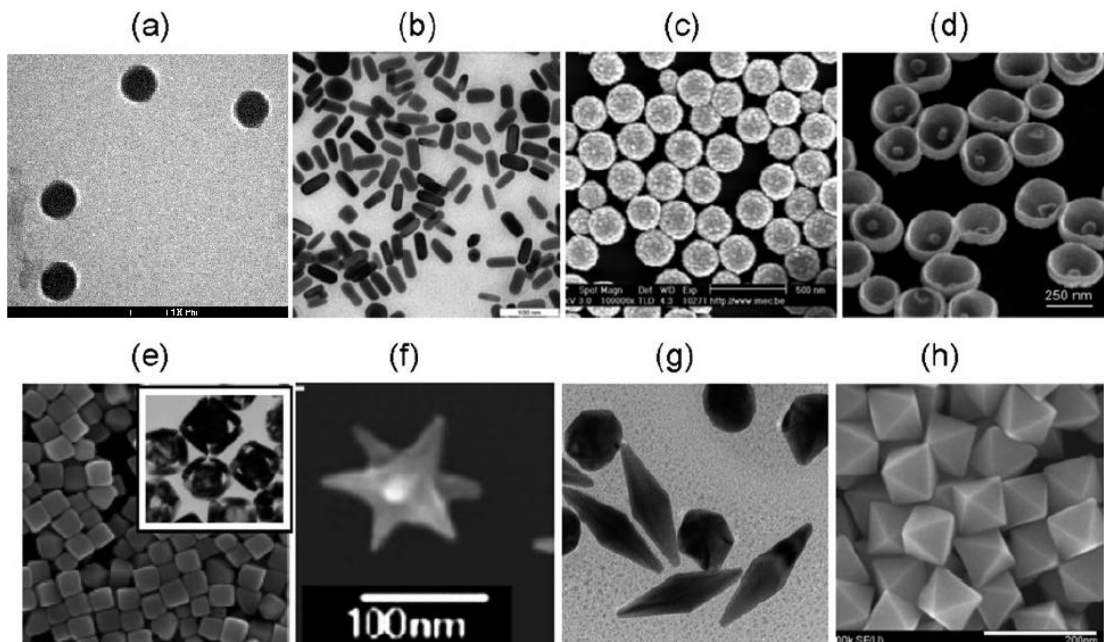

Figure 2-1- Nanoparticles formats: (a) nanospheres; (b) nanorods; (c) nanobowls with 55-nm Au seed inside; (d) coreshell; (e) nanocubes and nanocages (inset); (f) nanostars; (g) nanobipyramids; (h) octahedral nanoparticles (adapted from Khlebtsov and Dykman (2010))

Usually, the particles do not have the same size but a distribution of sizes. In that sense, the European Comission (EC) definition of nanomaterial is much broader than the ISO definition (European Commission, 2011), as the latter excludes solvated and self-assembled soft particles such as proteins and micelles as well as macroscopic nanostructured materials (Brown *et al.*, 2013).

The EC definition of nanomaterial comprise "natural, incidental or manufactured materials containing particles, in an unbound state as an aggregate or as an agglomerate and where, for 50% or more of particles in the number size distribution, one or more external dimensions in the size range 1 to 100 nm". Under this definition, particles are understood as tiny pieces of material with defined boundaries. The aggregates are defined as a body of two or more particles that are strongly bound or merged together, while agglomerate is defined as a body of two or more particles that are weakly bound together by long-range interactions (European Commission, 2011).

The EC definition for nanomaterial using only particle size has been subjected to some criticism. For example, the absence of a statement about specific surface area by volume is a fail point according to Brown *et al.* (2013), since it is an agglomerate--tolerant parameter, to identify potential nanomaterials (Kreyling *et al.,* 2010). According to Merkus (2009), the description of particle size and size distribution should provide the best discrimination for the quality of the particulate product regarding the properties and production process. If these properties also depend on particle shape, it should be characterized in addition to size.

The EC nanomaterial definition clearly advances over the ISO definition, but implies in several challenges in the area of particle metrology and also imposes the use of distribution parameters to characterize nanoparticles. The use of average particle size is not enough to specify the samples. The characterization of nanomaterials, as usually required for particles in general, should consider the histogram of particles sizes, or the D10, D50 and D90 parameters, which represent the particle sizes comprised under a given percentage (10, 50 and 90%) of the sample. Alternatively, the width of a particle size distribution may be expressed as the ratio of (D90-D10)/D50 or the ratio D90/D10.

2.2 Nanometrology

Metrology is the study of measurement and its applications. This encompasses all technical and practical aspects of measurement, whatever the measurement uncertainty and the field of application are (VIM, 2012).

When this study is devoted to nanomaterials properties measurement, it is called nanometrology (Kim *et al.*, 2014) and dimensional nanometrology when it is related to dimensions of objects or object features in the range from 1 nm to 1000 nm (Korpelainen, 2014). Nanometrology faces similar issues as the traditional metrology, such as precision, accuracy, cost and measurement speed at required scale (Liddle and Galatin, 2011)

2.2.1 Mesurement

Measurement is a process of experimentally obtaining one or more values that can be reasonably attributed to a quantity. This is done by comparing quantities or counting entities (VIM, 2012).

The selection of the best method and measurement system depends on a number of characteristics of the application for which the measurement is intended. The measurement velocity, stability over time, possibility of automation, desired uncertainty and also the cost of measuring and instruments should be considered when choosing the method. Under this perspective, one of the goals of this study is to investigate the variables associated with measuring techniques used to determine particle size and particle size distribution.

2.2.2 Error

When measuring a quantity, there is inevitably a concern in understanding the relationship between the obtained value and the actual value of the variable (Alves, 2003) and this difference always arises, because the error is undesirable, but also inevitable (Albertazzi and Souza, 2008). Thus, a measurement error will always be present to a greater or lesser extent (Albertazzi and Souza, 2008). There are numerous factors that lead to the occurrence of measurement errors (Figure 2-2) making it necessary to classify them, in order to reduce and, if possible, eliminate them (Alves, 2003).

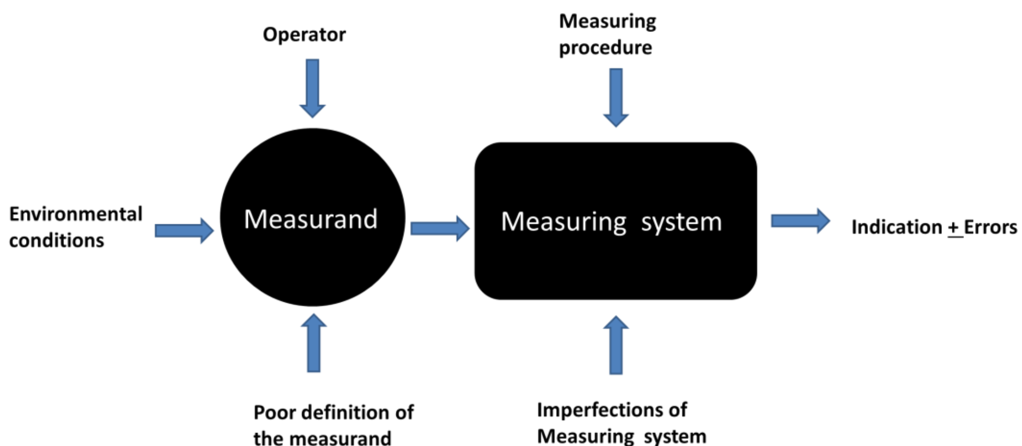

Figure 2-2- Causes for the measurement errors (adapted from Albertazzi and Souza, 2008).

According to the International Vocabulary of Metrology (VIM, 2012), measurement error is the difference between the measured value of a quantity and a reference value (since the true value is impossible to be known). These errors can be classified as systematic or random.

Systematic error is the parcel of the measurement error that remains constant or varies in a predictable way in repeated measurements. The estimate of this value is called trend. Systematic error, if known, can be corrected by adding it to the measured value of the quantity or by a correction factor. On the other hand, the random error is the part of the measurement error that varies unpredictably on repeated measurement (VIM, 2012). Its origin is often difficult to explain, being the accumulation of a large number of small effects. In practice, they are seen as the different values obtained when performing several measurements of a quantity that does not vary. Random errors can generically be regarded as the residue of the measurement error after avoiding gross errors and conveniently correcting the known systematic ones. In general the measurements show the two types of errors, which hinder accuracy.

Figure 2-3 outlines some possible situations during measurement, starting from a case with large random and systematic errors, with a result with no precision or trueness (Figure 2-3a) and culminating in a more accurate measure (Figure 2-3d).

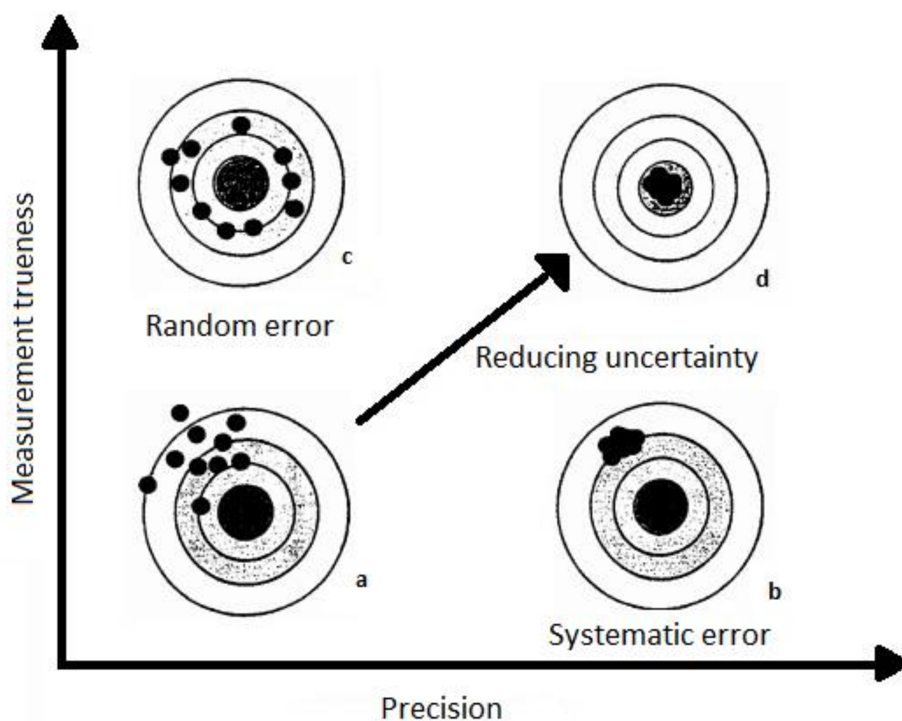

Figure 2-3- Schematic representation of the error types (Teixeira, 2006).

The improvement of the precision only in the measuring system is illustrated by Figure 2-3b. Precision is the degree of agreement between indications or measured values obtained by repeated measurements in the same or similar object under specific conditions. One result can be quite precise but distant from the reference value, as shown in the figure, influenced by the presence of a systematic error. The measurement precision is usually expressed numerically by variables such as standard

deviation, variance or coefficient of variation under specified experimental conditions (parameters). These parameters will specify the conditions of precision, as repeatability, intermediate precision or reproducibility (VIM, 2012). Table 2.1 shows the differences between these conditions.

Table 2.1- Parameters to be maintained for different conditions of precision.

Parameters to be repeated between two analysis	**Repeatability**	**Intermediate precision**	**Reproducibility**
Measurement procedure	X	X	
Operator	X		
Measurement system	X		
Operation conditions	X		
Local	X	X	
Object	X	X	X

When comparing techniques, the repeatability is an important parameter to be analysed. For particle size distribution measurements, there are two different repeatability cases. One is for an instrument or technique where the same sample aliquot is being measured for a given short period of time (in our case three days). The other case concerns the procedure where all the conditions and the sample batch are kept the same but for each analysis a new aliquot is prepared (Merkus, 2009).

Increasing only the accuracy of the sample (i. e., the degree of agreement between the average of repeated measures and a reference value) is exemplified in Figure 2-3 c. The trueness of the measurement can be high even if it has a high random error (they are independent), given that the average is close to the reference value, as in the example. Accuracy is the degree of agreement between a measured value and the true value of the measurand (VIM, 2012). Finally the Figure 2-3 d exemplifies a more accurate measure, i. e., with lower measurement errors and lower uncertainty.

2.2.3 Uncertainty

The measurement uncertainty is a non-negative parameter characterizing the dispersion of the values attributed to the measurand, based on the information used. This parameter includes components from systematic effects such as components associated with corrections and values assigned to standards, as well as the definitional uncertainty. Sometimes the estimated systematic effects are not corrected, but instead incorporated to the uncertainty. Various parameters represent the uncertainty of measurement. If the parameter is, for example, the standard deviation it is called the standard uncertainty (VIM, 2012).

The standard deviation of a normal distribution associated with the measurement error is used to quantitatively characterize the intensity of the random component of the

measurement error. An estimate of the standard deviation is obtained by the sample standard deviation (s), calculated from a finite number of repeated measurements of the same measurand by Equation 3.1:

$$s = \sqrt{\frac{1}{n-1}\sum_{i=1}^{n}(x_i - \overline{x})^2} \tag{3.1}$$

where n is the number of measurements, x is the variable being measured (e.g., particle size), and $\overline{x}$ its average. The coefficient of variation (CV) is reported as a percentage and represents the ratio of the standard deviation to the mean. The uncertainty of the measurement generally comprises many components. The uncertainty of type A is one that can be evaluated by a statistical analysis of the measured values obtained under defined conditions of measurement, for example, the condition of repeatability, intermediate precision condition and reproducibility condition (VIM, 2012). The type A evaluation of the standard uncertainty is inherent to the measurement process and is performed by a statistical processing of the set of replicate observations x_i. When one performs repetitions of measurements of the input variable x_i, under repeatability conditions, one of the assessment type A standard uncertainty is (Couto, 2008):

$$u(\overline{x_i}) = \frac{s(x_i)}{\sqrt{n}} \tag{3.2}$$

where $s(x_i)$ is the standard deviation of the individual values of the set of repetitions; and n is the number of replications of the assembly.

When the evaluation of the uncertainties of the input source is carried out by a different method (such as assuming a given distribution and a dispersion interval or by a calibration certificate) the evaluation of the standard uncertainty is denoted type B.

Each of the factors that are part of the measurement process has influence on the outcome and can bring systematic and random components. When properly corrected, the systematic components do not bring considerable uncertainty to the outcome. On the other hand, the random components will always bring uncertainties to the results. Each of the factors that contribute to the uncertainty of the measurement process is called uncertainty sources (Albertazzi and Souza, 2008).

2.2.4 Statistical analysis

A common problem in many areas of science is to compare average results with each other, certify that they are different, and to what level of significance. The hypothesis tests can be applied to evaluate the hypothesis of equality of the average of the results

(H_0 hypothesis, or null) (Montgomery, 2001). Among the decisions of a hypothesis test, there are errors and successes. The probability of rejecting a null hypothesis (H_0) given that it is true (should be accepted), or in other words, statistically state that there is significant difference when in fact there is not, is named type I error, whose probability is represented by α, also called significance level, and is normally fixed by the researcher. Another wrong decision is the type II error (represented by β) defined by the probability of accepting a null hypothesis given that it is false (it should be rejected), or in other words, statistically state that there is no significant difference when in fact there is. On the other hand, a correct decision is made by stating that there is significant difference between at least two means when this actually exists. The probability of making this decision is the power of the test ($1 - \beta$) (Girardi *et al.*, 2009).

After a hypothesis test is applied, the decision whether H_0 should be accepted or rejected will be given by the statistics of the test, or the analysis of the p-value. The analysis by statistical testing is generally performed by comparing the values obtained with the tabulated values according to the level of significance (α) chosen. In the analysis through the p-value, one rejects H_0 if the p-value is less than α and do not reject H_0 otherwise. The p-value is the lowest level of significance that does not reject the null hypothesis. It does not allow reasoning about the probabilities of hypotheses, but works only as a tool for deciding whether to reject the null hypothesis or not.

The use of p-values in statistical hypothesis tests are widely used in many fields of science, such as economics, psychology, biology, chemistry, criminology, and sociology (Babbie, 2007). The hypothesis tests used in this work will be described briefly in this work.

2.2.4.1 Normality test

The studies reports values from microscopy-based measurements are often the mean of all observed particles with one or two standard deviations about this mean, assuming a Gaussian distribution (MacCuspie *et al.*, 2011). However particle size distributions are not always normal. Usually particle size distributions are modelled by log-normal, Weibull or log-hyperbolic probability distributions (Purkait, 2002; Ujam and Enebe, 2013). The inconvenience comes from the fact that many statistical procedures such as t-tests, test F, linear regression analysis or and Analysis of variance (ANOVA) have an underlying assumption that the data has a normal distribution (Razali and Wah, 2011). Even to calculate the confidence interval it is necessary to know which distribution the data follow.

There are some methods to evaluate if the data can be well modelled by a normal distribution: graphical methods (histograms, boxplots, Q-Q-plots), numerical methods (skewness and kurtosis indices) and formal normality tests (Shapiro-Wilk test, Kolmogorov-Smirnov test, Lilliefors test, Anderson-Darling test). Shapiro-Wilk has the best power (Razali and Wah, 2011), and thus was chosen to test the particle size distribution founded. The Shapiro-Wilk test, calculates a W statistics that tests whether a random sample comes from a normal distribution. High values of W are evidence of

normality (Shapiro and Wilk, 1965).

2.2.4.2 Student's t-test

The t-test is used to evaluate the difference between the averages of two groups, which must have a normal distribution. This comparison is also possible by the Z-test, but when the population variance is estimated from the sample, as in the cases studied here, the t-test becomes more suitable. The t-test was developed in 1908 by William Sealy Gosset, a chemist at the Guinness brewery. He used the "Student" pseudonym for publishing the work, as demanded by his employer (Raju, 2005). There are three types of t-test: t-test one sample, paired t-test and independent two-sample t-test.

One sample t-test: consist in measuring the probability that the sample mean is equal to a established value (certificate), or compare it to the average of a population. This test does not consider the standard deviation of the reference value.

Paired t-test: This test should be used when it is necessary to compare the means of two samples that are dependent on one another. Examples of such situations are: repeated measures, two measures of the same population or same subjects at two different times.

Independent two-sample t-test: This test should be used when it is necessary to compare two independent samples. This is well divided in two cases: two distributions can be assumed to have the same variance or when the distributions have unequal variance. These parameters need to be analysed or tested before choosing which type of test should be applied in the samples under consideration.

2.2.4.3 F-test

The F test is used to compare whether two data sets have the same variance. It is a fairly simple test and assumes the distribution to be normal. One simply needs to divide the greater variance by the smaller one and compare with the F table, according to the number of samples of the numerator and denominator and the desired level of significance (Oliveira, 2008).

2.2.4.4 ANOVA

The analysis of variance (ANOVA) is the most common way to compare the effect of various treatments, or a series of measurements, and determine which of these methods produce different average results among themselves (Girardi *et al.*, 2009). In such cases it is common that there are two sources of variation in the measurement: the random errors that occur during measurement (always present) and systematic effects such as the change in treatment or parameters or, in the case of particle analysis, due to segregation, problems with dilution or dispersion, different measurement methods, various techniques (Merkus, 2009). ANOVA identify both variations, one within the set of results and the other one between the set of results. The null hypothesis is that these variations are the same (Merkus, 2009).

The variance estimates are obtained by the mean squares of the treatments and of the residues, obtained by the ratio of the sums of squares by the respective degrees of freedom. The variances of the residues are related to: random errors, particle size distribution, treatment, change in the day of the analysis, operator, technique, among others. The F statistics is obtained through the ratio of the mean square of the treatments and the mean square of the residues.The rejection of the null hypothesis signifies that there is sufficient evidence to state that the treatments have different effects on the studied variable (Girardi *et. al.*, 2009). In order to detect which treatments have different effects, one must employ the multiple comparison tests.

2.2.4.5 Dunnett's test

Dunnett's test is a test used for multiple comparisons. The analysis compares the means of the treatments taken two by two, or the mean of two treatment groups (Girardi *et.al.*, 2009). There are several tests for multiple comparisons and the choice should be guided by the type of comparison that one needs to perform, by the data group behaviour (number of data, balanced data or not, among others) and by the rate of the desired magnitude of the type I error.

Dunnett's test should be applied every time one needs to compare the treatment mean with the control mean only (Vieira *et al.*, 1989). This test keeps the type I error probability at a specified value α for the whole set of comparisons. The type I error probability is applied to all data sets in general and not individually, as occurs in other hypothesis tests (Girardi *et al.*, 2009). This implies the reduction of power of the test when a large number of treatments is tested. According to Oliveira (2008) an alternative is to use higher levels of significance. Dunnett's has an advantage over other tests, because it is the most powerful when the control treatment has larger sample size than the test treatments (Montgomery, 2001).

2.3 Nanoparticle characterization

European Research Strategy Planning had already highlighted the fundamental principles of scientific research about measurements at nanoscale that must be comparable and reliable even if performed with different instruments by different people at different times (Burke *et al.,* 2011; Korpelainen, 2014). However the metrology under which the materials are ''initially'' characterized may impact their reported size and size distributions, which are in turn used as the basis for interpretation of test results or nanoparticles properties. In that sense is important to know the proper usage of each analyses technique and its limitations, advantages and disadvantages, since these techniques provide the fundamental information on nanomaterial applications (Campbel, 2009). Thus the following paragraphs briefly describe the fundamentals of each technique used in this work as well as its main sources of error.

2.3.1 Transmission Electron Microscopy (TEM)

In 1931, the German physicist Ernst Ruska presented the transmission electron microscope, an instrument that is currently able to magnify images in sixteen million times, with a resolution of around 50pm. The operating power of these microscopes ranges from a few tens of kilovolts (kV) to several million volts (Barbosa, 2012). The function diagram is shown in Figure 2-4.

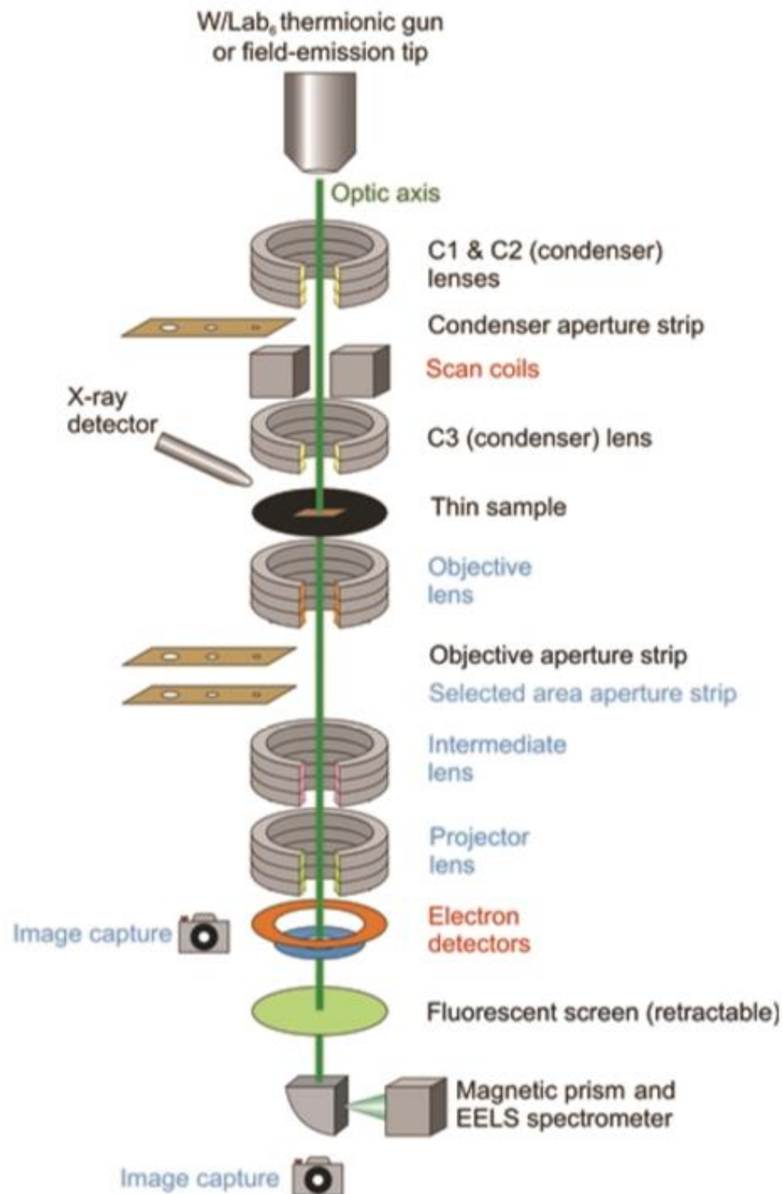

Figure 2-4- Function diagram of a TEM (Lee, 2010).

In a transmission electron microscope, a two-dimensional image of the inside of this on a screen is formed by passing a beam of electrons through extremely thin slices of the sample (Melo, 2002). In the TEM, the sample is inserted in the column under vacuum and "illuminated" with a beam of electrons at 100-300kV. A filament or a thermionic

source EGF generates this beam, as in SEM. The beam passes through a series of electromagnetic lenses, as well as electrostatic plates shown schematically in Figure 2-4. The last two allow the operator to manipulate and steer the beam as necessary (Galletti, 2003). The beam passes through the sample and images are generated simultaneously (Melo, 2002). The final image is projected on a screen of observation, coated with a material that fluoresces when irradiated with electrons, or on a photographic plate, if one wants to record the image permanently (Galletti, 2003).

Despite having a working principle and a very different mode of operation of a SEM, several concepts are common and can be availed here. As is the case of the interaction between electrons beam and sample, the difference now is that the signal of interest is transmitted.

2.3.1.1 Factors influencing the measurement quality

The small electron wavelength allows the electron microscope much higher resolutions than an optical microscope. In an optical microscope the best resolution achieved to date is 174nm. On the other hand a transmission electron microscope, could achieve 0.13nm at 10 kV (λ = 0,0037nm) and 0.09nm at 200kV (λ = 0,0025nm). This difference is due to the nature of electromagnetic lenses, which contains intrinsic imperfections that alter the microscope performance (Miquita , 2012), such as :

i. Spherical aberration: The field lines are more intense in the region of the lens edges. As a result, the electrons passing through the lens by the edges suffer greater deviation than passing through the center. This limits the size of the image in the condenser lens, corrupts the details of the sample in the objective and since the image is generated in the objective and expanded by other lenses, these errors will be magnified by other lenses.
ii. Chromatic aberration: occurs due to the beam (during image formation) being not monochrome, due to the initial distribution generated in the beam cannon or the electron energy loss when interacting with the samples.
iii. Astigmatism: happens when the focus on the horizontal axis is at a different focus point of the vertical axis (Figure 2-5). Astigmatism is due to the inhomogeneous distribution of the field lines, asymmetry of the coils or dirt in the openings.
iv. Thickness of sample: samples, which are not too thin, can cause problems in the contrast of the sample.
v. Atomic number of components of the sample can affect the contrast of the sample.

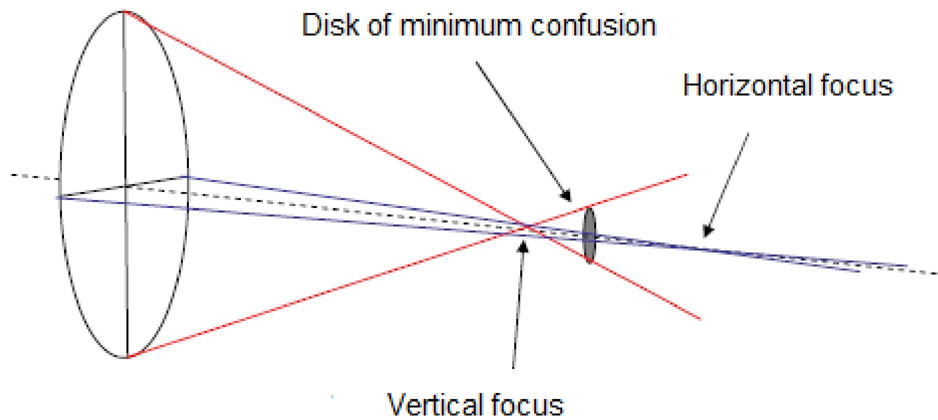

Figure 2-5- Different focus position in the horizontal and vertical axis (adapted from Goldstein *et al.,* 1977).

There are factors that may influence the particle size measurement, which are common to SEM, such as the degradation of the sample at high vacuum, or intensity of the beam incident electrons, or the spreading of the beam due to a low vacuum (Lee, 2010), or even the image definition.

2.3.2 Scanning Electron Microscopy (SEM) (Barbosa, 2012).

The scanning electron microscopy is based on scanning the sample by an electron beam. The technique allows obtaining information about the topography of the sample surface and chemical composition (Vernon - Parry, 2000).

The first scanning electron microscope was developed by Knoll in 1935, and on a commercial scale in the 40's. The resolution obtained at the time was around 1µm, which was very poor, since an optical microscope reached resolutions of 0.5µm. Currently magnifications of 1,000,000 times can be achieved with a resolution of 1.0nm. In a scanning electron microscope (Figure 2-6), an electron beam is generated in the cylinder and is collimated within the column through a condenser lens system and then focused on the sample through an objective lens and coil system. The beam collimated and not magnified by the objective lens, scans the sample and interacts with it. This beam has diameters in the order of a few nanometres in high-resolution microscopes.

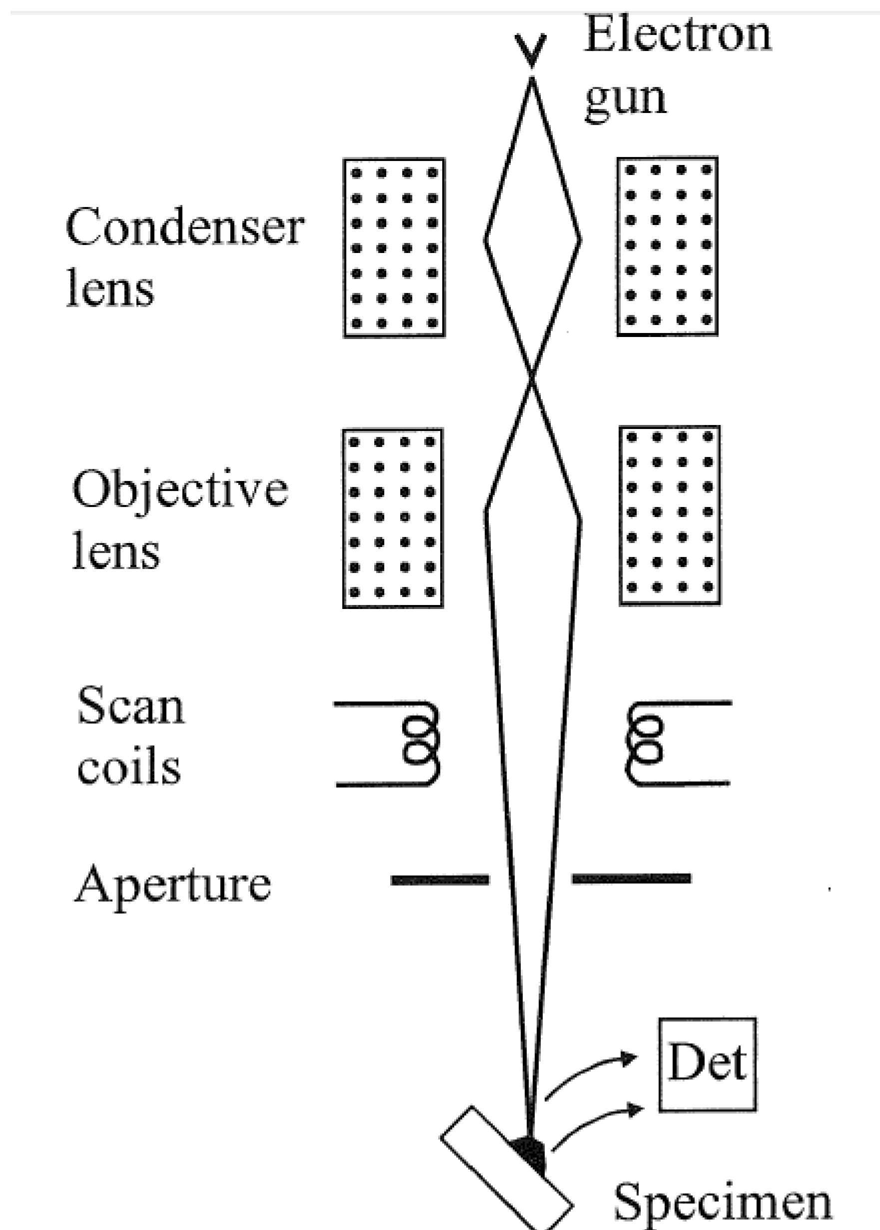

Figure 2-6- Schematic drawing of a scanning electron microscope (Goodhew *et al.*, 2000).

2.3.2.1 Electron beam

The electron beam, after emission, increases in diameter and then passes through a set of collimating lenses and apertures that make its final diameter as small as possible, thereby increasing the resolution of the analysis. That is generated in the cylinder where the beam is extracted from a filament. The extraction system can be thermionic or emission by field effect (Field Emission Gun - FEG). There are three main types of filament: tungsten, lanthanum hexaboride and FEG with tungsten monocrystal (Figure 2-7).

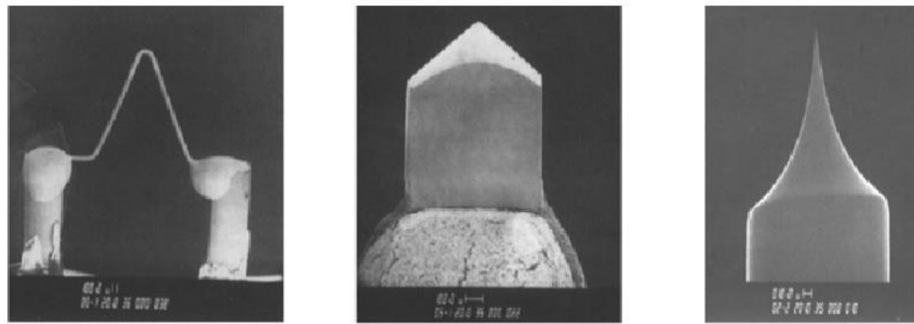

Figure 2-7- Tungsten filament, lanthanum hexaboride and tungsten single crystal (Goldstain *et al.*, 2003)

For a conventional SEM, with tungsten filament as a source of electron beam, this diameter may reach 3.0nm in ideal conditions, which means that the best resolution can be 3.0nm. Due to the method of extraction of the electron beam, and also to the tungsten monocrystal shape, the FEG system leads to a lower filament detrition and a beam with smaller diameter. For a SEM with FEG beam source this resolution can be 1.0nm.

2.3.2.2 Electron beam-sample interaction (Barbosa, 2012).

There are many possible interactions between the beam of high-energy electrons and the sample (

Figure 2-8).

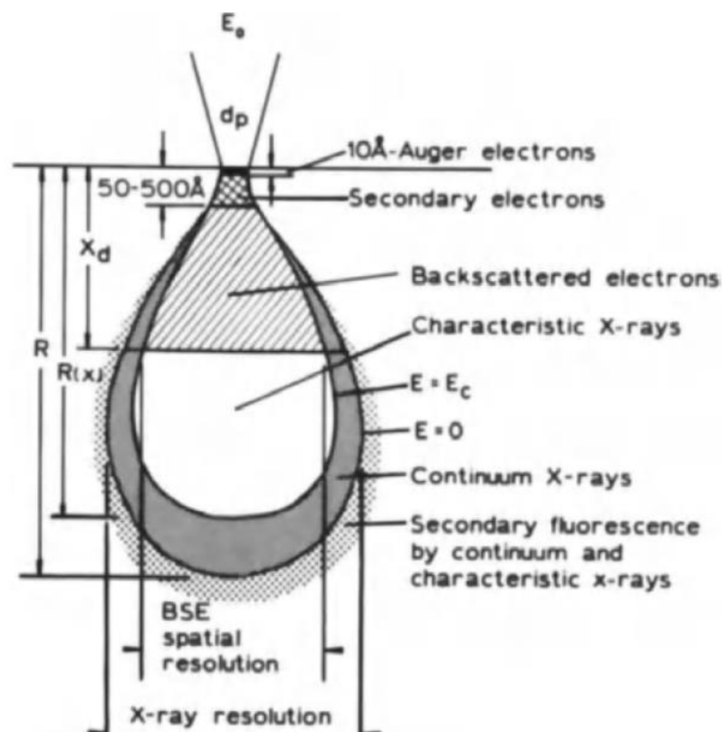

Figure 2-8- Signals resulting from the beam-sample interaction (Goldstein *et al.*, 1977, apud Goldstein , 1974).

The sample-beam interaction occurs in different ways according to the applied voltage, the chemical composition of the material and the microscope conditions. The Figure 2-9 shows these differences. The sample-beam interaction volume changes for each of the three signals: back-scattered electrons, secondary and characteristic X-rays.

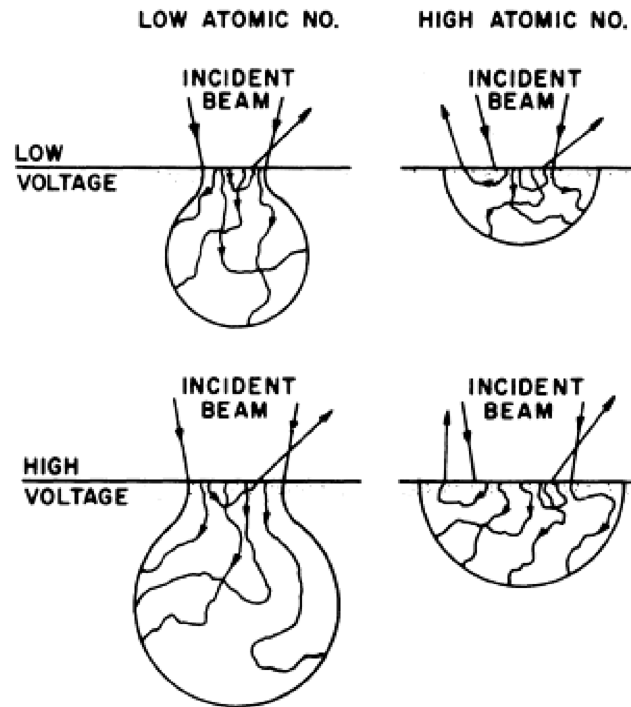

Figure 2-9- Scheme of the sample-beam interaction volume in different situations (Duncumb and Shields, 1963).

The secondary electrons (SE) are low-energy electrons (<50eV) generated from the sample's surface by inelastic collision. Its signal comes from an area with approximately the same radius of the incident electron beam (Vernon-Parry, 2000). In turn, the back-scattered electrons (BSE) are not as numerous as the SE, but are more energetic, since they are generated by elastic collisions. The incident electron beam is deflected when passing near the core of a sample, usually from its deepest region, and only some of them reach the detector. The electron image allows checking the morphology of the sample with lower resolution, since the image contrast variation is mainly related with the atomic number of the elements present in the sample. The lower the atomic number, the darker the region in the image becomes. In addition to the contrast variation due to different chemical composition, it is also possible to analyse the crystallographic orientation due to the diffraction of backscattered electrons.

Thus, although it is possible to make images with these back-scattered electrons, they do not represent truthfully the surface topography, because the generated signal is the result of an interaction that occurs within the sample, while the secondary are those generated closer to surface.

2.3.2.3 Working distance and vacuum

Although the same terminology is used for the optical and electron microscopy, there are numerous differences between the behaviour of light and electron beam. One is that electrons are much more scattered by gases than light and therefore all electron microscopes have to work under vacuum (Goodhew et al., 2000). The scattering of the electron beam is very small in high vacuum.

The distance between the end of objective lens and sample is called working distance Changing working distances affects the depth of image focus and the scattering of the electron beam (Figure 2-10). Under low vacuum smaller working distances promote less scattering of electron beam, improving resolution, but in turn leads to less focus depth (Wittke, 2008).

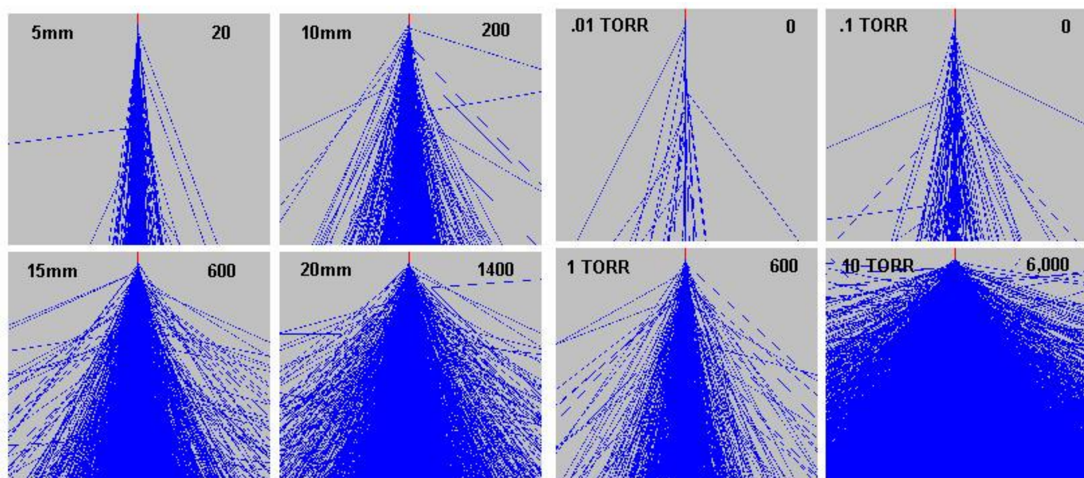

Figure 2-10- Scattering of the incident electron beam for different working distances and vacuum (Wittke, 2008).

The low-vacuum mode allows air molecules present in the chamber to remove the charge of the surface of non-conductive materials, in addition to preventing the degradation of some types of samples, such as biological samples or some minerals. But these molecules also interfere with the incident electron beam scattering it. The effect is so intense that the working distances need to be, in general, smaller than 10nm.

2.3.2.4 Factors influencing the measurement quality

Several factors affect the quality of the image (Wittke, 2008) and size particle measurement, among them:

i. Diameter of the electron beam: the smaller the diameter of the electron beam that scans the sample, the larger will be the image resolution and depth of focus;
ii. Accelerating voltage: the diameter of the electron beam decreases with the increase of accelerating voltage, thus increasing resolution. However, there are some side effects such as sample degrading and charging, reduction of surface detail since the beam penetrates more.
iii. Objective aperture: The smaller the objective aperture, the smaller the diameter of the electron beam, but this also reduces the amount of electrons arriving in the sample, increasing the signal/noise ratio.
iv. Working distance: as mentioned above, this is directly connected to the vacuum inside the machine. For short distances less scattering is observed, but also less focus depth.
v. Astigmatism: occurs more sharply in magnifications over 5000 times, which is not enough for nanoparticle measurements, and should be corrected to improve the resolution of images.
vi. Brightness and contrast: influence the quality of the image, but it is a difficult parameter to assess as it varies according to the user/operator (Figure 2-11).

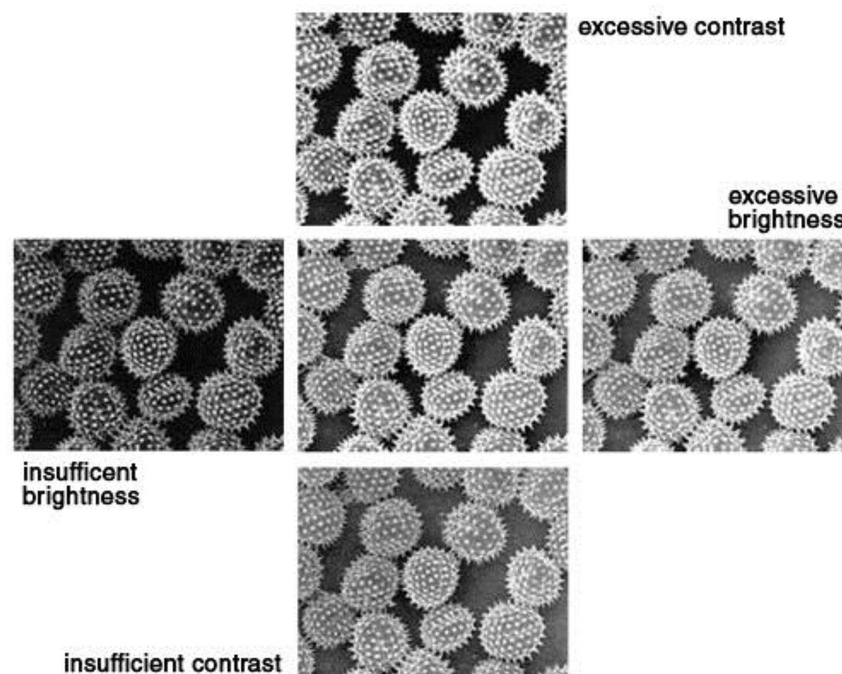

Figure 2-11- Optimum brightness and contrast (Wittke, 2008).

vii. Sample charging: recurring problem in non-conductive samples. One can minimize it by depositing a layer of conductive material thereon, which however may compromise the surface roughness and size measurement. Other alternatives are to reduce the accelerating voltage or the use of low vacuum, considering the effects that such changes may cause.
viii. Sample preparation: the sample preparation should guarantee that it is

representative of the whole material (as in any analysis) and is not trivial to determine representative shape, number of particles, size, and size distribution from the bulk sample in a small volume analysed (Kim *et al.*, 2014; Merkus, 2009). Also it may facilitate particle size measurement by a well dispersed deposition of the particles.

The peculiarities of the samples may not allow the use of the best analyses conditions. High accelerating voltage beam may cause the degradation of the sample or the high vacuum may imply in increasing sample charge. In summary, each situation should be evaluated, regarding the detrimental effects caused by selected analysis condition.

2.3.3 Atomic force microscopy (AFM)

The invention of the atomic force microscope has contributed significantly to nanotechnology and received the Nobel Prize in 1986 (Taboga, 2001). The AFM uses tip-sample interaction to draw a "map" of the sample. A stem called cantilever supports a needle called tip. While the tip scroll through the sample, the rod deflects according to the interaction tip-sample. A mirror behind the tip is illuminated by a laser and traces the profile of the sample in a photodiode as shown in Figure 2-12.

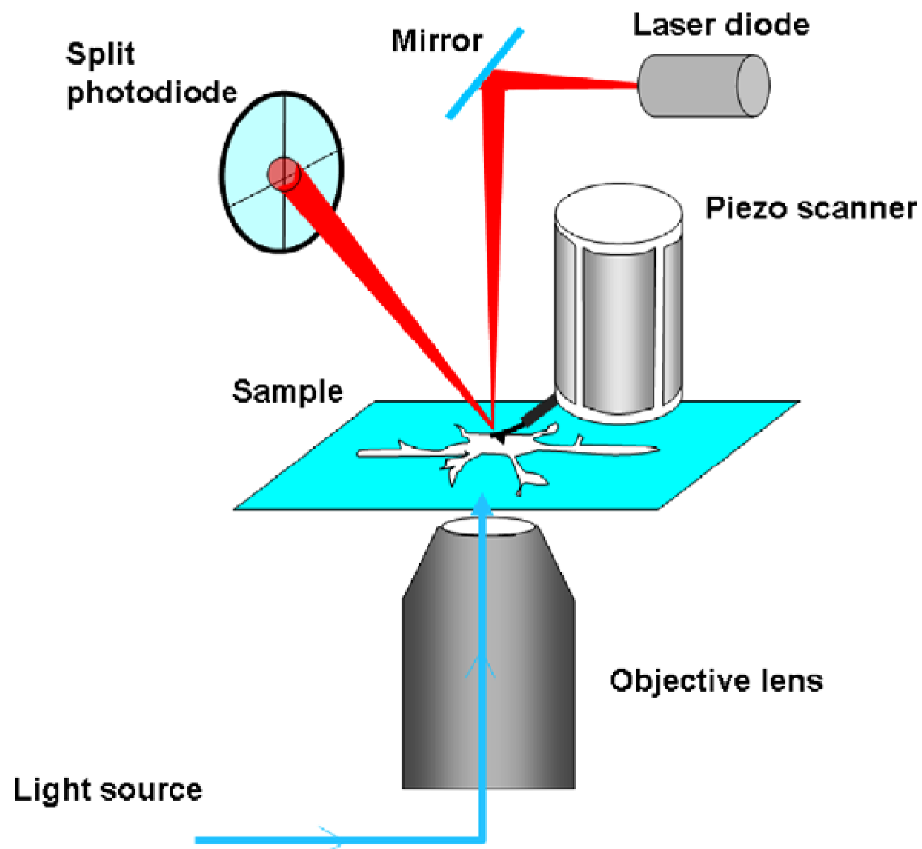

Figure 2-12- Function diagram of an AFM (Alessandrini and Paolo, 2005).

The type of interaction tip - sample reflects the equipment operation mode. There are three modes of image acquisition: non-contact mode, contact mode and tapping mode. In non- contact mode the cantilever vibrates at the natural resonant frequency or near to it, slightly away from the surface. Mounting the cantilever over a piezoelectric ceramic and measuring the deviation from natural frequency due to the attraction with the sample, topographical information can be extracted (Basso et al., 1998). In the contact mode this information is obtained by monitoring the interaction forces while the probe keeps in contact with the sample (Fung and Huang, 2001). The tapping mode combines the qualities of both modes, the cantilever oscillate in natural resonance frequency and the tip touch the sample for a minimum period of time, as shown in the Figure 2-13 (Salapaka e Chen, 1998). Depending on the distance between the tip and sample the AFM can operate in the attraction or repulsion mode (Figure 2-14).

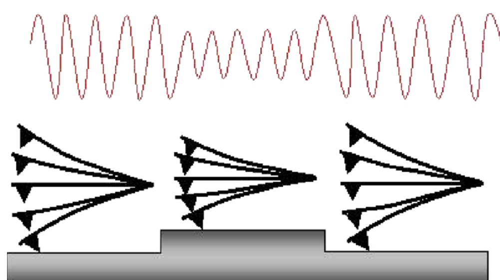

Figure 2-13- Tapping mode AFM (Alessandrini and Paolo, 2005).

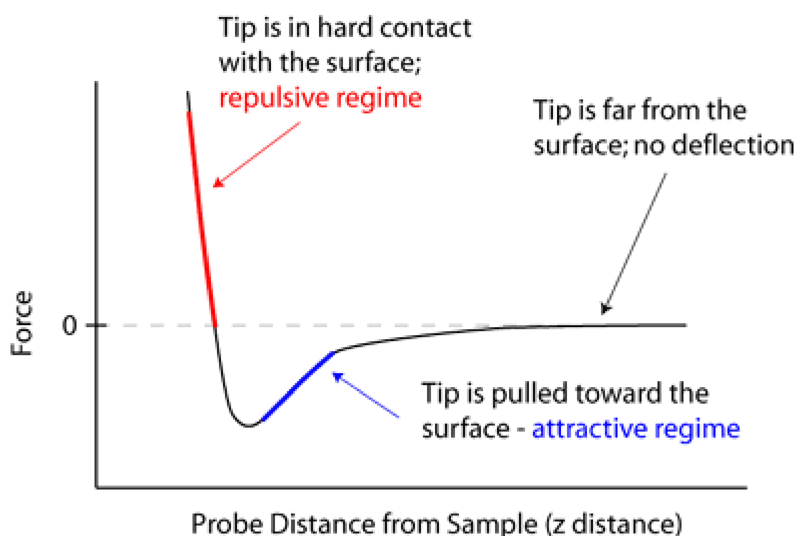

Figure 2-14- Operating regime of the AFM (Nanoscience, 2011).

In summary, when the tip approaches the sample it is first attracted by the surface due to a wide range of attractive forces existing in the region, such as van der Waals

forces. This attraction increases until the tip gets very close to the sample, both atoms are so close that their electronic orbitals begin to repel. This repelling electrostatic attractive force weakens as the distance decreases. The force vanishes when the distance between atoms is about a few angstroms (the characteristic distance a chemical bonding). When the forces become positive, we can say that the atoms of the tip and the sample are in contact and the repulsive forces dominate.

2.3.3.1 Factors influencing the measurement quality

AFM is a very versatile microscope. It can be used to measure samples at ambient pressure, dry or in a liquid medium (Alessandrini and Paolo, 2005) and achieve high resolutions on the Z-axis reaching 1 angstrom at ideal conditions (Li, 2007). However, the measurement is susceptible to a number of interferences.

i. Modes of operation: Each mode of operation has advantages and disadvantages. The atomic resolution, for example, is obtained when the probe operates in contact mode (Mannheimer, 2002). The use of non-contact or tapping mode implies on the increase of tip convolution. One drawback regarding the contact mode is the ability to drag the sample fragments of this displacement, deteriorating sample and creating artifacts in the image (Alessandrini and Paolo, 2005). Furthermore, the non-contact scan mode is subject to interference by moisture Figure 2-15.

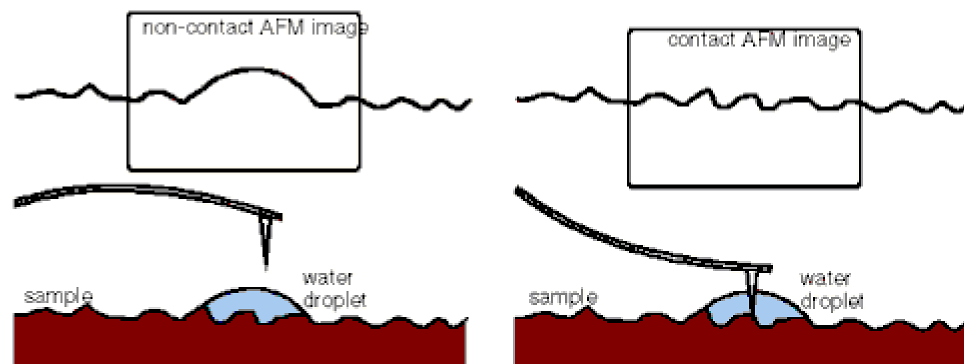

Figure 2-15- AFM contact and non-contact mode (SSP, 2003).

ii. Cantilever and Tip: this set is the heart of AFM. There are several types. Some specially treated to measure a specific interaction, such as coated with magnetic material to measure the magnetic force. The selection of tip and cantilever should be also in accordance with the mode of operation used. The AFM mode of operation in which the cantilever does not have to vibrate should use a cantilever as soft as possible to deflect with minimal change in tip-sample interaction. While using vibration modes, the cantilever should be harder and thus reduce noise (Alessandrini and Paolo, 2005). Besides the composition and hardness of the cantilever, the tip may have different formats. The conical and

the triangular may have different results if the particle has reduced dimensions. Figure 2-16 shows an example of artifact due to the tip shape. The distance of tip to the sample also influences the results, biggest distances enable the appearance of artefacts.

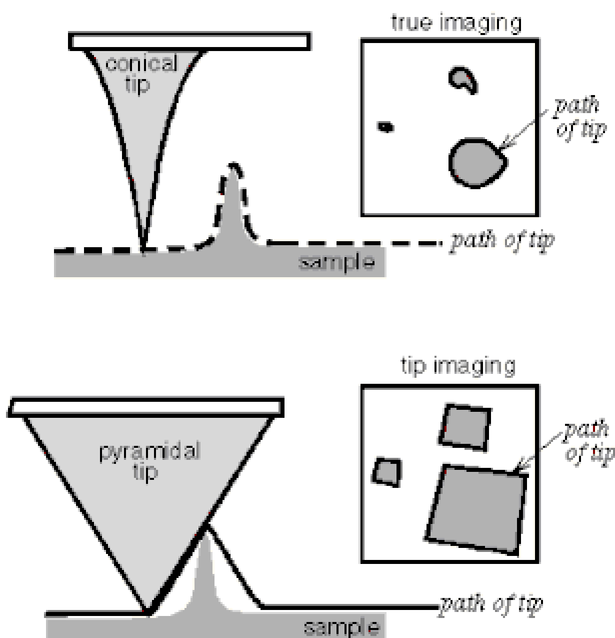

Figure 2-16- Formation of artifacts in the image of AFM (SSP, 2003).

iii. Imaging: Every particle size measured by image carries uncertainties related to the imaging program that will perform these measures and the method chosen to do so. In the AFM images there is an issue that should be evaluated: the image processing before the measurement that aims to correct own mistakes measurement by AFM. Artifacts are common at raw images and the software for imaging and data processing are essential to treat these images before particle size measurements. Each program has its own method in a way that the selection of the software may also influence the final results.

iv. Sample preparation: The sample preparation should provide satisfactory deposition density and minimize aggregate formation (Grobelny *et al.,* 2009). The nature of the substrate is one variable to be considered since nanoparticle samples need to be well dispersed on flat surfaces for AFM measurements. Some substrates require a change of the substrate surface by adequate functionalization (Dubrovin, 2012).

2.3.4 Dinamic light scattering (DLS)

The particle size measurements by the dynamic light scattering technique consists in measuring the Brownian motion of particles in a suspension and relate this to the size of the particle. For this purpose, the particles in suspension are illuminated with a laser and the intensity fluctuation is analyzed by the scattered light (Figure 2-17). The random changes in the intensity of light scattered can be interpreted using an

autocorrelation function (Horiba, 2014). The diffusion coefficient is proportional to the lifetime of the exponential decay. It can be calculated by fitting the correlation curve to an exponential function and from that the hydrodynamic diameter can be calculated by using the Stokes-Einstein equation (Malvern, 2011).

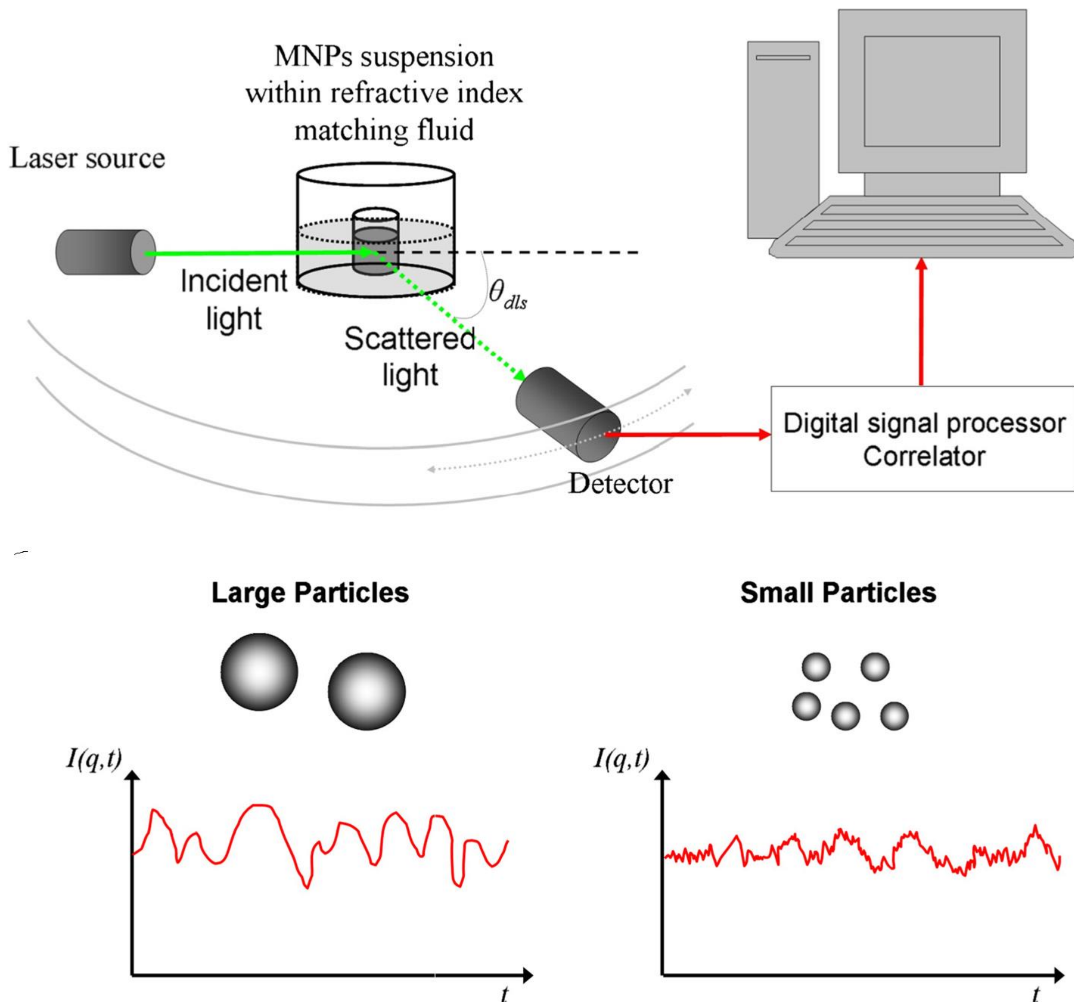

Figure 2-17- Hypothetical DLS of two samples, one with larger particles, other minor (Lim *et al.,* 2013)

The DLS analysis provides particle size distribution, and from these data it is possible to calculate the average hydrodynamic diameter of the particle. When calculated from the intensity distribution it is usually called Z-average. There are three types of distributions: intensity, volume and number. A description of the differences between these three distributions can be made by considering a sample containing particle sizes with 5nm and 50nm and having the same quantity of particles for each size. The distribution graphics for this sample are shown in Figure 2-18.

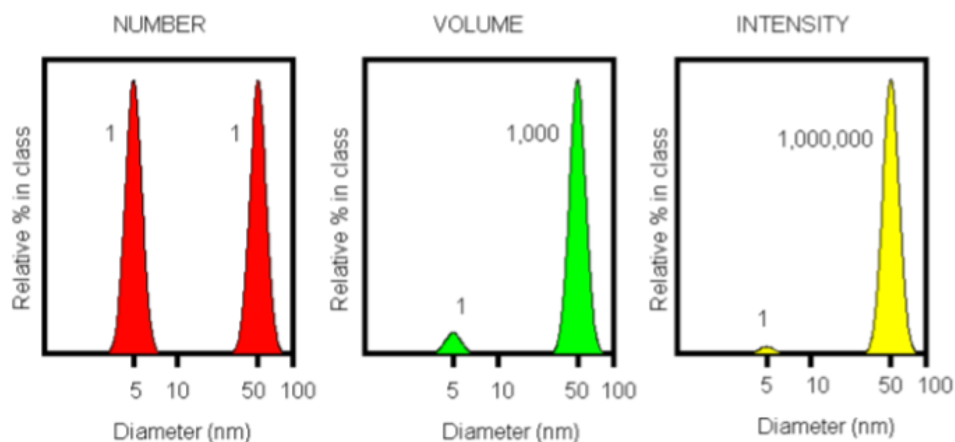

Figure 2-18- Particle size distribution by number, volume and intensity for a hypothetical sample with 50% of the particles with 5nm and the remainder with 50nm (Malvern, 2003).

The distribution by number shows two peaks with the same intensity of 1:1 for each size since there are an equal number of particles. The distribution by volume shows that the peak for the larger particles (50 nm) is 1000 times larger than the peak for the smaller particles, since the radius is 10 times bigger and the volume of a sphere is given by $4 / 3\pi r^3$. The distribution by intensity is strongly dependent on the presence of large particles and agglomerates, since the scattering intensity is proportional to the square of the particle volume (i. e., the radius to the sixth power). Thus, the particle size distribution graph shows that the peak for the 50nm particles has intensity 1,000,000 times greater than the peak of 5nm (Instruments, 2003).

Each type of distribution has an application. The distribution by volume, for example, has major practical advantages in formulations containing nanoparticles, since the volume may be related to the mass by the density, and this is a readily measurable quantity. For purposes of comparison between different microscope techniques, such as this study, the distribution of numbers is the most appropriate, because there will be a particle counting as well as in other techniques. The distribution obtained from the DLS measurement is based on intensity, and it is important to analyse its raw data (Horiba, 2014). In general, the technique of DLS gives good results for monodisperse samples. If the intensity distribution graph shows a substantial tail, or more than one peak, it is important to convert it to the volume distribution to provide a more realistic view of particles distribution of the sample, since the intensity distribution will increase the contribution of the larger particles (Figure 2-18). The polydispersity index indicates the width of the distribution, and so, it will suggest if the particles are monodisperse. Because of this, polydispersity index is used to indicate the measurement reliability. It should be less than 0.5, preferably less than 0.1.

2.3.4.1 Factors that influence the measurement quality

Analysis by this technique is very fast and simple to perform, in part because much of the method is automated. However there are numerous variables that can alter quality

measure (Microtrac, 2010):

i. Fluid temperature: could affect the results since the measure is based on the Brownian motion and this is influenced by temperature. Both the fluid analysis and the solvent must be used for background at the same temperature.
ii. Solvent Viscosity: this needs to be reported correctly to the software because the machine uses this information to calculate the temperature of the analysis cell. The viscosity should be preferably between 0.3 and 3CP. High viscosities imply loss of speed and hence, lower frequency signals. The equipment detection limit is determined by viscosity. In samples 1cp the equipment detection limit is 6.400nm, while for samples with 10cP the detection limit is 640nm. A practical advice is to keep the product Viscosity (cP) X particle size (microns) between 0.0008 and 6.54.
iii. Acquisition time: it may vary with the particle size or viscosity. The higher the viscosity the higher should be the measurement time, since high viscosities reduce the particle velocity and so low frequency signals are generated which require a greater acquisition time. A good estimate of the time is to multiply the value of the particle size by the viscosity of the sample. The smaller the particles, the lesser time required to measure, as shown in Table 2.2

Table 2.2- Running time variation in function of particle size

Particle Size Range (nm)	Minimal running time (s)
<60	30
60-300	90
300-900	120
>900	80

iv. Refractive index: The particles are only visible to the equipment if their refractive index is different from the carrier liquid. In systems in which these values are close, the scattered energy is very low as the signal intensity. The refractive index is also used to convert intensity distribution to volume or number distributions.
v. Sample concentration: Very low concentrations are susceptible to errors influenced by environmental changes or minimal contamination. Having excessive concentrations may favor the interaction between particles generating false results or creating optical artifacts responsible for the generation of so-called "ghost peaks". The ideal concentration may vary depending on the sample.

2.3.5 Digital image

The images obtained from electronic and atomic force microscopes are digital, monochromatic, indirectly obtained images (Gonzalez and Woods, 2008). In electronic

microscopes for example, the electrons coming from the sample are captured by specific detectors, transformed into electrical pulses and converted to images (Barbosa, 2012). The images may be defined as a function of the spatial coordinates x, y, where the value of f(x,y) is given by the intensity or grey level. The digital image is one whose values of x, y and f are finite and discrete (Gonzalez and Woods, 2008).

A digital image may be represented by a set of elements called pixel. Each pixel is stored and the whole set forms a bitmap, whose mapping is used to reproduce the image digitally. The quality perception of the image is influenced by spatial resolution. This resolution is determined by the number of pixels per image area or the size of the pixel in the image. The more pixels an image has (or smaller pixel size), the greater is its resolution and the better is the image quality (Thomas, 2004).

For a monochromatic image, the grey level is the tone scale, ranging from 0 (zero) for black to 255 for white (Figure 2.19). The grayscale level assigned to each pixel is called quantization. The abrupt changes in pixel values in relation to the neighbours are used by some algorithms for segmenting images and delimiting particles, for example, for counting and automated measurement (Barbosa, 2012).

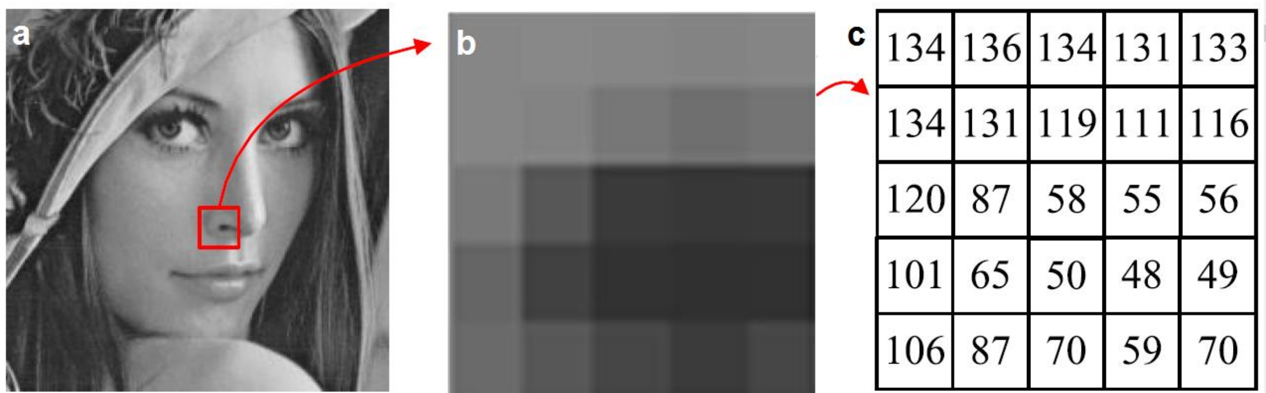

Figure 2-19: Representation of the mean value of a pixel: (a) original image, (b) region of red rectangle, (c) gray-scale value (Lien *et al.,* 2013).

3 An assessment of errors in sample preparation and data processing for nanoparticle size analyses by AFM

Accurate measurements of particle size, which are essential for a better understanding of nanoparticle properties, are often influenced by sample preparation and image data treatment. In this work, we discuss the errors associated with different methods of sample preparation and data treatment in AFM size measurements using polystyrene nanoparticles with sizes of (102 ± 3)nm on silicon and mica substrates. Silicon has the advantage over mica of being conductive. The dilution of the polymeric nanoparticle suspension was sufficient to achieve good dispersion on the mica substrate, but not on silicon. Sample preparation on silicon was significantly improved by treating the substrate with glow discharge. The addition of a dispersant can cause errors of approximately 20% if the height of the coating that is formed is not considered in the particle size measurement. Both the software for data treatment and the type of flattening procedure were shown to influence the particle size measurement. Particle size has been significantly influenced by data treatment and the type of flattening procedure. No meaningful effect of the interpolation method on the measurements of the average particle size was observed under the experimental conditions, but the variance was affected. The results also demonstrated that image size and pixel size should be carefully selected to obtain an accurate measurement in a short period of time. The results were compared using Student's t-test at a 99% confidence level.

3.1 Introduction

Nanoparticles have unique properties that are directly correlated to their size, shape and size distribution, making it important to be able to measure these features outside and inside of suspensions a (Cadene *et al.*, 2005; Hoo *et al.*, 2008). Scanning probe microscopy (SPM), especially with atomic resolution capability, is a tool that provides reliable measurements at the nanometre scale (Jalili and Laxminarayana, 2004). AFM (atomic force microscopy) has been broadly applied for morphological analyses, mainly in the measurement of particle size. Several aspects influence the ability of these methods to produce accurate results, such as sample preparation, type of substrate, resolution, software used, operation mode of the instrument, measurement (Hristu *et al.*, 2012), cantilever, tip and tip-sample interaction(Yacoot and Koenders, 2008), pixel size and scan speed (Klapetek *et al.*, 2013; Dufrêne, 2002).

The sample preparation should provide a satisfactory deposition density and minimize aggregate formation (Grobelny *et al.*, 2009). The nature of the substrate is one variable to be considered because nanoparticle samples must be well dispersed on flat surfaces for AFM measurements. The surface roughness should be much smaller than the nominal size of the nanoparticles to provide a consistent baseline for size measurements. The nature of the substrate also influences the number of the nanoparticles and their distribution over the substrate surface. For some materials (e.g., TiO_2), the adhesion of the nanoparticles to the substrate decreases with increasing surface hydrophobicity (Rao *et al.*, 2007).

Mica and silicon are accepted as good substrates for AFM analyses (Grobelny *et al.*, 2009). Mica refers to a group of *minerals* having almost perfect basal cleavage, which are therefore called phyllosilicate or sheet minerals. In addition to a flat surface, silicon has the advantage of being conductive, which allows the same substrate to be used in electric force microscopy (EFM) and in other microscopy analyses, such as scanning electron microscopy. Aqueous samples commonly agglomerate on the silicon, requiring the substrate's surface to be modified by adequate functionalisation (Dubrovin *et al.*, 2012).

The software for imaging and data processing is also essential for SPM analysis. Artefacts are common, and the software helps to address them. Samples that are not fixed perfectly perpendicular to the AFM tip generate tilt that is not actually present on the sample's surface. Other sources of artefacts include thermal drift and non-linearity in the scanner. The flattening technique, present in all programs, corrects these non-idealities by fitting each scan line with a polynomial and subtracting it from the data (Grobelny *et al.*, 2009). Each program has its own methods; thus, the selection of software may also influence the final results. It was used the free software Gwyddion and the software Asylum MFP-3D developed by Asylum.

Resolution is another important feature in microscopic analyses that strongly influences particle size measurements. Because 3D images are obtained by AFM, two types of resolution must be taken into account: lateral and vertical resolutions (García and Pérez, 2002). AFM has an excellent resolution on the Z-axis that reaches one angstrom under ideal conditions (Li, 2007) and is limited by both the noise from the detection system and the thermal fluctuation of the cantilever (García and Pérez, 2002). It is known that measurements in X and Y axes, common in other microscopy analyses, cause errors due to artefacts related to the tip size, shape and interactions with the sample (i.e., tip convolution) (Ukraintsev *et al.*, 2012). The in-plane or lateral resolution has long been recognized to be crucial because of the non-vanishing size of the probe; thus, a convolution of the tip shape on the sample topography is expected at large magnifications. This phenomenon corrupts the resolution or the possibility of distinguishing two points far apart from each other (Tranchida *et al.*, 2006). The general lateral resolution is also difficult to define due to the pixel size, tip-surface Sepäration, tip-surface force and sample compliance (García and Pérez, 2002).

AFM provides an image resolution of several nanometres or even atomic resolution (Linkov *et al.*, 2013) depending on variables, including the scan speed. The resolution is also determined by the scan size (once images are collected with a fixed pixel number); decreasing the number of image pixels reduces the resolution (Tranchida *et al.*, 2006). As no result can have a smaller error than the raw image, the image resolution is the limiting factor. For example, in acquiring a 10μm × 10μm image with 512 pixels, the pixel size is 19.5nm. In this case, it is not possible to resolve features smaller than 19.5nm, making it important to consider the particle size when choosing the scan size.

As full images are typically a few hundred pixels in width and height and because AFM

data are coarsely sampled compared to measured details, when a line is drawn to extract a profile, there is a high probability of not crossing the pixel centres. Some software gives the closest value by interpolating neighbouring points. The interpolation method (e.g., round or key interpolation) can be critical for proper quantitative analysis of data properties (Klapetek *et al.*, 2009).

The present work intends to contribute to more accurate measurements of particle size by AFM. To better understand and quantify the errors associated with AFM measurements, a certified material with a particle size of (102 ± 3)nm was analysed under different preparation conditions using mica and silicon substrates as supports. Dilution of the suspension, addition of a dispersant and modification of the substrate surface by glow discharge were investigated. The influence of software (Gwyddion and Asylum MFP-3D) and parameters for data treatment on image resolution, such as the flattening technique, were also studied. The importance of resolution and image size for accurate results was also evaluated. The statistical significance of the results was evaluated by Student's t-test at a 99% confidence level.

3.2 Materials and methods

A standard reference material (SRM) traceable to NIST (National Institute of Standards and Technology) was obtained from Microtrac Instruments. The SRM consists of a 0.1% (v/v) aqueous suspension of polystyrene spherical nanoparticles with diameters of (102 ± 3)nm diameter (5.2nm standard deviation). This colloidal suspension was dropped onto substrates (silicon or mica) followed by drying for 24h at 25°C, as described by Dubes and co-workers (Dubes *et al.*, 2003). Single-crystal silicon and mica (V-1 quality) from Electron Microscopy Sciences were used as substrates to minimize the effect of surface roughness on the nanoparticle measurements, as recommended by the NIST Protocol (Grobelny *et al.,* 2009). The silicon substrates were cleaned by ultrasound for 10 min in a glass container with ethanol and then dried by blowing air. The mica substrates were freshly cleaved before use (Grobelny *et al.,* 2009).

Table 3.1 summarizes the experimental conditions. The stock solution was analysed without any further preparation over a silicon wafer (sample SRM-S). All of the other samples were prepared by a dilution of the stock solution with deionized water to 2 x 10^{-3}% (v/v). The diluted stock solution was then dropped onto silicon (SRM-SW), mica (SRM-M) and silicon modified by glow discharge (SRM-SG) under 9mA, 0.2 mTorr vacuum and ionized argon gas for 30s in a Baltec Med020. One further sample was prepared by dropping the diluted stock solution with 2% (w/w) dispersant (disperByk 348) (SRM-SD) onto a silicon wafer. All of the samples were analysed by AFM and scanning electron microscopy (SEM). Triplicate samples were made for each sample preparation.

Table 3.1: Experimental conditions employed and their acronyms

Sample	Preparation	Substrate
SRM-S	SRM undiluted	Silicon wafer
SRM-SW	SRM diluted 50x in deionized water	Silicon wafer
SRM-M	SRM diluted 50x in deionized water	Muscovite mica
SRM-SG	SRM diluted 50x in deionized water	Silicon wafer treated with glow discharge
SRM-SD	SRM with 2% diperByk 348 in 50x dilution in ionized water	Silicon wafer

AFM analyses were performed on an Asylum Research MFP-3D atomic force microscope in tapping mode to avoid damaging the particle surfaces or to carry them on. An Olympus AC160TS cantilever composed of Si with a nominal resonance frequency approximately 300kHz, a force constant of 42N/m and a tetrahedral tip with a radius of 7nm was used. SEM analyses were carried out using an FEG scanning electron microscope (Quanta 200 FEI) at an accelerating voltage of 15kV under high vacuum. All analyses were performed at Microscopy Center of Federal University of Minas Gerais.

Two different software programs were employed for scanning probe microscopy data analyses for the particle size measurement and image processing: Gwyddion 2.3.1 developed by Czech Metrology (Nečas and Klapetek, 2012); and Asylum MFP-3D software developed by Asylum on the Igor Pro 6.22 platform. All of the results obtained were evaluated for statistical significance against the certified value using one-sample Student's t-test, while paired-sample Student's t-test was employed for the comparison between methods. The statistical significance level was set at $p \leq 0.01$ with the help of the free R Software (R Core Team, 2014).

3.3 Results and discussion

3.3.1 Sample Preparation

3.3.1.1 SRM nanoparticle dilution:

Initially, undiluted and diluted samples (SRM-S and SRM-SW, respectively) were deposited on freshly cleaned Si substrates, as shown in Figure 3-1. Despite the reduction of the nanoparticles by increasing the dilution, agglomeration was still observed. The higher-resolution versions Figure 3-1b and d) show that the particles are clustered and attached to each other in both cases, which makes the measurement of individual particle size difficult and imprecise. Therefore, sample preparation should ensure lesser agglomeration and good particle distribution on the substrate. The sample agglomeration may be related to the drying process or to an inefficient spreading of particles over the surface, both of which are related to interfacial tension phenomena. The SEM image on similar regions (Figure 3-2) provides more details on the agglomeration pattern of the diluted sample on the silicon substrate.

Heterogeneous particle scattering on the substrate is evident; agglomeration is observed even at a lower population density (e.g., in peripheral areas). In conclusion, a 50x dilution of SRM-S nanoparticles in water did not significantly improve the sample preparation on the silicon substrate, which is likely related to the high interfacial tension and the electrical nature of the silicon-water system. This behaviour is specific to the silicon substrate because a good dispersion was obtained with the mica substrate, as will be shown further. In view of these results, an attempt to modify the silicon substrate was examined.

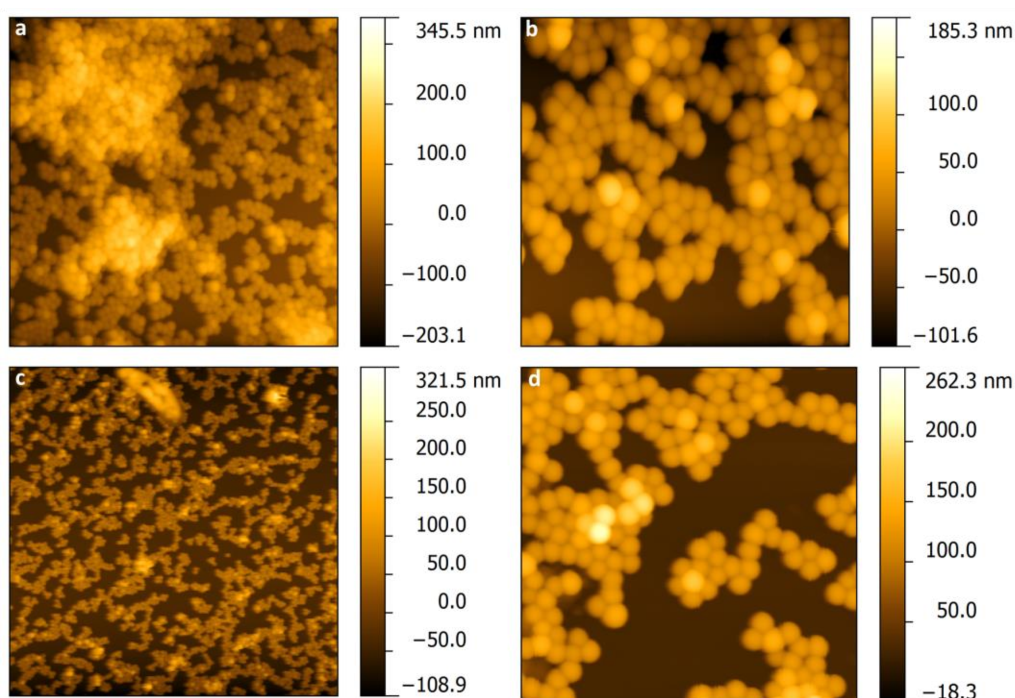

Figure 3-1- AFM images of (a and b) SRM-S and (c and d) SRM-SW. Images acquired at 10 x 10 µm and 2 x 2 µm.

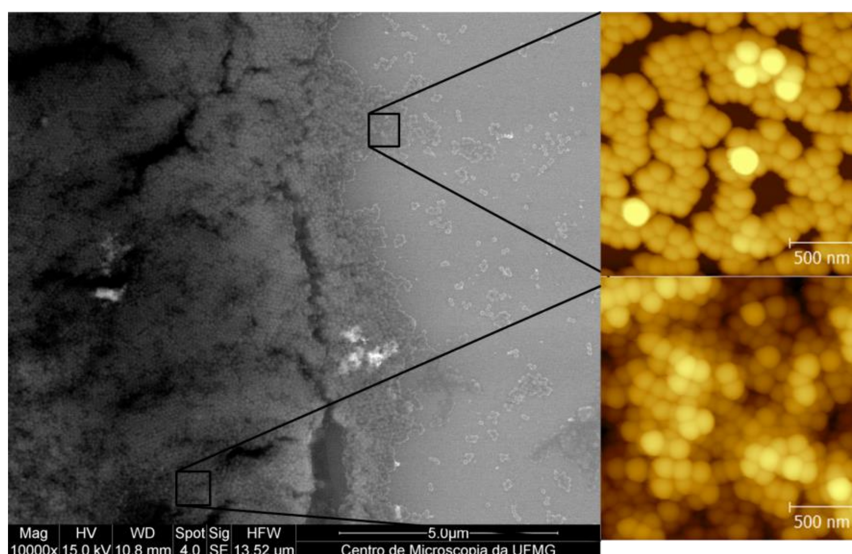

Figure 3-2- SEM image of sample SRM-SW and AFM microscopy images of similar highlighted regions.

3.3.1.2 Effect of the substrate surface:

Figure 3-3 compares the particle dispersions on silicon, silicon treated with glow discharge and mica. The typical agglomeration observed on the untreated silicon substrate is illustrated in **Figure 3-3**Figure 3-3 a. The dispersion and the quality of the prepared sample (Figure 3-3 b) were significantly improved by treating the silicon with glow discharge. Homogeneous particle distribution was observed throughout the silicon substrate. The quality of the prepared sample in Figure 3-3 b is similar to that obtained with mica (Figure 3-3 c). One may assume that the negatively charged mica surface (Liberelle et al., 2008) improves the polymeric nanoparticle-substrate interactions and prevents particle agglomeration during the drying process.

Glow discharge, a plasma medium consisting of positive and negative charges and several neutral species, is used for the heat sputtering, etching, nitriding and ionization of surfaces (Chiad et al., 2010). This surface treatment is used to treat several types of materials; for instance, in carbon-coated grids for TEM analysis, this treatment enhances the adhesion of some samples to the grids (Böttcher et al., 2005). Our results showed that glow discharge significantly improved the sample preparation on the silicon substrate (Figure 3-3 b). Two mechanisms can explain this finding. By cleaning the organic impurities generally present on surfaces exposed to ambient conditions, the glow discharge treatment increases hydrophilicity (Droz et al., 1994), which in turn favours the spreading of the aqueous suspension. The other mechanism involves the creation of charged centres at the silicon wafer surface (Norstrom et al., 1978) via the bombardment of a wide variety of species existing in the glow discharge. These species include radicals, excited species and various fractured gas molecules created by collisions between electrons and gas molecules or atoms (Chiad et al., 2010). This charge will attract the polymer particles because they are non-conductive. Therefore, glow discharge is one treatment to be considered in the preparation of samples for AFM.

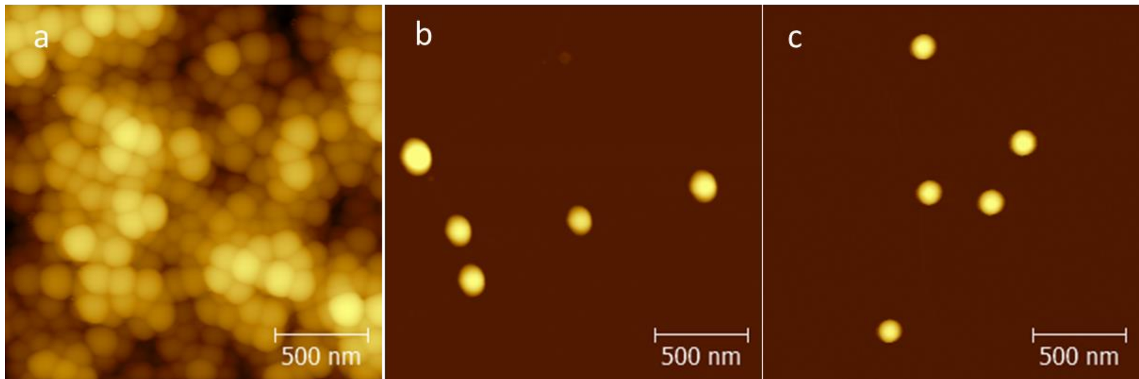

Figure 3-3- AFM images of samples (a) SRM-SW, (b) SRM-SG and (c) SRM-M.

3.3.1.3 Effect of dispersant

The SRM-SD sample on the freshly cleaned Si substrate is shown in Figure 3-4. The addition of the dispersant decreases the surface tension, keeping the nanoparticles well Sepärated after drying. However, the presence of the additive creates a shadow around the particle images that may affect the size measurement. The dispersant may interact with the AFM tip, thus hindering the measurement. The aura is even more evident in the phase contrast image of SRM-SD (Figure 3-4b) because these images typically show changes in the material composition or texture.

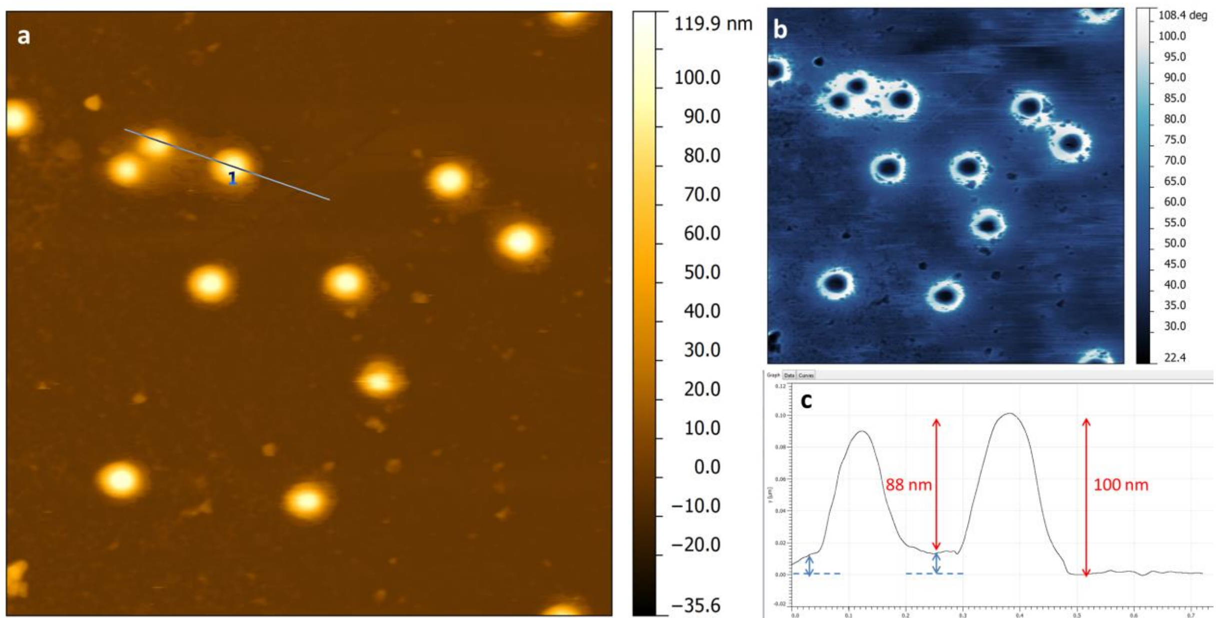

Figure 3-4- AFM images of the SRM-SD samples: (a) height and (b) phase contrast images and (c) the profile of region 1.

The aura of the dispersant was measured, and this thickness varied from 9 to 25 nm at the base of the particle (Figure 3-4 c). Therefore, if the particle size is measured from the film surface to the top of the particle, it will yield errors of approximately 20%. Particles measured in the absence of the surfactant (SRM-SG) presented particle sizes

of 100 ± 2 nm. The height of the dispersant accumulated around the particles should be considered by quantitative analysis. Otherwise, the height found from the surfactant-free substrate surface to the top of the particle 103 ± 3 nm agrees with the value expected for this sample (Table 3.2). The increase in particle height from the experiment with the dispersant was shown to be statistically irrelevant; the standard deviations in the particle sizes of both SRM-SG and SRM-SD indicate that precision does not allow the results to be differentiated. The t-test, at a 99% confidence level, confirms that the results are statistically equal (p-value = 0.13). The negligible contribution of the dispersant capping layer to the measured height has been reported by others (MacCuspie *et al.*, 2011). This finding has been ascribed to the decrease in the thickness of the dispersant as a result of solvent evaporation during drying (Tsai *et al.*, 2010).

Table 3.2- Particle size measurements of SRM-SG and SRM-SD samples

Sample	SRM-SG	SRM-SD
Average particle size (nm)	100.43	102.89
Variance	42.71	34.94
Standard deviation	6.54	5.91

Same factors affecting sample preparation were studied, as this stage is the main source of error in AFM analysis. It is well established that silicon and mica are adequate substrates for sample preparation, but some difficulties may arise depending on the nature of the sample to be analysed. Our results have shown that treatment by glow discharge significantly improved particle dispersion and adhesion on the traditional silicon substrate. Silicon has the advantage over mica of being conductive. The use of dispersant has certain restrictions because performing measurements without considering the height of the dispersant film on the substrate introduces errors of approximately 20%. In addition to sample preparation, data processing can also be a source of error in AFM particle size measurements. The main errors related to data processing are addressed in the following paragraphs, and the results obtained with two different software programs are compared.

3.3.2 Effect of Data Processing

3.3.2.1 Influence of the flattening technique:

Figure 3-5 illustrates typical errors in AFM analysis due to the scanning process. As the AFM probe scans the sample parallel to the X axis, dark regions appear. This plane distortion is very common in AFM images (Grobelny et al., 2009); thus, image treatment is required before measuring particle sizes (Klapetek et al., 2009). Usually (as described for treatments 1 and 3 below), the first step involves a line-wise flattening to remove artefacts created by the image acquisition process. In the presence of nanoparticles, the flattening procedure becomes more difficult because the software available for image treatment attempts to fit polynomials to both the substrate and the

nanoparticles instead of just fitting the substrate. To “eliminate” artefacts that can appear during the flattening process, it is necessary to exclude all nanoparticles by applying masks prior to substrate flattening; in this way, the baseline should become relatively flat over the line scan (Grobelny et al., 2009).

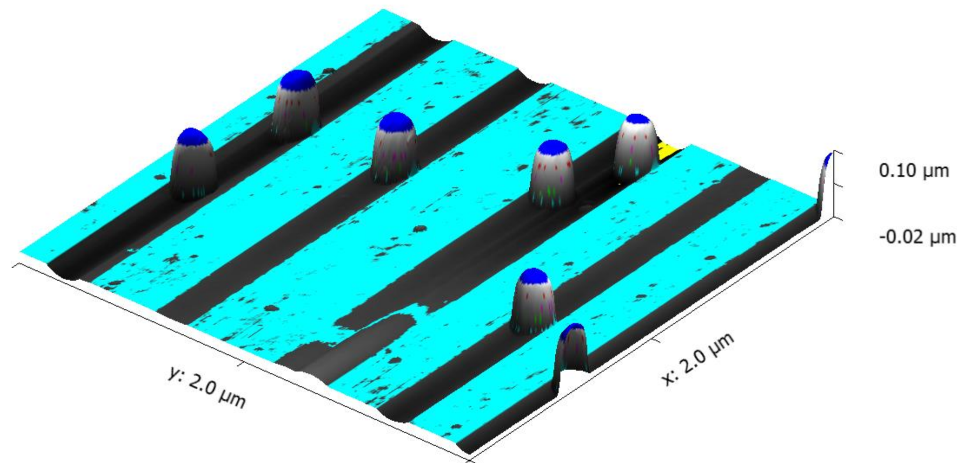

Figure 3-5- 3D image of the SRM-SG sample (original image with artefacts).

Three different treatments were applied to the original image to test the elimination of artefacts (Figure 3-6). In treatment 1, a mask was applied to the nanoparticles followed by surface flattening using a first-order polynomial. This treatment was tested with two types of software (Gwyddion and Asylum MFP-3D) using the same fixed height as a threshold value for the masks. Treatment 2 (Gwyddion software) involved the application of the Revolve Arc function, which revolves a virtual “arc” of a given radius horizontally or vertically over (or under) the data. The envelope of this arc is treated as a background, which allows the removal of features larger than the arc radius (approximately) (Klapetek *et al.*, 2009). Treatment 3 (Magic Flatten in Asylum MFP-3D) performs sequential flattening with zero- and first-order polynomials. After treatment, the particle sizes were determined according to the usual procedure, which involves drawing a line to the top of the highest part of the particle and then extracting the vertical profile along that line. The average baseline height was subtracted from the peak height to obtain the nanoparticle height. The results are presented in Table 3.3 .

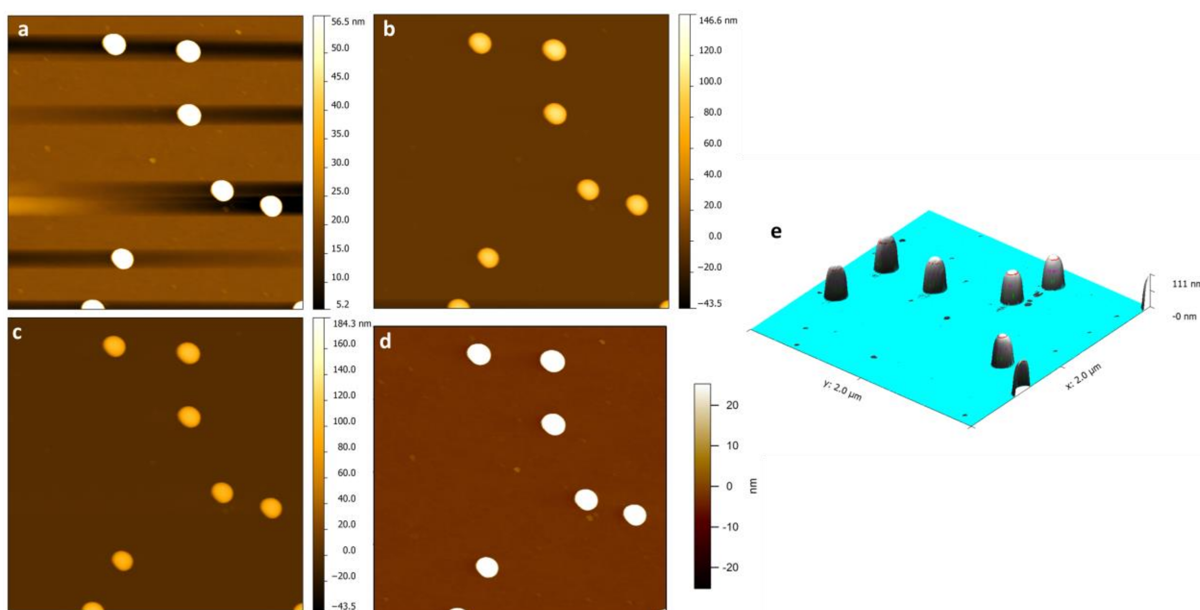

Figure 3-6- Height retrace images of the SRM-SG sample: (a) 2-D original with artefacts; (b) 2-D after treatment 1 with Gwyddion; (c) 2-D after treatment 2 with Gwyddion, (d) 2-D after treatment 3 by Asylum MFP-3D; and (e) 3-D after treatment 2 with Gwyddion.

Table 3.3- Height measurements (SRM-SG sample) without and with treatments by Gwyddion and Asylum MFP-3D software

	No treatment	Treatment 1		Treatment 2	Treatment 3
Software	Gwyddion	Gwyddion	Asylum MFP-3D	Gwyddion	Asylum MFP-3D
Average particle size (nm)	94.69	99.10	101.3	101.43	101.3
Variance	68.21	65.95	36.68	42.71	36.56
Standard deviation	8.26	8.12	6.06	6.53	6.05

The mean particle diameter according to the supplier is 102 ± 3 nm. The particle size measured without image treatment was 95 ± 2 nm. This value rejects the null hypothesis of the t-test at the 99% significance level, demonstrating the need for image treatment. All treatments provided values close to the certified SRM value. However, the mean particle size determined using Gwyddion after treatment 1 (99 ± 2 nm) is significantly different than the certified value. Conversely, when treatment 1 is applied to the same images and particles using Asylum MFP-3D, the result (101 ± 2 nm) is statistically equal to the certified value (p-value > 0.01). This conclusion also applies to the value measured by Asylum MFP-3D for treatment 3. For the treatments with Gwyddion, while a significant difference was observed with treatment 1 (99 ± 2 nm),

the result from treatment 2 (101 ± 2 nm) agreed with the certified value and was statistically equal to both values measured by Asylum MFP-3D . This shows that the software selected for data treatment and the type of flattening procedure may influence the particle size measurement.

To evaluate the magnitude of the error caused by tip convolution, a measurement of the full width at half maximum (FWHM) was also performed to simulate an X,Y axis measurement (Figure 3-7), and the results were compared to the height measurement (Table 3.4).

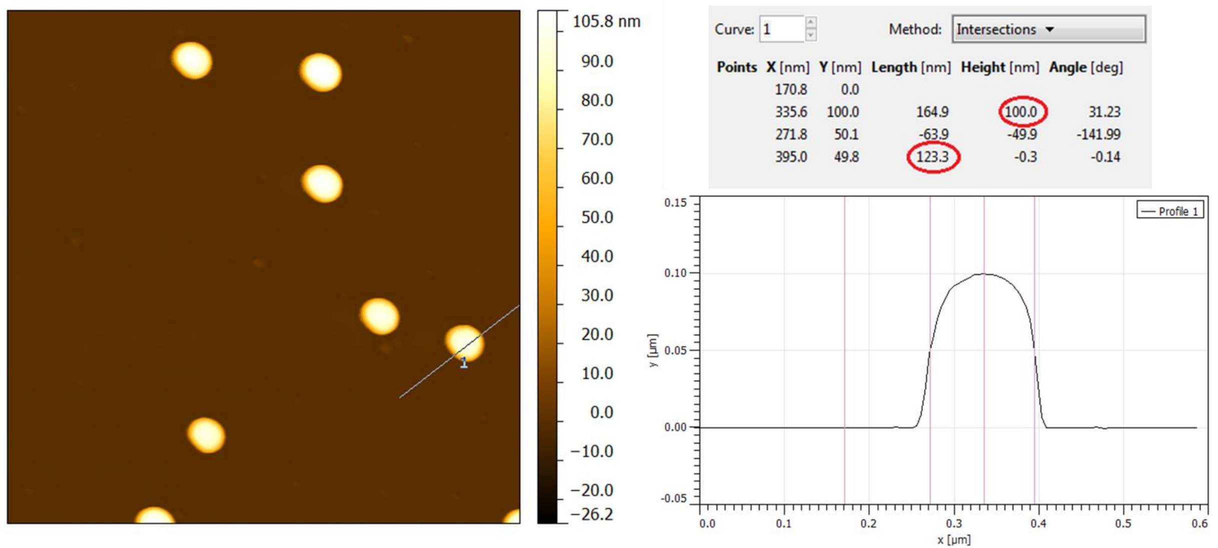

Figure 3-7- Profile, height and length measurements of sample SRM-SG with treatment 2 using Gwyddion.

Table 3.4- Measurements of height and FWHM of sample SRM-SG with treatment 2 using Gwyddion and with treatment 3 using Asylum MFP-3D

Software	Gwyddion		Asylum MFP-3D	
Measurement	Height (nm)	FWHM (nm)	Height (nm)	FWHM (nm)
Average particle size (nm)	101.51	131.75	101.2	128.05
Variance	53.13	96.35	47.47	203.92
Standard deviation	7.29	9.82	6.88	14.28

The heights measured by both software programs (102 ± 2 nm by Gwyddion and 101 ± 2 nm by Asylum MFP-3D) agreed with the certified value according to the t-test at the 99% confidence level. As expected, FWHM measurements indicated average errors of up to 30% due to tip convolution. These errors will vary depending on the tip size and shape as well as the particle size. The results shown in Table 4 indicate a significant difference between the FWHM variances obtained using Gwyddion and Asylum MFP-

3D. This suggests that the use of key interpolation by the former software program (compared to round interpolation) reduces the variance in the x-y plane measurements. The different interpolation approaches are analysed in more detail in the following paragraphs.

3.3.2.2 Influence of data interpolation methods and of pixel size

Figure 3-8 compares the round (round value of the expected position) and key interpolation calculated in Gwyddion because the MFP-3D package in Asylum MFP-3D does not offer these tools. The key interpolation takes values in the before-preceding and after-following points, as described elsewhere (Klapetek *et al.*, 2009). It is possible to improve the image quality using key interpolation as well as by smoothing the profiles used to measure particle size.

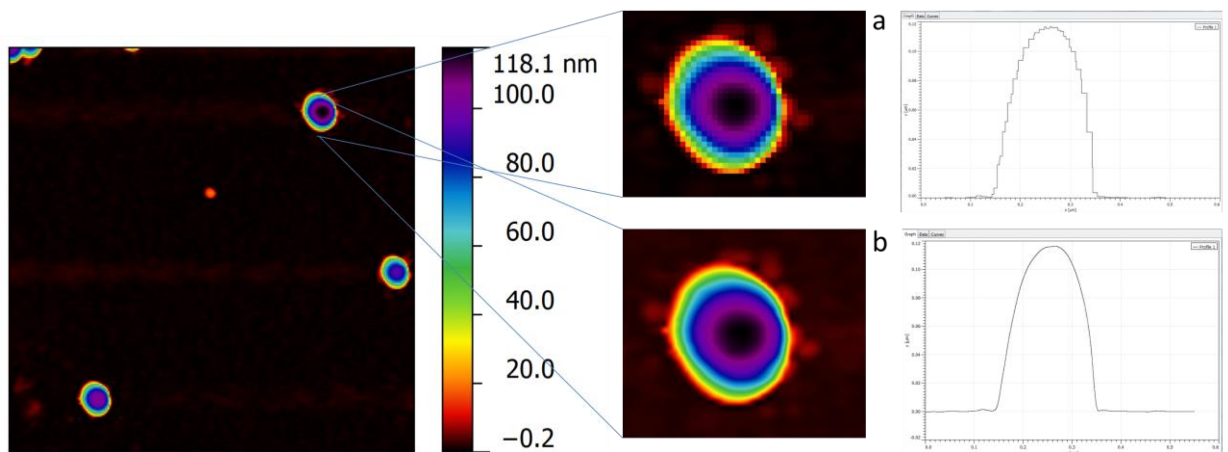

Figure 3-8- Round (a) and key (b) interpolation using Gwyddion software and their profiles from the AFM image of the SRM-SG sample.

The influence of the interpolation method on the quality of the results was evaluated with both height and FWHM measurements and two different image resolutions (Table 3.5). At the lower image resolution (10 x 10 µm), none of the measured particle sizes agreed with the certified value (t-test at the 99% confidence level), regardless of the selected interpolation method. For FWHM measurements, the particles sizes determined using round and key interpolations were 127 ± 6 nm and 128 ± 3 nm, respectively. The larger errors associated with the FWHM measurements are evident, and in this case, the variance is affected by the interpolation method, as suggested by the results shown in Table 3.4. The key interpolation led to significantly lower variance compared to round interpolation. The same effect, although smaller in magnitude, was observed at the higher resolution. It is possible that the interpolation method has a greater influence at a lower resolution, where the pixel size is bigger. For height measurements, the particles sizes determined using the round and key interpolations were 95 ± 2 nm and 98 ± 2 nm, respectively. Despite the fact that none of the values agreed with the certified value, the key interpolation reduced measurement error from 7 to 4%. It is known that the X-Y plane resolution is influenced by pixel size, explaining

the reduction in the variance of the FWHM measurements; however, the results showed that key interpolation also influences the height measurement.

At a higher resolution, the height measurements (102 ± 2 nm) agreed with the certified value, while the FWHM measurements did not. In both cases (height and FWHM), the interpolation method had no significant observable effect on the average particle size. Similarly, at a lower resolution, only a decrease in FWHM variance was observed as a result of interpolation method (highlighted in Table 3.5)

Table 3.5- Comparison of values obtained using round and key interpolation.

Image size	**2 x 2 µm (256 x 256)**				**10 x 10 µm (256 x 256)**			
Interpolation	**Round**		**Key**		**Round**		**Key**	
Measurement	Height	FWHM	Height	FWHM	Height	FWHM	Height	FWHM
Average size (nm)	101.77	131.09	101.75	132.59	94.80	126.51	97.91	128.06
Variance	44.74	**150.65**	45.02	**106.04**	36.31	**169.24**	41.75	**30.24**
Standard deviation	6.7	12.3	6.7	10.3	6.03	13.0	6.46	5.5

Table 3.6 relates the pixel size, ranging from 3.9 to 39 nm, with image size and resolution (pixel amount) for particles analysed at two resolutions and image sizes using key interpolation in Gwyddion.

Table 3.6- Particle size measurements from the height with two different resolutions and the key interpolation in Gwyddion

Image size	**2x2 µm**		**10x10 µm**	
Pixels	**256**	**512**	**256**	**512**
Pixel size (nm)	**7.8**	**3.9**	**39.1**	**19.5**
Average size(nm)	101.75	101.00	97.91	100.70
Variance	45.02	41.70	41.75	38.74
Standard deviation	6.7	6.5	6.46	6.22

By increasing the resolution (decreasing the pixel size) and using the key interpolation, it was possible to obtain accurate measurements (p-value > 0.01) of particle size (101 ± 2 nm) at a larger image size (Table 3.6). On the other hand, for the 2 x 2 µm images, the decrease in pixel size did not improve the results (102 ± 2 nm and 101 ± 2 nm), possibly because in this case, the size of a pixel is similar to the standard deviation of the measurements. This finding has important implications for the time required for AFM analyses, as the use of a larger pixel size implied a reduction in image acquisition time by a factor of two in this case.

3.4 Conclusions

The errors associated with sample preparation and data treatment in the AFM measurements of a certified polymeric material were measured. Changes in sample-substrate interfacial tension, surface modification and the addition of a dispersant were efficient to achieve dispersion and particle attachment to the substrate during AFM scanning. The use of dispersant is effective at keeping the particles dispersed and attached to the substrate but may cause errors of up to 20% if the height of the film is not considered. Dilution was not effective at preventing agglomeration on a silicon wafer, as observed for mica. However, treatment of the silicon substrate by glow discharge was shown to significantly improve the quality of the prepared samples for particle size analyses. The use of glow discharge creates charges that will attract the nonconductive polymer particles, attaching them to the substrate. The size measurement was affected by the software selected for data treatment or by the type of flattening procedure. The key interpolation method led to the lowest variances. An adequate combination of the particle size and pixel size allow reliable measurements in shorter periods of time.

4 Errors associated to basic metrology methods applied to the characterization of non-conductive nanoparticles

Measurements at the nanoscale must be comparable and reliable even if performed with different instruments by different people at different times. Each technique has its own limitations and it is important to be aware of the influence that each parameter may have, in order to capture all of the relevant information when reporting nanoparticles (NP) size and size distributions. In this work we discuss several parameters that may influence the NP size measurements by analysing polystyrene nanoparticles with certified sizes of (102 ± 3)nm using transmission electron microscopy (TEM), scanning electron microscopy (SEM), atomic force microscopy (AFM) and dynamic light scattering (DLS) techniques. It was shown that by an adequate manipulation of their parameters and regarding their inherent limitation (e.g. hydrodynamic diameter for DLS) all techniques allow finding values compatible with the certified ones, according to one sample Student's t-test at a 95% confidence level. The method (area vs. diameter) of measuring the NPs size was shown to be relevant to SEM but not to TEM analyses, probably due to the best image definition particle's border in the latter. The TEM technique presented the best results in terms of repeatability and bias to the certified value. Measurements by SEM did not present repeatability over time and showed the highest bias to the certified value. Among the microscopy techniques, AFM presented the highest standard deviation, despite its high precision associated with the Z-axis, showing that the other parameters involved in particle size measurements are responsible for the associated errors. The results obtained from the DLS technique proved to be sensitive to several operating parameters and presented a large standard deviation. Furthermore, a comparison of the results of NPs sizes obtained by DLS with those obtained by microscopy techniques must be performed carefully, since the technique measures hydrodynamic diameter and provides intensity distribution (not by number). Thus, extreme care should be taken when comparing results from techniques with different principles.

4.1 Introduction

The importance of nanotechnology both scientifically and in the increasing industrial applications is undeniable (Malinovsky *et al.,* 2014; Linkov *et al.,* 2013). Due to its unique properties, nanoparticles have increased applications in the fields of microelectronics, catalysis, composite materials and biotechnologies, among others (Brown *et al.,* 2013) and many of these properties of interest are related to the nanomaterial size (Hoo *et al.*, 2008). The European Commission (EC, 2011) Framework Programme 7 highlights the importance of size distribution in the definition of a 'Nanomaterial' as: "materials containing particles, in an unbound state or as an aggregate or an agglomerate, and where, for 50% or more of the particles in number size distribution, one or more external dimensions is in the size range 1-100 nm.The measurement of nanomaterial properties is called nanometrology (Kim *et al.*, 2014"..

One of the nanometrology functions is to provide better measurements to support the nanoparticle research and industrial applications(Malinovsky *et al.*, 2014) since it is not possible to compare results or to sell products without trusted and internationally accepted measurements (Burke *et al.,* 2011; Korpelainen, 2014). Methods for the implementation of reliable, commensurate, and repeatable measurements are central to all techniques and crucial for research, industry and legal measurements (Sepä, 2014; Korpelainen, 2014). Unfortunately the problem of characterizing nanoscale is vast (Campbell, 2009). One example is the need of the comparability of measurement results by different research groups, performed with different instruments, by different people, and at different times, which is required for nanotechnology development. This is highlighted by the European research strategy planning (MacCuspie *et al.*, 2011; Burke *et al.,* 2011; Korpelainen, 2014).Gold nanoparticle measurement by TEM technique was discussed by Rice and cooworkers (2013). Different laboratories tested different measurement approaches but the results showed that it was not possible to identify a method that would achieve the certified value by all. The reasons for the different results as well as solutions to overcome the difficulties were not indicated. A comparison of different measurement methods is one of the aims of the present work. The determination of nanopolymer sizes by atomic force microscopy (AFM) and dynamic light scattering (DLS) showed that is possible to reach similar results for monomodal distribution (Cadene et al. 2005; Hoo, 2008). Another study compared the average size values of silver nanoparticles (NPs) and also the uncertainties associated with techniques such as scanning electron microscopy techniques (SEM), transmission electron microscopy TEM, and DLS, among others (MacCuspie et al., 2011). However, sample preparation approaches were not examined in detail and may explain, for instance, some discrepancies of AFM and TEM results. Each analytical technique has its limitations, advantages and disadvantages, which is important to know for proper usage as these techniques provide the fundamental information for nanomaterials applications (Campbel, 2009). The TEM uses a beam of electrons that are transmitted through an ultra-thin specimen. It has excellent resolution (lateral), down to 0.1 nm depending on sample thickness (Linkov *et al.*, 2013). Regarding particle size measured by TEM and in addition to the thickness of the sample, other error sources important are sample stability under the electron beam, aberrations of the lens and sample preparation (Lee, 2010; Linkov *et al.,* 2013).

SEM is another technique widely used in the characterization of nanoparticle size. It has a lateral resolution from 1 to 10nm (Linkov *et al.*, 2013), which is poor for tiny particles. However it has large focus depth and does not impose strong restrictions on the specimen size, in contrast to TEM (Shimizu and Mitani, 2010). SEM has another advantage over TEM, which is to allow sample imaging under low pressure and fairly high humidity (Sapsford *et al.*, 2011). On the other hand, these conditions may be a source of errors to influence image quality. The beam energy, work distance or the use or not of conducting overcoat also may be a source of errors.

AFM is another technique used to analyse structures and processes on the nanometric scale. Its resolution in the vertical direction may reach angstrom scale, but the lateral resolution is lower (Linkov *et al.*, 2013) and depends on tip convolution. Besides that, the measured Z-height may present errors related to the nanoparticle shape, if spherical asymmetry exists, and may not reflect the maximum dimension of the nanoparticle (MacCuspie *et al.*, 2011). Some advantages of AFM is not requiring staining, contrasting with special agents or conductive coatings (Linkov *et al.*, 2013).

For nanoparticles dispersed or dissolved in solvents, DLS is a suitable technique (Linkov *et al.*, 2013), since it may allow access not just to particle size but also to the presence of agglomerates and aggregates. Its resolution may reach 0.5nm (Linkov *et al.*, 2013). However, the particle size distribution obtained using DLS is different from microscope techniques as well as the dimension, which is called the hydrodynamic radius and commits the comparison with microscope techniques. There are many sources of errors at DLS technique such as counting time, temperature, carrier viscosity, and sample concentration, among others.

The sample preparation is one of the largest sources of error of most analysis techniques of nanoparticles, not just TEM, since is not trivial to determine representative shape, number of particles, size, and size distribution from the bulk sample in a small volume analysed (Kim *et al.*, 2014; Merkus, 2009). It has been discussed thoroughly and should be tested and improved for each system.

This work compares different techniques for particle size analyses of a polymeric material. The non-conductive nature of the sample adds additional difficulties when compared to the metallic samples' analyses reported in previous investigations. Here, measurements from TEM, SEM, AFM and DLS were compared against reported NIST traceable polystyrene nanoparticle size distributions. The uncertainty as well as the reliability and reproducibility of each procedure are also investigated. Both average size and the particle size distribution are reported.

The metrology under which the materials are "initially" characterized may impact their reported size and size distributions, which are in turn used as the basis for interpretation of test results or nanoparticles properties. Thus, this work aims to explore several parameters that may influence the nanoparticles size measurements using TEM, SEM, AFM and DLS techniques as well as their underlying metrology. It has also the aim to discuss potential mistakes when reporting nanoparticles average sizes and size distributions. Finally, it intends to develop approaches for comparison of the wide range of reported results, by using statistical tools to verify the reliability and reproducibility of the replication procedure.

4.2 Materials and methods

Standard Reference Material

The SRM is a well-dispersed and uniform standard, traceable to NIST (National Institute of Standards and Technology), obtained from Microtrac Instruments. The SRM consists of a 0.1% (v/v) aqueous suspension of polystyrene spherical nanoparticles with diameters of (102 ± 3)nm diameter (5.2nm standard deviation). All the samples were prepared by dilution of the stock solution with de-ionized water to 2 x 10^{-3} % (v/v).

Transmission Electron Microscopy (TEM)

The diluted stock solution was dropped onto carbon film TEM grids and then dried at

environmental conditions. Images were acquired at 120 kV using a Tecnai G2-12 – SpiritBiotwin Transmission Electron Microscope, from FEI, with high contrast, which is important in analysing polymeric samples. At least 10 locations on the TEM grid were examined. The quantity of NPs necessary to obtain reliable measurements was evaluated similarly as described in NIST protocol (Bonevich and Haller, 2010). Image J software was used for image analysis, freely available on the internet (Rasband, 1997). Sizes were measured by using the line distance tool across the diameter of the SRM NPs, previously calibrated to the scale bar imprinted on the TEM images. The considered value was the mean of three measurements at each NP. Size measurement was also performed by using the area enclosed by the oval selection tool. The diameter was obtained considering perfectly spherical shape.

Scanning Electron Microscopy (SEM)

The diluted stock solution was dropped onto glow-discharged silicon wafers and then dried at environmental conditions. Other samples were coated with 5nm thickness of conductive carbon. Images were acquired at a FEG - Quanta 200 Scanning Electron Microscope from FEI under high and low vacuum and 10 and 15 keV. The image acquisition and size particle measurement procedures were the same as that used for TEM analysis.

Atomic Force Microscopy (AFM)

The same samples prepared for SEM analyses onto glow-discharged silicon wafers, without carbon coat, were analysed by an Asylum Research MFP-3D Atomic Force Microscope in tapping mode, intending to avoid damages at particles surfaces or to carry it on. An Olympus AC160TS cantilever, made of Si, with a nominal resonance frequency of approximately 300kHz, force constant 42 N/m and tetrahedral tip was used. The quantity of NPs necessary to reliable measurements was evaluated similarly as described in NIST protocol (Grobelny *et al.,* 2009). All AFM images were treated to eliminate artefacts as described at previous chapter. The NPs size were obtained by drawing a line over the highest part of the particle and extracting the vertical profile along that line using the cross-section analysis tool of the Gwyddion 2.3.1 software, freely available on the internet (Nečas and Klapetek, 2012) and manually selecting a point on the substrate surface and a point at the peak of the SRM NP and recording the difference in Z-height between these points. The sample preparation and particle size analyses were performed according to the best results described in chapter 3.

Dynamic Light Scattering (DLS)

The DLS methodology followed recommendations outlined in the NIST-Nanotechnology Characterization Laboratory (Hackley and Clogston, 2007) Assay Cascade protocol PCC-1.23. The DLS measurements were performed using a Microtrac Intruments-Zetatrac 173. Measurements were performed at 25°C. The stock solution was diluted to 1×10^{-4} % (v/v) and 1×10^{-5} % (v/v) with deionized water to illustrate the concentration effect at DLS measurements. A sample was also

concentrated at 5% (v/v). The results were presented at intensity, volume and number-based distributions. The use of the *monodisperse mode* of analysis was also tested.

Statistical analysis

The SRM NPs were prepared and analysed in triplicate from the same batch for each technique, under condition of repeatability. In addition, to compare the strengths and weaknesses of each measurement technique, the same sample was analysed three times following the time interval of 6 to 9 days. Student's t-test (one sample) was used to compare the measured values to SRM certified values. The similarity of variances was tested by F-test. One-way analyses of variance (ANOVA) were employed in the comparison of the experimental data. Multiple comparisons tests among results and SRM certified value were performed by Dunnett's test. A p-value of ≤ 0.05 was considered statistically significant for all analyses, and ran using the R free Software (R Core Team, 2014), with interface integrated to Excel via Action Software (Estatcamp, 2014). The standard deviation was used to report uncertainty as it is a measure of the width of the distribution and also contains the uncertainty associated with determining the mean size. For DLS measurements the standard deviation was calculated by (D84 - D16)/2. It is not an indication of variability for multiple measurements.

The results of analyses of the same samples in different days were combined to obtain an improved result for variance of the technique. For the general case, where the mean values, X_1, X_2, X_3, etc. have been calculated from sets of N_1, N_2, N_3, etc. measurements, this can be done by using the following equation (Merkus, 2009):

$$s_x^2 = \frac{\sum(x_1-\overline{x_1})^2+\sum(x_2-\overline{x_2})^2+\sum(x_3-\overline{x_3})^2+.....}{(N_1-1)+(N_2-1)+(N_3-1)+.....} \tag{4.1}$$

4.3 Results and discussion

4.3.1 Number of particles to count

Analysis by microscopy-based techniques enables direct observation of the powders but erroneous results may happen due inadequate sample preparation (Jillavenkatesa *et al.,* 2001). Some of the statistical errors typically encountered when using microscopy-based techniques are due to counting a quantity of particles that does not represent the particles actually present in the whole powder (Merkus, 2009). A comprehensive mathematical procedure to determine the number of particles to be counted, in order to minimize the error associated with size determination, has been proposed by Masuda and Linoya (1971). The authors have studied the scatter of experimental data due to particle size distribution. Their hypothesis has been confirmed by computer simulation (Jillavenkatesa *et al.*, 2001), where it was found that size and distribution (calculated by the model) are similar when a smaller number of particles

are counted. The optimum amount of particles to be counted varies with the size distribution thereof. Thus for each material and analysis technique the minimum amount of particles necessary for a representative analyses was calculated prior to the measurements. Starting from 144 nanoparticles (NPs) to be analysed by TEM (Table 4.1) the evaluation of similarity of results and variances by the F-test indicate a statistically meaningful results for a minimum of 30 SRM particles.

Table 4.1-Calculated nanoparticles diameters from TEM. Random Sampling Summary

# NPs counted	Mean diameter (nm)	Variance	F value	F critical
144	101.76	18.81		
100	101.90	17.95	1.05	1.36
100	101.24	19.64	1.04	1.35
100	101.54	20.50	1.09	1.35
70	102.54	16.95	1.11	1.42
70	101.20	18.94	1.01	1.39
70	101.96	22.72	1.21	1.39
30	101.76	23.66	1.26	1.54
30	101.38	20.89	1.11	1.54
30	101.52	25.54	1.36	1.54
20	**103.66**	**10.70**	**1.76**	**1.89**
20	101.91	12.55	1.50	1.89
20	101.65	26.36	1.40	1.64
20	99.93	24.79	1.32	1.64
15	102.05	19.68	1.05	1.74
15	**100.76**	**50.14**	**2.41**	**1.74**
15	101.71	15.42	1.22	2.11
15	103.43	13.08	1.44	2.11

The F-test (Snedecor and Cochran, 1989) was used to test if the variances of data from fewer particles counted were statistically equal to18.81, which is the variance when 144 NPs were counted. The F value from 15 counted NPs was found to be higher than F critical for one series of measurements. This indicates more NPs should be analysed to ensure reliable results. The mean diameter value was higher than the expected (101.76 nm) for one series of 20 particles. Moreover, the F value is too close to the F critical. For the further experiments at least 30 NPs were analysed, as the t-test and F-test ensure, with 95% confidence level, that the results from the analyses of 30 NPs are statistically equal to the analyses of 144 NPs. This relatively low NPs number is reasonable if one considers that SRM particle's sizes are relatively uniform. The F-test and t-testapplied to the data obtained by SEM and AFM also pointed to minimal value of 30 particles. This finding suggests that the microscopic technique has no influence on the number of particles that will be accurately represented the sample, but the dispersion of the particles over the substrate has instead. According to Rao and cooworkers (Rao, 2007), the nature of the substrate is the one who influence on the dispersion and particle number on it. Thus, when two techniques will be used to

analyse a sample, this study needs only be carried out once. For both techniques applied to the same substrate, the minimum amount of particles will be the same.

4.3.2 Test for normality

The values reported from microscopy-based measurements are often the mean of all observed particles with one or two standard deviations, assuming a Gaussian distribution (MacCuspie *et al.*, 2011). However, particle size distributions are not always normal. The inconvenience about that is related to the fact that many statistical procedures such as t-tests, F-test, linear regression analysis or analysis of variance (ANOVA) have an underlying assumption that the data has a normal distribution (Razali, 2011). Even to calculate the confidence interval it is necessary to know which distribution the data follows. Usually particle size distributions are modelled by log-normal, Weibull or log-hyperbolic probability distributions (Purkait, 2002; Ujam and Enebe, 2013). At this work most results can be represented by log-normal distributions. There are some methods to evaluate if the data can be well-modelled by a normal distribution: graphical methods (histograms, boxplots, Q-Q-plots), numerical methods (skewness and kurtosis indices) and formal normality tests (Shapiro-Wilk test, Kolmogorov-Smirnov test, Lilliefors test, Anderson-Darling test). The Shapiro-Wilk test has the best power (Razali, 2011), which means it is the most effective one in affirming that the data cannot be regarded to be well modelled by normal distribution. Figure 4-1 shows that data from all microscopy-based techniques may be well modelled by normal distributions, as demonstrated by line fitting and by p-values higher than 0.05.

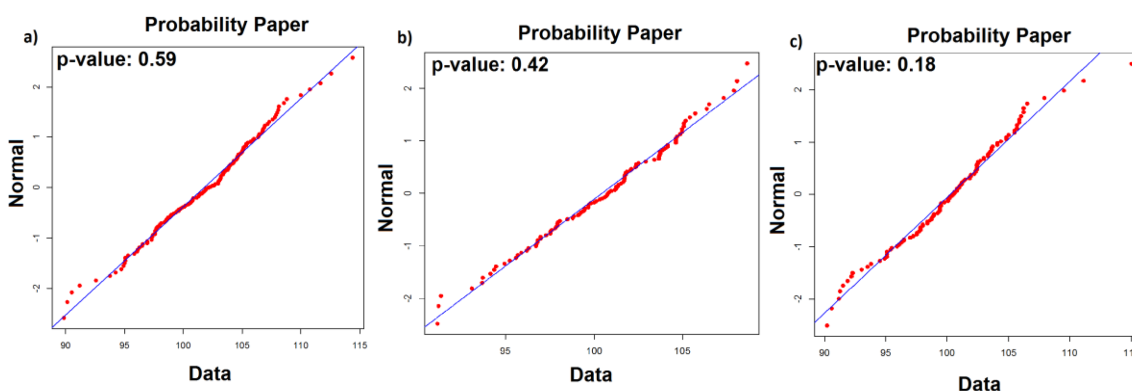

Figure 4-1- Probability paper and p-value for normality tests of nanoparticles sizes analyzed by a) TEM, b) SEM and c) AFM, by Shapiro-Wilk test..

4.3.3 Microscopy analysis

The the measurement techniques as well as sample preparation will impact the NPs size and size. Microscopy-based techniques such as TEM, SEM or AFM typically require dried samples fixed on a solid support, and the sample preparation method may impact the results considerably by drying-induced agglomeration. The chosen sample preparation protocol - dropping the diluted SRM sample over an substrate

adequate for each technique - was performed in triplicate to ensure reliable preparation. Figure 4-2 shows the results from TEM, SEM and AFM. These images are representative of all the replicates.

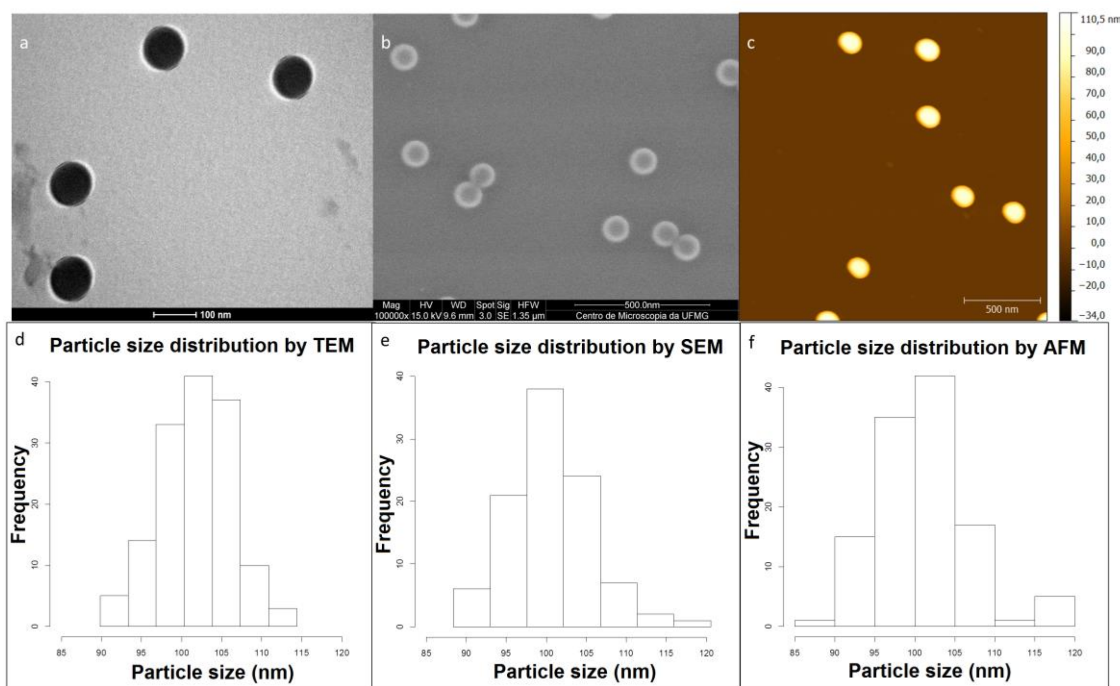

Figure 4-2- Images of SRM NPs by TEM (a), SEM (b) and AFM(c) showing low drying-induced agglomeration. Particle size distribution of SRM NPs measured by TEM (d), SEM (e) and AFM (f).

All the replicates showed the same pattern of well disperse particles over the substrate. Even at high contrast TEM, an organic capping layer, very commonly found in dispersed samples, was not identified. The absence of a capping layer will also allow a better comparison between the results from microscopy techniques and from DLS. The latter measures the hydrodynamic diameter, which may be influenced by the presence of capping agents (MacCuspie *et al.*, 2011).

TEM

The particle size measurement by TEM was calculated by both the mean of diameters and the area to evaluate de difference between these two approaches, both used in particle size measurements. A comparison of the results for spherical SRM particles will allow evaluating the intrinsic errors of both approaches. The particle size of each three sample replicates, measured at least 30 particles each, at the same day and conditions are summarized in Table 4.2.

Table 4.2- Mean diameter of three replicate (n=30 each) of SRM particles obtained by TEM

Measure	by mean of diameters		by area	
Replicate	**Mean diam. (nm)**	**SD (nm)**	**Mean diam. (nm)**	**SD (nm)**
1	101.54	4.89	102.30	4.37
2	101.24	4.36	100.75	4.47
3	102.73	4.51	101.94	5.06

The t-test for paired samples (since the same sample was compered) was applied to the data obtained by mean of diameters and by area of the particle. The p-values> 0.05 for each replicate ensure that both methods lead to statistically equal results and can be used without loss of measurement reliability.

The histogram of residuals confirms the normal behaviour of the treated data allowing the use of ANOVA (Figure 4-3). A p-value > 0.05 shows that differences in the results from the three sample preparations and from the two methods for particle size measurements are not statistically meaningful. The plot of residuals against fitted values shows that the variation of the amplitude is the same for each test, which corroborates that the particle size values at three replicates are not significant. The particle size analysis is subject to several sources of errors as at the technique, the operator or the image analysis. Thus it is important to evaluate the plot of residuals against the order of collection since they suggest the existence of systematic measurement error, which should be eliminated to ensure the evaluation of random measurement errors. The similar evaluation was undertaken during each ANOVA test.

Now the errors resulting by measuring the same batch of particles by the same operator, in three different days, using the same equipment will be discussed. These conditions create an intermediate precision condition or repeatability for the technique (Merkus, 2009). Table 4.3 contains all the measures of the particles performed by the same analyst.

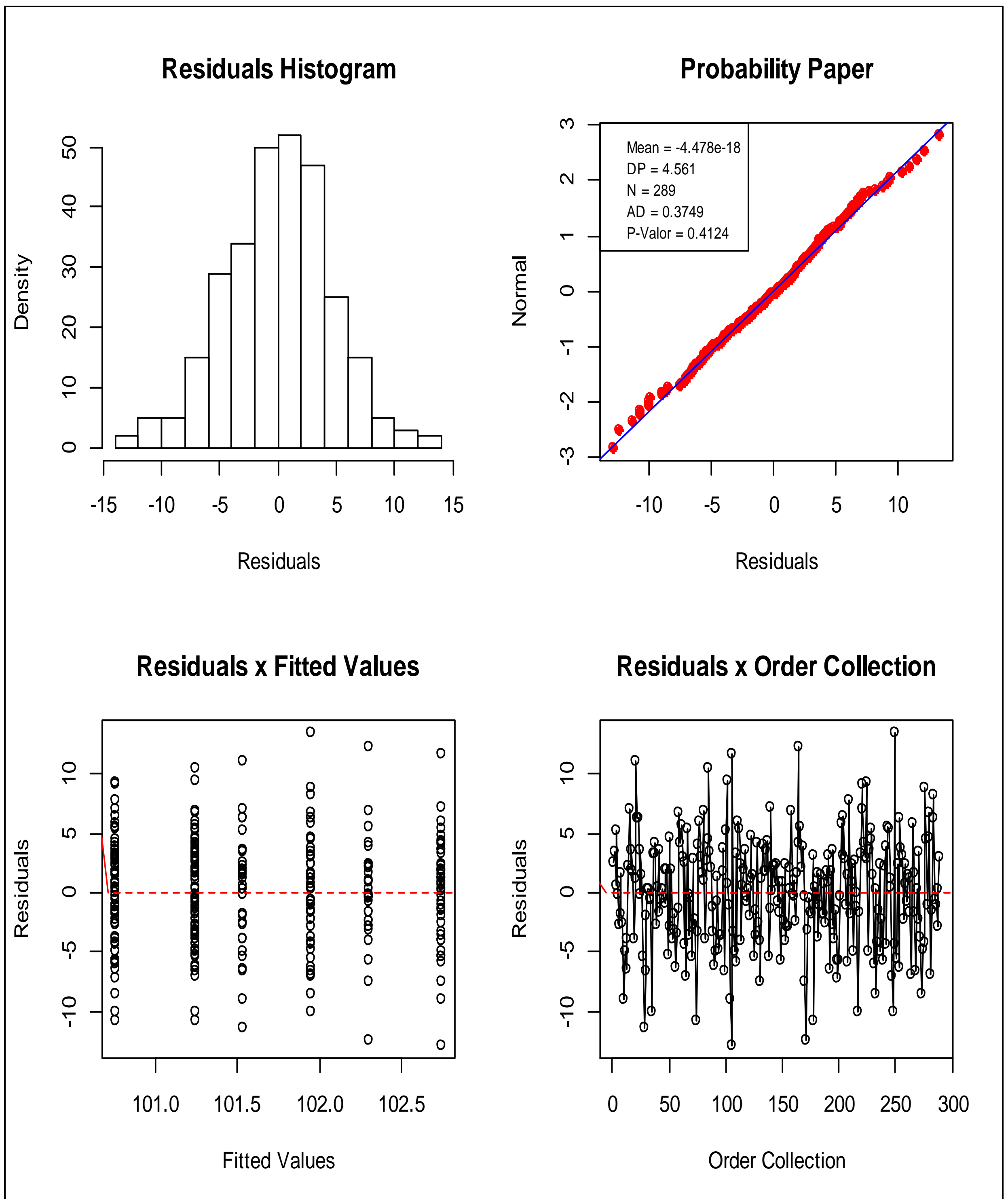

Figure 4-3- ANOVA results for SRM nanoparticle measured using TEM at three replicated sample and two image measurement methods.

Table 4.3- Mean particle size of SRM samples and their standard deviation (SD) on three different days measured using TEM.

PARTICLE	DAY 1- Size (nm)	DAY 2- Size (nm)	DAY 3- Size (nm)	SD
1	102.06	100.01	101.01	1.03
2	101.03	99.01	98.99	1.17
3	99.99	101.01	100.01	0.58
4	96.24	94.95	96.00	0.69
5	96.99	96.00	93.00	2.08
6	94.95	96.00	97.00	1.03
7	100.00	101.00	100.05	0.56
8	102.02	100.01	100.00	1.16
9	105.05	105.00	103.01	1.16
10	89.57	86.00	86.00	2.06
11	103.07	100.00	100.00	1.77
12	103.00	103.00	102.97	0.02
13	100.00	102.00	100.00	1.15
14	110.10	110.00	108.08	1.14
15	109.10	111.00	111.11	1.13
16	108.08	108.01	105.00	1.76
17	102.02	101.01	101.00	0.58
18	103.03	99.01	100.00	2.09
19	96.00	95.00	97.00	1.00
20	104.00	104.00	105.00	0.57
21	101.01	101.00	102.00	0.57
22	103.03	105.00	105.00	1.14
23	103.03	100.00	103.03	1.75
24	98.99	100.00	101.01	1.01
25	101.00	99.00	101.00	1.15
26	97.00	98.00	97.00	0.58
27	104.00	106.01	103.00	1.53
28	101.02	100.00	99.00	1.01
29	109.01	110.00	113.14	2.16
30	103.00	101.00	102.02	1.00
31	102.00	100.00	103.00	1.53
32	103.00	103.03	102.00	0.59
33	102.00	104.00	103.01	1.00
AVERAGE	**101.65**	**101.18**	**101.19**	
SD	**4.22**	**4.90**	**4.84**	

The variances were calculated per particle analyzed at three different days and also for the set of particles analyzed at each day. The latter also represents the width of the particle size distribution. The measurements show particles with diameters ranging from 86 to 113nm, with particle average size of (102 ± 2)nm in the first day and (101 ± 2)nm in the second and third days, at 99% confidence level. The standard deviations were 4.2, 4.9 and 4.8 respectively. The mean values are in agreement with the sample certified value (102 ± 3nm and 5.2 of standard deviation). Thus TEM analysis yields a size range within the limits of the specified range. When each particle is individually evaluated on days 1, 2 and 3, it can be seen that the standard deviation due to the different days of analysis are smaller than those obtained for the whole set at one day or the dispersion associated with the SRM itself. The variation within a day represents the uncontrolled variation of the measurement and microscope conditions. The results indicate that the sample variance is greater than the procedure as a whole. This finding demonstrates that the technique and method associated with nanoparticle size measurement by TEM are reliable and the variations are mainly due to the sample itself.

SEM

SEM analysis of polymeric materials exhibits some drawbacks. First, the material is non-conductive and that generates sample charging. This is illustrated by the lighter circles around the particles (Figure 4-2). Secondly, polymeric samples show instability in the presence of the electron beam. As the beam scans the sample it decomposes, as shown in the sequence of images on Figure 4-4. This prevents evaluating the same particle in different days, as performed by TEM. Changing operational parameters can improve the measurement as discussed later.

Three sample replicates from the same batch were measured by SEM at the same day and conditions and their results are summarized in Table 4.4, similar to the tests performed with the TEM analyses. For the measurements by mean of diameters, the results were consistent and agreed with the certified value to SRM, as tested by ANOVA and one sample t-test (p-value> 0.05). However, the measurements performed by area differ greatly among themselves. According to Dunnett's test the replicates 2 and 3 disagree with the certified value. Thus the measures by area were shown to be inaccurate to assess the particles size. This finding is related to the low quality of the images obtained by SEM (Figure 4-4). Even when images are acquired at high resolution (2048x1887dpi), the border of the particles is not clear, for the reasons discussed previously.

Table 4.4- Mean diameter of three replicate of SRM particles obtained by SEM at the same day, with : same operator, resolution of 2048x1887dpi, 100.000 times magnification, high vacuum and 15 kV.

Measure	**mean of diameters**		**by area**	
Replicate	**mean (nm)**	**SD (nm)**	**mean (nm)**	**SD (nm)**
1	100.48	5.40	100.18	6.10
2	100.88	5.20	98.09	5.02
3	100.14	5.62	95.29	5.43

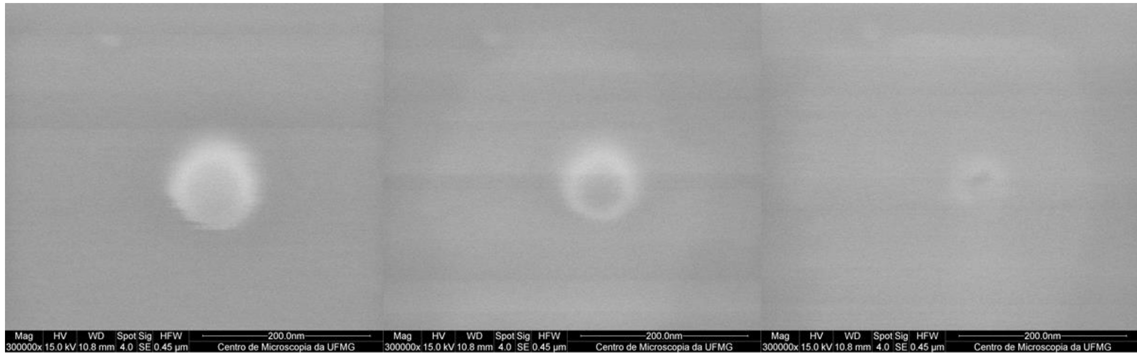

Figure 4-4- Sequential images of the same particle, by SEM with high vacuum and 15kV.

To test the reproducibility over time, the same sample (but not the same batch of particles) was analysed on three different days, with approximately one week between each of them, under fixed conditions. The results are sumarized in Table 4.5.

Table 4.5- Particle size of SRM samples on three different days, by SEM, with : same operator, resolution of 2048x1887dpi, 100.000 times magnification, high vacuum and 15 kV.

Measure	**mean of diameters**			**by area**		
Day	**Mean (nm)**	**Variance**	**SD (nm)**	**Mean (nm)**	**Variance**	**SD (nm)**
1	100.14	31.58	5.62	95.29	29.48	5.43
2	96.54	26.83	5.18	91.34	35.28	5.94
3	99.76	25.60	5.06	93.31	42.90	6.55

The results varied considerably from one day to another and the differences can be considered significant by ANOVA (p-value< 0.05). The values determined by SEM were not reproducible over time. Other factors, such as the electron beam stabilization, besides the controlled ones (vacuum, operator, beam energy and magnification) may influence accurate particle size measurement by this technique.

The measurements from the area are biased to lower values if compared with certified

value for diameter. It can be also noted at replicate results (Table 4.4). In summary, particle size measurements by SEM showed higher errors and inaccuracy when compared to TEM.The impact of operational parameters (e.g. vacuum, beam energy and sample coverage with conductive film) on the particle size measurement was analysed. The results are summarized in Table 4.6.

Table 4.6- Influence of analyses parameters at particle size measurement by SEM.

	Beam energy (keV)	**Magnification (1000x)**	**Carbon covering**	**Mean of diameters**			**by area**		
				Average(nm)	**SD**	**Variance**	**Average(nm)**	**SD**	**Variance**
High Vaccum	5	50	yes	125.47	7.95	63.23	123.19	6.74	45.46
	5	100	yes	129.02	8.52	72.56	125.73	9.76	95.22
	15	50	no	100.85	6.56	43.08	99.92	7.08	50.15
	15	100	no	100.88	5.20	27.05	97.44	4.11	16.87
	10	100	no	100.28	5.21	27.10	94.22	4.32	18.62
Low Vacuum	10	100	no	102.54	5.60	31.31	95.03	5.37	28.82
	15	100	no	103.05	5.41	29.28	98.50	6.71	45.01

The average diameters of particles covered with conductive carbon layer are significantly higher than those in the absence of the carbon coating (Figure 4-5). In addition, the values do not agree with the certified one. The carbon film is expected to be 5 nm, but the range of diameters (105 to 151nm) shows that the film thickness is larger and not uniformly distributed. This is also evidenced by the high variances. On the other hand, carbon coating allows sharper images and avoids charging effects even at high vacuum (Figure 4-5-a) as compared to the NPs without any covering (Figure 4-5-c). The low vacuum reduces the charging effect (Figure 4-5- b and d) but reduces also sharpness, especially at beam energy of 10 keV (Figure 4-5 d). The reduction of the charging effect under low vacuum happens because air molecules in the chamber remove charge from the surface of a non-conducting material. However, the air also scatters the beam, thus decreasing sharpness of the images (Wittke, 2008). The energy beam (10 and 15kV) did not influence the measured diameters (Table 4.6), but the low vacuum presented, in general, higher average size values, which may be related to the reduced degradation from the sample. The variance decreases with increasing magnification, and in the presence of a conductive layer..

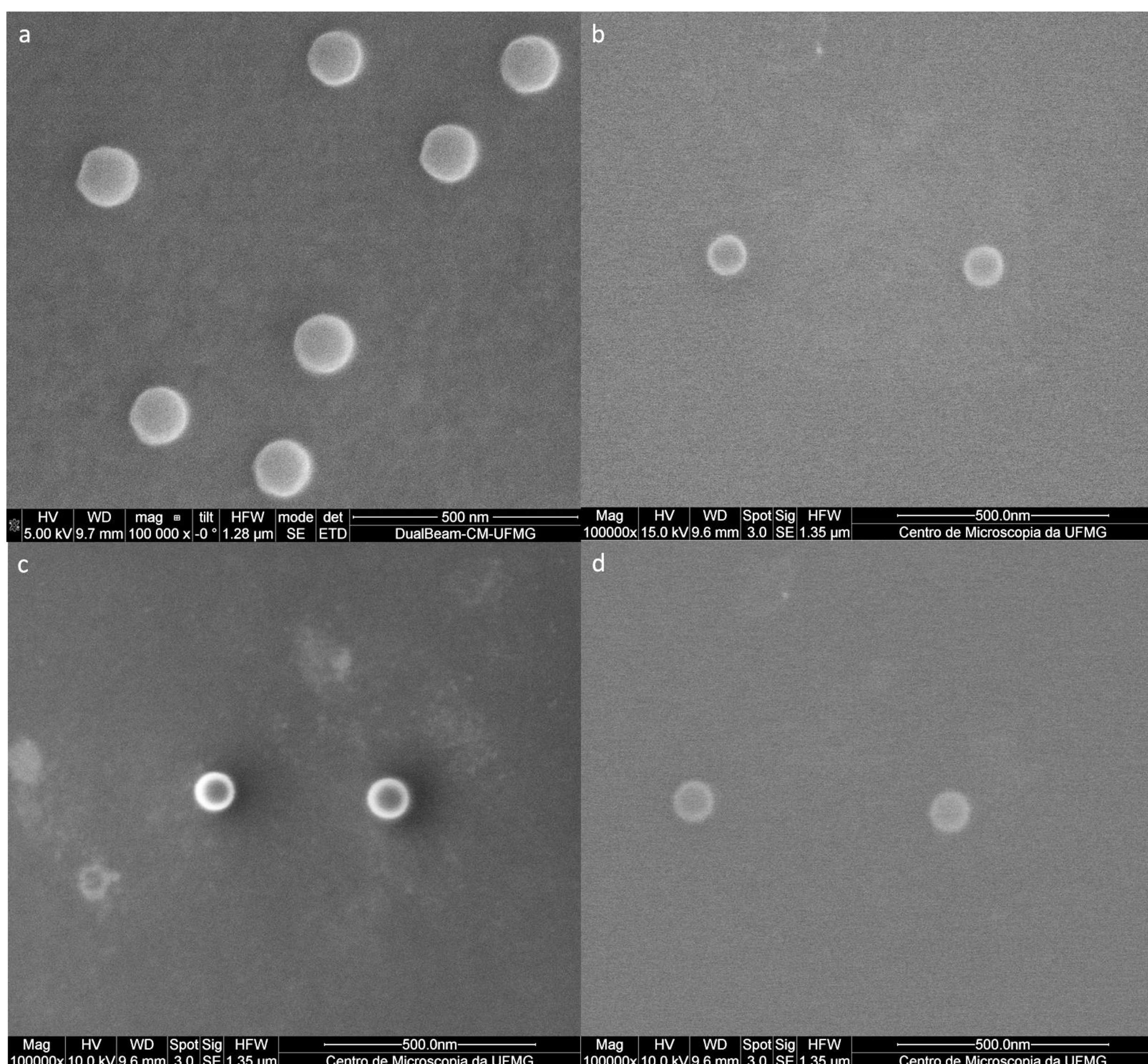

Figure 4-5- SEM images from SRM NPs with (a) carbon coating, high vacuum and low energy; (b) no coating, low vacuum and energy beam of 15keV; (c) no coating, high vacuum and energy beam of 10keV and (d) no coating, low vacuum and energy beam of 10keV.

AFM

The AFM probe scans the sample and dark regions appear on the image (Figure 4-6). This plane distortion is very common to AFM images (Grobelny *et al.,* 2009) and because of this, it is necessary to treat the images before measuring nanoparticle sizes (Klapetek *et al.,* 2009). This treatment should be done carefully since is also a source of errors as described in the previous chapter. The established procedure involves drawing a line over the highest part of the particle and extracting the vertical profile along that line. The average baseline height was subtracted from the peak height to find each nanoparticle height. The measurements by AFM found NPs size from 88 to 119nm and the mean values are summarized in Table 4.7.

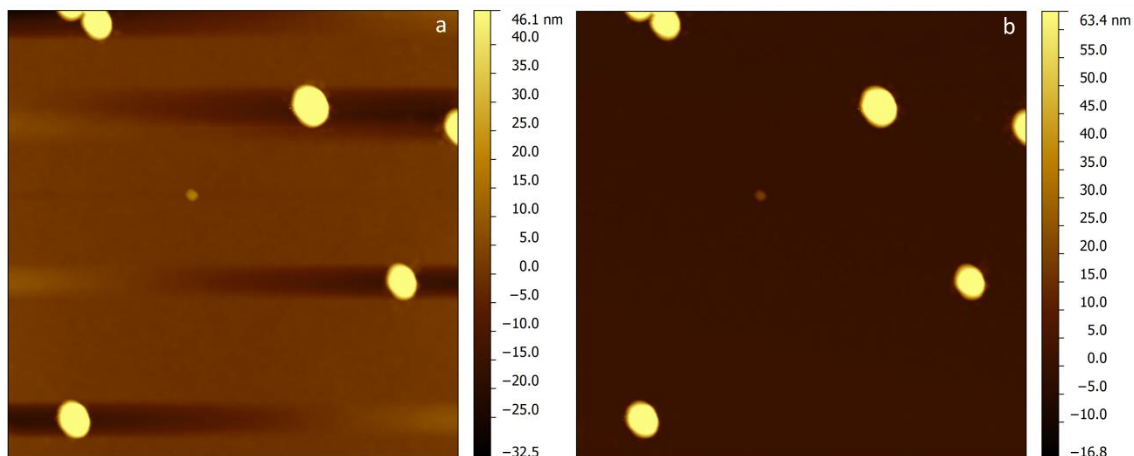

Figure 4-6- Height retrace image from the SRM-sample (a) with artifacts; (b) after image treatment at Gwyddion.

Replicate measurements were performed under fixed conditions and can be considered statistically equal by ANOVA (p-value > 0.05). This finding demonstrates the reproducibility of sample preparation and measuring procedures. The sample preparation and image treatment are major sources of errors in NPs measurement. Reproducibility of the technique over time was shown according to ANOVA tests (p-value> 0.05) by the measurements performed in three different days. The average particle size values for each day are presented in Table 4.7.

Table 4.7- Average particle size and standard deviation associated to SRM measurement by AFM with replicate and at different days

Replicate Same day	Mean (nm)	SD (nm)	Day	Mean (nm)	SD (nm)
1	101,12	5,13	**1**	101,67	5,16
2	101,08	6,36	**2**	100,97	4,83
3	100,16	5,57	**3**	101,13	6,80

4.3.4 Dynamic light scattering (DLS)

The DLS has inherent limitations (Linkov *et al.*, 2013) (such as the measurement of hydrodynamic diameter) and several parameters may influence the results, such as counting time, temperature, and carrier viscosity. The measured diameter, called hydrodynamic diameter, is different from those measured by microscopy techniques, and comprises the particles itself, capping agents and other molecules sorbed on the surface as well layers of solvent molecules that moves with the NP due to Brownian motion (Merkus, 2009). The mean hydrodynamic diameter found for SRM NPs was 105nm with 23nm of standard deviation as showed in

Table **4.8**. This size is found with the intensity-based size distribution (Figure 4-7-a) as recommended by ASTM standard E2490-09. Different particle size techniques report primary results based on number (microscopy) or volume, weight, surface area, and intensity (DLS) (Horiba, 2014). The softwares from DLS equipments are usually capable of converting intensity-based results to number or volume distribution based on Mie theory (Malvern, 2003). Table 4.8 presents the DLS results according to volume, number and intensity distributions. The values calculated from volume and number distributions present a large bias to the certified value, with errors up to 20%.

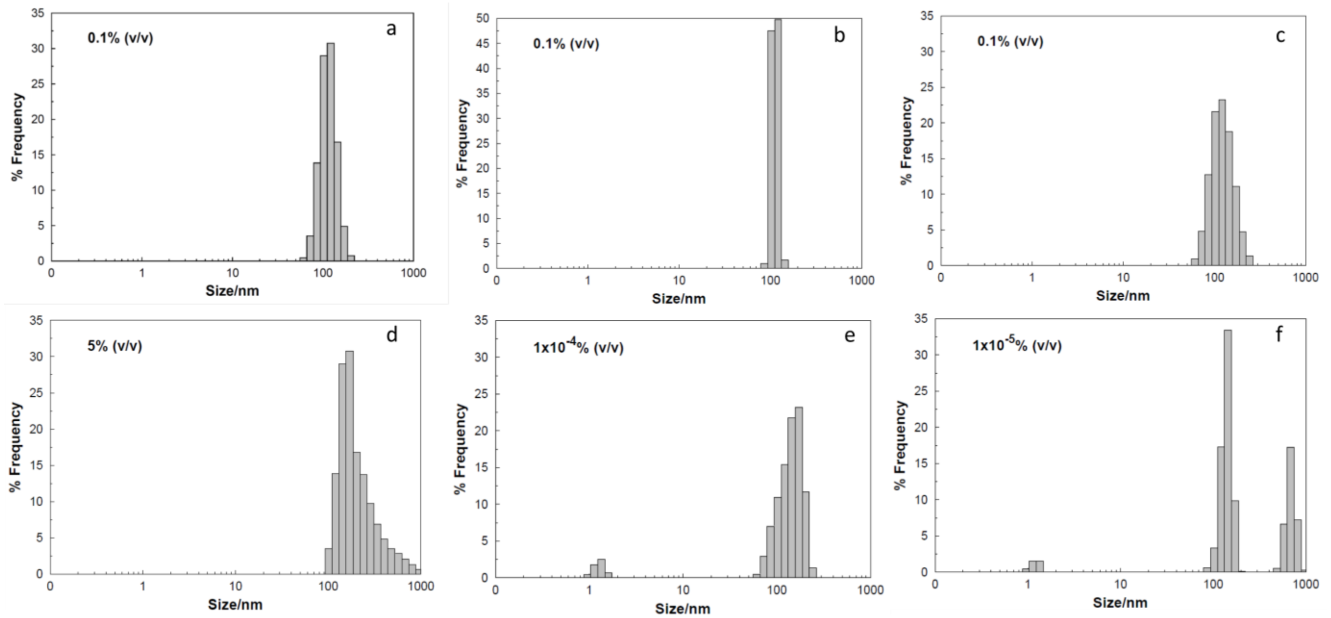

Figure 4-7- Particle size distribution of SRM by DLS: at normal operational mode, no dispersant, and SRM concentrations of 0.1%(v/v) (a), 5%(v/v) (d), $1x10^{-4}$%(v/v) (e) and $1x10^{-4}$%(v/v) (f). At monodisperse operational mode, no dispersant, and SRM concentration of 0.1%(v/v) (b). At normal operational mode, with dispersant (disperbik 348), and SRM concentration of 0.1%(v/v) (c);

Table 4.8- Average particle size and standard deviation associated to SRM measurement by DLS.

	Distribution	Mean (nm)	SD (nm)
Day 1	number	81.6	20
Day 1	volume	94.3	18
Day 1	intensity	104.7	23
Day 2	intensity	101.2	20
Day 3	intensity	101.2	18
Monodisperse mode	intensity	103.0	11
Dispersant	intensity	114.9	32

The particle size distribution found by DLS (intensity distribution) showed a particle size range from 60 to 204 nm and therefore larger than the range observed with the other

techniques (89 to 114 nm for TEM, 86 to 121 nm for SEM and 90 to 115 nm for AFM). There are algorithms to improve the processing of the correlation function based on available information of the sample, the monodisperse mode is one of them. The results obtained in monodisperse mode, which calculates a Gaussian distribution centered around the mean diameter, (Figure 4-7-b) are closer to those found with microscopy techniques (Table 4.8). The particle size range was kept between 85 and 145nm, which suggests that very small and very large particles, probably the result of some interaction between particles, multiple scattering, noise, and other, have been eliminated. Another parameter that may influence the particle size measurement by the DLS technique is the use of dispersants, which is a common practice as the analysis requires particles being in suspension. However, the presence a surfactant increased the SRM size measured by 10% (Figure 4-7-c) and also the width of particle size distribution (mean particle size of 115 nm and 32nm of standard deviation). The magnitude of these errors will vary with the size of the NP and the nature of dispersant molecule.

As for microscopy techniques, sample preparation is crucial for DLS results. If the sample concentration is to high there is a risk of erroneous results due to multiple scattering (light scattered by one particle undergoing scattering by another) (Linkov *et al.*, 2013). If the sample concentration is to low, the noise or even same dust may yield spurious peaks called "ghost peaks" (Hackley and Clogston, 2007). Figure 4-7 exemplifies these errors. Care should be taken with excess dilution to achieve monodispersed distribution as this may lead to errors. Each system has an ideal concentration, which depends on parameters such as carrier fluid viscosity, refractive index, particle size, among others (Hackley and Clogston, 2007). Large particles will require lesser quantities due to their higher scattering. In general, it is necessary about 500 particles at the measurement zone (Merkus, 2009).

It was not possible to test repeatability over time by ANOVA as with the other techniques. It happened because the results are provided in the format of histograms. It is possible to note that the results are closer to each other (taking into account the high SD) (Table 4.8) and to the certified value. Due to measurements based on hydrodynamic diameter, a limitation inherent to this technique, it was expected that all average values were bigger than 102nm, but this has not been observed. The t-test confirmed that all results are statistically equal (at 95% confidence) for 500 particles measurements,

4.3.5 Comparison of NPs size distribution by the different measurement techniques

When comparing techniques, the precision is an important parameter to be analysed. For particle size distribution measurements, there are two important intermediate precision conditions. One concerns the procedure where all the conditions are kept the same but for each analysis a new aliquot from the same batch is prepared (Merkus, 2009). For all microscopy techniques this precision (or repeatability of procedure) was tested and the results were very similar (Table 4.2,Table 4.4, and Table 4.7). The

coefficient of variation (CV) of the SRM average particle size prepared to TEM, SEM, AFM and DLS analyses were 0.8%, 0.4%, 0.5%, and 0.3%, respectively. These values can be related to the relative sample preparation uncertainties (Rice *et al.,* 2013) and suggest that this technique is the most sensitive to variations on this procedure. Another intermediate precision condition is for an instrument or technique, where the same sample aliquot is measured for a given short time interval, three times in our case. The repeatability of each technique is illustrated by Figure 4-8, which shows the relationship between the certified SRM value and the average particle size obtained by the four techniques at three different days.

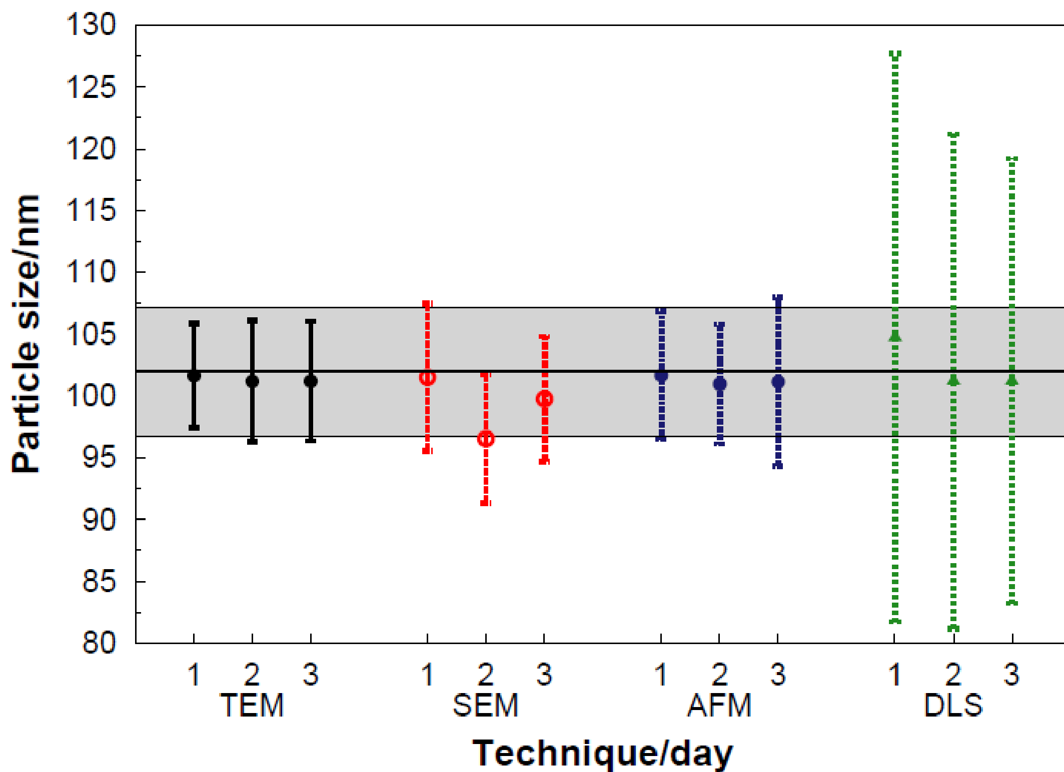

Figure 4-8- Mean value for SRM obtained by TEM, SEM, AFM and DLS. The centre line represents the certified value and the gray zone indicates the standard deviation of each measurement.

The CV of the average particle size, at the three days tested, for TEM, SEM, AFM, and DLS were 0.3%, 2.0%, 0.4%, and 2.0% respectively. These results indicate that TEM and AFM showed similar repeatability and the techniques SEM and DLS are equally worse than the previous two. On the other hand, when the entire distribution is considered the findings are different. The variance of techniques calculated from equation 4.1 was 1.02 for TEM, 29.30 for SEM, 32.33 for AFM and 417.67 for DLS. TEM results present the smallest SD compared to the other techniques, indicating to be the most precise technique. The SEM measurements show generally smaller average values and higher variances than TEM measures. SEM is also not reproducible over time and presents the highest bias from the certified value. AFM results agree with the certified value but show the highest SD values among the

microscopic techniques. DLS results present the highest SD values compared to the four tested techniques. Even the result at monodisperse operational mode presents SD of 11nm (Table 4.8) higher than any microscopic technique.

Note that the standard deviation contains the uncertainty associated with determining the mean size but also reflects the width of particle size distribution. The broad particle size distribution of DLS is inconsistent with the narrow SRM particle size range confirmed by the other techniques. Due to the fundamental metrology of DLS measurements, any agglomerates or aggregates present in the suspension will be measured and will contribute to the mean size (MacCuspie *et al.*, 2011). The light intensity scattered by a NP is proportional to its diameter to the sixth power, and thus larger diameter particles contribute much more to the signal intensity (Microtrac, 2008). Thus, distributions with the presence of smaller particles may not be observed by the intensity distribution. On the other hand, number-based distributions may show these particles. Therefore, it is important to observe the size distribution by number and volume when analysing NPs systems despite to the errors present at absolute values due to the conversion from intensity distribution. At number distribution, for example the mean particle size was found to be 89nm.

Horiba suggests including other parameters, such as D10 and D90, in order to describe the width of the distribution rather than using a single point in the distribution as the mean. The width of an arbitrary PSD can be expressed as the ratio (D90/D10) (Merkus, 2009) as shown in Table 4.9.

Table 4.9- Span ratio and median values from SRM by TEM, SEM, AFM and DLS.

Technique	D10 (nm)	D90 (nm)	D50 -median (nm)	D90/D10
TEM	95.85	107.14	102.16	1.12
SEM	94.17	107.30	100.70	1.14
AFM	93.00	106.20	100.60	1.14
DLS	76.80	136.00	102.20	1.77
DLS (monodisperse mode)	90.00	116.50	102.70	1.29

All the microscopy techniques present similar span ratios. These results indicate that the increased SD values are not associated to the sample dispersion and corroborate the results of technique variance described before. DLS presents the largest distribution. The monodisperse mode of operation makes the ratios closer to those found by the microscopy techniques but the bias is kept.

4.4 Conclusions

The four techniques described above - TEM, SEM, AFM and DLS - can provide accurate size measurements and size distributions of non-conductive polystyrene NPs. Prior to the measurements, it is important to be aware of the limitations and the specific influence of the pertinent parameters of each technique to report NP size and NP size

distributions with minimal errors. A preliminary investigation should be carried out to define a representative number of particles to be count, the distribution shape, the adequate concentration or the sample preparation procedure, among other factors, prior to selecting a lower-cost routine and a time efficient characterization method. The TEM technique showed the best results in terms of technique repeatability and the agreement with the certified value. The sample variance was found greater than that of the procedure as a whole, thus indicating that variations are mainly due to the sample itself. The SEM technique showed no repeatability over time and the worst agreement to the certified value. These results may be related to electron beam-sample instability, and image quality, among other parameters in addition to the controlled ones (vacuum, operator, beam energy and magnification).The methodology (area vs. diameter) of measuring the NPs size was shown to be relevant to SEM but not to TEM analyses, probably due to the better image definition at the particles' border of the latter Among the microscopy techniques, AFM allowed high precision associated to Z-axis but the highest SD, showing that other parameters (such as image treatment) contribute most to the errors associated with size measurements. Reproducibility of the technique over time was shown by the measurements performed in three different days. Therefore, it is recommended a more focused approach to imaging and measurements standardization than for obtaining the image itself.
The DLS technique is excellent for routine analysis. It is a less expensive and quick method. However, many parameters may affect the results. The use of dispersant, common at sample preparation, lead to errors of 10% relative to the certified value. Therefore prior to optimizing the operational parameters for DLS routine analysis, it is suggested to undertake the measurements with a microscopy technique (TEM or AFM). Values calculated from volume and number distributions present a large bias to the certified value, with errors up to 20%. DLS has also an advantage over microscopic techniques that is to evaluate NP dispersions at the original environment, which allows studying nanoparticles agglomeration in the carrier fluid.

Each analytical technique has its own limitations, advantages, disadvantages, and associated errors. Identification of the deviations in size measurements together with the parameters affecting the results will contribute to more precise and reliable size determination in NP manufacture and applications.

5 Final considerations

The parameters that may influence the NPs size measurements by TEM, SEM, AFM, and DLS techniques were evaluated in order to identify all of the relevant information to be provided when reporting NP size and size distributions. Sample preparation, the inherent limitation of each technique, and image treatment was shown to contribute more to increase the reliability of the measurements than the equipment's nominal resolution.

All the four selected techniques (TEM, SEM, AFM, and DLS) were able to provide accurate particle size and particle size distribution of the certified polystyrene NPs, according to one sample Student's t-test at a 95% confidence.

The TEM technique presented the best results in terms of repeatability and agreement with the certified value and therefore it is the most recommend for comparison and validation with other techniques. The sample preparation is the major source of errors of this technique. The results obtained by SEM did not show repeatability over time and presented the worst agreement with the certified value, according to the Dunnett's test at 95% confidence level. These results may be related to electron beam-sample instability, and image quality, among other parameters in addition to the controlled ones (vacuum, operator, beam energy and magnification).

In AFM analyses, it was found that dilution of the polymeric nanoparticle suspension provide good dispersion on the mica substrate, but not on silicon. The sample preparation on silicon was significantly improved by treating the substrate with glow discharge. The use of dispersant was effective to keep the particles dispersed and attached to the substrate, but may cause errors of up to 20% if the height of the film is not considered. AFM results presented higher standard deviation when compared to TEM and SEM, despite its high precision associated with the Z-axis. It was found that both the software for data treatment and the type of flattening procedure influence particle size measurement by the AFM technique.

The results obtained by DLS were shown to be very sensitive to the technique's operational parameters and presented a large standard deviation. However, DLS has advantages of relatively low cost and short time for routine analyses in addition to carrying out measurements in the presence of the carrier fluid. Comparison of DLS and other techniques should be performed with caution as DLS measures hydrodynamic diameters in intensity distribution and not in number, as the others.

The particle size distribution obtained by DLS diverged in width from the TEM results, which demonstrates that a particle size characterization should contain more than just the average size. Other information, such as the number of counted particles, the distribution (such as format or width) and the measurement conditions should also be reported.

As a conclusion, we may say that by enabling a better understanding of the techniques and methods applied to nanoparticle size analyses, the present investigation is expected to contribute to the development of nanometrology.

6 References

Albertazzi, G. Jr. A. and Souza, A. R. (2008) *Fundamentos de Metrologia Científica e Industrial.* São Paulo: Manole.

Aleksandrov, V. S.; Trunov, N. N. and Lobashev, A. A. (2012) “Systematizing and parameterizing nanosystems” *Measurement Techniques.* 55 (7), 763-769.

Alessandrini, A. and Paolo, F. (2005) “AFM: a versatile tool in biophysics” *Measurement Science and Technology.* 16, 65-92.

Alves, M. F. (2003) *ABC da Metrologia Industrial.* Portugal: Departamento de Engenharia Eletrotécnica: ISEP.

Attota, R. and Silver, R. (2011) “Nanometrology using a through-focus scanning optical microscopy method” *Measurement Science and Technology.* 22, 1-10.

Babbie, E. (2007). *The practice of social research.* 11th Belmont: Thomson Wadsworth.

Barbosa, B. (2012) *A Transformada de Hough aplicada à Difração de Elétrons Retroespalhados.* Monografia apresentada ao Programa de Pós–graduação em Matemática para Professores com Ênfase em Cálculo da Universidade Federal de Minas Gerais.

Basso, M. (1998) “Numerical analysis of complex dynamics in atomic force microscopes” *Proceedings of the 1998 IEEE International Conference on Control Application.*1026-1030.

Bonevich, J. E. and Haller, W. K. (2010) *Measuring size of nanoparticles using transmisson electron microscopy (TEM).* Version 1.1, Gaithersburg:National Institute of Standards and Technology, 20p.

Böttcher, C.; Schade, B.; Ecker, C.; Rabe, J. P.; Shu, L. and Schlüter, A. D. (2005) “Double-Helical Ultrastructure of Polycationic Dendronized Polymers Determined by Single-Particle Cryo-TEM” *Chemistry - A European Journal.* 11, 2923-2928.

Brown, S. C.; Boyko, V.; Meyers, G.; Voetz, M. and Wohllebe, W. (2013) "Toward advancing nano-object count metrology: a best practice framework" *Environmental Health Perspectives.* 121, 1282-1298.

Burke, T. et al. (2011) European Nanometrology 2020. Co - Nanomet Consortium. [Internet] disponível em: http://www.nano.org.uk/files/home/european-nanometrology.pdf. Acessado: 22/10/2014 às 18:23.

Cadene, A.; Durand-Vida,l S.; Turq, P. and Brendle, J. (2005) “Study of individual Na-montmorillonite particles size, morphology, and apparent charge” *Journal of Colloid and Interface Science.* 285, 719–730.

Campbel, T. A. (2009) "Measuring the nano-world" *Nano Today.* 4, 380-381.

Chiad, B. T.; Al-zubaydi, T. L.; Khlaf, M. K. and Khudiar, A. I. (2010) “Characterization of low pressure plasma-dc glow discharges (Ar, SF6 and SF6/He) for Si etching” *Indian Journal of Pure & Applied Physics.* 48, 723-730.

Couto, P. R. G. (2008) A estimativa da incerteza de medição pelos métodos do ISO GUM 95 e de simulação de Monte Carlo. Nota Técnica. INMETRO.

Droz, E.; Taborell,i M.; Descouts, P. and Welles, T. N. C. (1994) “Influence of surface and protein modification on immunoglobulin G adsorption observed by scanning force microscopy” *Biophysical Journal.* 67(3),1316-1323.

Dubes, A. *et al.* (2003) “Scanning electron microscopy and atomic force microscopy imaging of solid lipid nanoparticles derived from amphiphilic cyclodextrins” *European Journal of Pharmaceutics and Biopharmaceutics.* 55, 279–282.

Dubrovin, E. V.; Fedyukina, G. N., Kraevsky, S. V.; Ignatyuk, T. E.; Yaminsky, I. V. and Ignatov, S. G. (2012) “AFM Specific Identification of Bacterial Cell Fragments on Biofunctional Surfaces” *The Open Microbiology Journal.* 6, 22-28.

Duncumb, P. and Shields, P. K. “The present state of quantitative X-ray microanalysis Part 1: Physical basis” *British Journal of Applied Physics,* 14, 617-625.

Dufrêne Y. F. (2002) “Atomic Force Microscopy, a Powerful Tool in Microbiology” *Journal of Bacteriology.* 184,5205–5213.

EC (European Commission). (2011) “Commission Recommendation of 18 October 201 1 on the definition of nanomaterial” *Journal of European Union.* [Internet] disponível em: http://eur-lex.europa.eu/legal-content/EN/TXT/?uri=CELEX:32011H0696, acessado em: 15/10/2014 às 21:34.

Equipe Estatcamp (2014). Software Action. Disponível em: http://www.portalaction.combr/, acessado em : 06/04/ 2014 às 23:15.

Fung, R. and Huang S. (2001) “Dynamic modeling and vibration force microscope” *ASME Journal Vibration and Acoustics.*123 (4), 502-509.

Galleti, S. R. (2003) *Introdução à Microscopia Eletrônica.* São Paulo: Centro de Pesquisa e Desenvolvimento de Sanidade Vegetal.

García, R. and Pérez, R. (2002) “Dynamic atomic force microscopy methods” *Surface*

Science Reports. 47, 197-105

Girardi, L. H.; Filho, A. C. and Storck, L. (2009) "Erro tipo I e poder de cinco testes de comparação de múltipla de médias" *Revista brasileira de biometria.* 27(1), 23-26.

Goldstein, J.; Yakowitz, H,; Newbury, D.E.; Lifshin; Colby, J. W. and Coleman, J. R E. (1977) *Practical scanning electron microscopy: Electron and ion microprobe analysis 3rd* Nova York: Plenum Press, 582p.

Goldstein, J.; Newbury, D.E.; Joy, D.C.; Lyman, C.E.; Echlin, P.; Lifshin, E.; Sawyer, L. and Michael, J.R. (2003) *Scanning Electron Microscopy and X-ray Microanalysis 3rd* Nova York: Springer, 689p.

González, R.C and Woods, R. E.(2008) *Digital Image Processing*. 3nd ed. New Jersey: Pearson Education, Inc., 103p.

Goodhew, P. J.; Humphreys, J. and Beanland, R. (2000) *Electron Microscopy and Analysis.* Reino Unido: Taylor and Francis Books.

Grobelny, J.; DelRio, F. W.; Pradeep, N.; Kim, D.; Hackley, V. A. and Cook, R. F. (2009) *Size Measurement of Nanoparticles Using Atomic Force Microscopy*.version 1.1, Gaithersburg:National Institute of Standards and Technology, 20p.

Hackley, V. A. and Clogston, D. J. (2007) *Measuring the Size of Nanoparticles in Aqueous Media Using Batch-Mode Dynamic Light Scattering.* version 1.0, Gaithersburg:National Institute of Standards and Technology, 22p.

Hoo, C. M.,; Starostin, N.; West, P. and Mecartney, M. L. (2008) “A comparison of atomic force microscopy (AFM) and dynamic light scattering (DLS) methods to characterize nanoparticle size distributions” *Journal of Nanoparticle Research.* 10, 89-96.

Horiba Scientific (2014) *A guidebook to particle size analysis.* Irvine:Horiba Insruments, Inc.32p.

Hristu, R.; Stanciu, S. G.; Stanciu, G. A.; Çapan, I.; Güner, B. and Erdoğan, M. (2012) “Influence of atomic force microscopy acquisition parameters on thin film roughness analysis” *Microscopy Research and Technique.* 75, 921-927.

Jalili, N. and Laxminarayana, K. (2004) “A review of atomic force microscopy imaging systems: application to molecular metrology and biological sciences” *Mechatronics.* 14, 907-945.

Jillavenkatesa, A.; Dapkunas, S. and Lim, L. H. (2001) *Particle Size Characterization.* Gaithersburg:National Institute of Standards and Technology, 20p.

Kim, H. A.; Seo, J. K.; Kim, T. and Lee, B. T. (2014) "Nanometrology and its perspectives in environmental research" *Environmental Health and Toxicology.* 29, 1-9.

Klapetek, P.; Nečas, D. and Anderson, C. (2009) *Gwyddion User Guide.* Disponível em: http://gwyddion.net acessado em: 04/03/2013.

Klapetek, P.; Picco, L.; Payton, O.; Yacoot, A. and Miles, M. (2013) “Error mapping of high-speed AFM systems” *Measurement Science and Technology.* 24, 025006.

Korpelaine, V. (2014) Traceability for nanometre scale measurements- Atomic force microscopes in dimensional nanometrology.Tese de doutorado apresentada ao Department of Physics da University of Helsinki, Finlandia.

Kreyling, W. G.; Semmler-Behnke, M. and Chaudhry, Q. (2010) "A complementary definition of nanomaterial" *Nano Today.* 5,165-168.

Leach, R. et al. (2012) “Advances in engineering nanometrology at the National Physical Laboratory” *Measurement Science and Technology.* 23, 1-9.

Lee, M. R. (2010) “Transmission electron microscopy (TEM) of Earth and planetary materials: A review” *Mineralogical Magazine.* 74(1), 1-27.

Li Y. (2007) *Microelectronic Applications of Chemical Mechanical Planarization*. Hoboken, NJ, USA: John Wiley & Sons.

Liberelle, B.; Banquy, X. and Giasson, S. (2008) “Stability of Silanols and Grafted Alkylsilane Monolayers on Plasma-Activated Mica Surfaces” *Langmuir.* 24, 3280-3288.

Liddle, J. A. and Gallatin, G. M. (2011) "Lithography, metrology and nanomanufacturing" *Nanoscale*. 3, 2679-2689.

Lien C. Y; Huang, C. C.; Chen, P. Y and Lin, Y. F. (2013) “An efficient denoising architecture for removal of impulse noise in images” *IEEE Transactions on Computers.* 62(4), 631-643.

Lim, J.; Yep, S. P.; Che, H. X. and Low, S. C. (2013) “Characterization of magnetic nanoparticle by dynamic light scattering” *Nanoscale Research Letters* 381 (8), 1-14.

Linkov, P.; Artemyev, M.; Efimov, A. E. and Nabiev, I. (2013) “Comparative advantages and limitations of the basic metrology methods applied to the characterization of nanomaterials” *Nanoscale*. 5, 8781-8798.

Lojkowski, W.; Turan, R.; Proykova, A.; Daniszewska, A. [eds] (2006) Eighth Nanoforum report: Nanometrology. [Internet] disponível em: http://www.nano.org.uk/members/MembersReports/NANOMETROLOGY_Report.pdf, acessado em: 19/06/2013 às 21:43

MacCuspie, R. I.; Rogers, K.; Patra, M.; Suo, Z.; Allen, A. J.; Martin, M. N. and Hackley, V. A. (2011) “Challenges for physical characterization of silver nanoparticles under pristine and environmentally relevant conditions” *Journal of Environmental Monitoring.* 13, 1212-1226.

Malinovsky, I. *et al.* (2014) "Imaging interference microscope for nanometrology" *Acta Imeko.* 3(3), 28-32.

Malvern Instruments (2003) *Zetasizer nano series user manual.* England: Malvern Instruments.

Malvern Instruments (2011) "Dynamic Light Scattering: An Introduction in 30 Minutes" Nota Técnica: Malvern Instruments [internet] disponível em: www.malvern.com. Acessado em 03/12/2013 às 11:34.

Mannheimer, W. A. (2002) *Microscopia dos materiais-Uma introdução.* Rio de janiero: e-paper Serviços Editoriais, 221p

Melo, R.C.N. (2002) *Células & Microscopia: princípios básicos e práticas.* Juiz de Fora: Ed. UFJF.

Merkus, H. G. (2009) *Particle Size Measurements.* e-book:Springer, 533p.

Microtrac (2010) *Zetatrac operational and maintenance manual*. USA:Microtrac Inc. 42p.

Minary-Jolandan, M.; Tajik, A.; Wang, N. and Yu, M. F. (2012) “Intrinsically high-Q dynamic AFM imaging in liquid with a significantly extended needle tip” *Nanotechnology.* 23, 5704-5710.

Miquita, D. R. (2012) *Microscopia eletrônica de Transmissão: Aspectos básicos e aplicações*. [Internet] Disponível em: http://www.microscopia.ufmg.br/index.php?option=com_content&view=article&id=33&Itemid=88, acessado em: 18/10/2013 às 16:54:42.

Montgomery, D. C. and Runger, G. C. (2002) *Applied statistics and probability for engineers.* Third Edition, New York:John Wiley & Sons, 822p.

Nanoscience Instruments (2011) [Internet] disponível em: http://www.teachnano.com/education/AFM.html, acessado em: 26/02/2015 às 23:18.

Nečas, D. and Klapetek, P. (2012) “Gwyddion: an open-source software for SPM data analysis” *Central European Journal of Physics.* 10, 181-188.

Norstrom, H.; Grusell, E.; Anderso,n L. P and Ber, S. (1978) “Barrier Formation by Glow Discharge Induced Centers on Silicon Surfaces” *Physica Scripta.* 18, 421-423.

Oliveira, A. F. G. (2008) " Testes estatísticos para comparação de médias" *Revista Eletrônica Nutritime.* 5(6), 777-788.

Postek, M. T. *et al.(*2011) "Development of the metrology and imaging of cellulose nanocrystals" *Measurement Science and Technology.* 22, 24005-24015.

Purkait, B. (2002) “Patterns of grain-size distribution in some point bars of the Usri River” *India Journal of Sedimentary Research.* 72(3), 367–375.

R Core team (2014) “R: A language and environment for statistical computing” Disponível em: http://www.R-project.org/, acessado: 07/08/2013.

Raju, T.N., (2005) "William Sealy Gosset and William A. Silverman: two "students" of science" *Pediatrics.* 116 (3), 732–738.

Rao, A.; Schoenenberger, M.; Gnecco, E.; Glatzel, T.; Meyer, E.; Brändlin D. and Scandella L. (2007) “Characterization of nanoparticles using Atomic Force Microscopy” *Journal of Physics: Conference Series.* 61, 971–979.

Rasband, W. S. (1997) ImageJ [Internet] disponível em: http://rsb.info.nih.gov/ij/, acessado em: 17/09/2013 às 17:35.

Razali, N. and Wah, Y. B. (2011). "Power comparisons of Shapiro-Wilk, Kolmogorov-Smirnov, Lilliefors and Anderson-Darling tests" *Journal of Statistical Modeling and Analytics.* 2 (1), 21–33.

Salapaka, M.; Chen, D. (1998) Stability and sensitivity analysis of periodic orbits in tapping modeatomic force microscopy. *Proceedings of the 37th IEEE International Conference on Decision and Control.* 2047-2052.

Sapsford, K.E.; Tyner, K.M.; Dair, B.J.; Deschamps, J.R. and Medintz I.L. (2011) " Analyzing nanomaterial bioconjugates: a review of current and emerging purification and characterization techniques" *Analitical Chemistry.* 83(12),4453-4488.

Sau, T. K. and Rogach, A. L. (2012) *Complex-shaped Metal Nanoparticles: Bottom-Up Syntheses and Applications.* Germany: Wiley-VCH Verlag & Co KGaA, Weinheim, 582 p.

Sepä, S. J. (2014) *Linear and traceable scales for nanometrology.* Tese de doutorado apresentada como pré requisito para obtenção do título de doutor em ciências a Aalto University School of Electrical Engineering, Finlandia.

Shapiro, S. S. and Wilk, M. B. (1965) "An analysis of variance test for normality (complete samples)" *Biometrika.* 52, 591-611.

Shimizu, K. and Mitani, T. (2010) In:. Ertl, D. G.; Luth, D. H. and Mills,D. L. *New*

Horizons of Applied Scanning Electron Microscopy. Berlin: Springer, 182p.

Snedecor, G. W. and Cochran, W.G. (1989) *Statistical Methods.* Eighth Edition, Iowa State: University Press.

SSP (2003) Solid State Physics group [Internet] Disponível em: http://www.dfs.unito.it/solid/CARATTERIZZAZIONE/Afm/, acessado em: 26/02/2015 às 23:30

Taboga, S. R. (2001) "Micoscopia" In: Recco-Pimentel, S. M. & Carvalho, H. F. [eds] *A célula.* São Paulo: Manole Ltda.

Tanaka, M.; Baba, T. and Postek, M. T. (2011) "Nanometrology" *Measurement Science and Technology.* 22, 1-2.

Teixeira, P. R. F. (2006) *Noções de Metrologia-Encarregado de Instrumentação.* Brasil: Petrobrás- Petróleo Brasileiro S.A..

Thomé, A. G. (2004) "Processamento de imagens" [Internet] Disponível em: http://equipe.nce.ufrj.br/thome/p_grad/nn_img/transp/c2_aquis_v2.pdf, acessado em 16/06/2015 às 19:17.

Todua, P. A. (2008) "Metrology and standardization in nanotechnologies and the nanoindustry" Measurement Techniques. 51(5), 5-10.

Tranchida, D.; Piccarolo. S. and Deblieck, R. A. C. (2006) "Some experimental issues of AFM tip blind estimation: the effect of noise and resolution" *Measurement Science and Technology.* 17, 2630–2637.

Tsai, D. H.; DelRio, F. W.; MacCuspie, R. I.; Cho, T. J.; Zachariah, M. and Hackley, V. A. (2010) "Competitive Adsorption of Thiolated Polyethylene Glycol and Mercaptopropionic Acid on Gold Nanoparticles Measured by Physical Characterization Methods" *Langmuir.* 26, 10325-10333.

Ujam, A.J. and Enebe, K. O. (2013) "Experimental Analysis of Particle Size Distribution using Electromagnetic Sieve" *American Journal of Engineering Research.* 2(10), 77-85.

Ukraintsev E., Kromka A., Kozak H., Remeš Z. and Rezek B. (2012) *Artifacts in Atomic Force Microscopy of Biological Samples, Atomic Force Microscopy Investigations into Biology - From Cell to Protein* Available from: http://www.intechopen.com/books/atomicforce-microscopy-investigations-into-biology-from-cell-to-protein/artifacts-in-atomic-force-microscopy-of-biological-samples.

Vernon-Parry, K.D. (2000) "Scanning eletron microscopy: an introduction" *Analyses.* 13, 40-47.

Vieira, S. and Hoffmann, R. (1989) Estatística experimental São Paulo: Atlas, 175p.

VIM (2012) Vocabulário Internacional de Metrologia: conceitos fundamentais e gerais de termos associados. Duque de Caxias, RJ : INMETRO.

Wikipedia (2014) [Internet] Disponível em:http://en.wikipedia.org/wiki/Dynamic_light_scattering, acessado em: 24/02/2015 às 15:22.

Wikipedia (2015) [Internet] Disponível em: http://en.wikipedia.org/wiki/Atomic_force_microscopy, acessado em: 26/02/2015 às 22:42.

Wittke, J. H. (2008) Planetary Materials Microanalysis Facility. [Internet] Disponível em: http://www4.nau.edu/microanalysis/Microprobe-SEM/Imaging.html, Acessado em: 15/10/2013 às 21:34:21.

Yacoot A., Koenders L. (2008) “Aspects of scanning force microscope probes and their effects on dimensional measurement” Journal of Physics D: Applied Physics. 41, 103001.